



International Symposium of Chemical-Environmental-Biomedical Technology 2013



The 5th International Symposium of Environmental Leaders

Date: September 8th - 12th

Venue: Montana Resort Iwanuma, Japan



Table of Contents

Organizers	2
Sponsors	3
General Information	4
Access Map to Montana Resort, Iwanuma	6
Traffic Information	7
Map of Montana Resort, Iwanuma	8
Program Overview	10
Scientific Program	11
Keynote Speakers	18
Invited Speakers	21
Oral Presentation	31
Poster Presentation	55

Organizers

Committee

Dr. Hiroshi Inomata (Professor)
Dr. Tomokazu Matsue (Professor)
Dr. Richard Lee Smith Jr. (Professor)
Dr. Takao Tsukada (Professor)
Dr. Toshiaki Yoshioka (Professor)
Dr. Keiichi Tomishige (Professor)
Dr. Makoto Kobayashi (Assistant Professor)

Shogo Kumagai (D2): Student leader
Shiho Matsuda (M2): Student co-leader
Yuri Hamabe (M2): Student co-leader
Keita Abe (D2): Website creator, in charge of abstract submission and registration
Fonseca Ashton Juan Diego (D1): Supervisor of English and international liaison
Yoshiharu Matsumae (D2): Recreation planner, including welcome party, sports meeting, sightseeing of Sendai city and culture tour to Matsushima
Yuanshu Zhou (D2): Recreation planner and Chinese translator
Dr. Masayoshi Honda (PD): Conference host

Contact

E-mail: iscebt2013@gmail.com

Sponsors



Tohoku University, Graduate School of Environmental Studies

<http://www.kankyo.tohoku.ac.jp/en/>



Tohoku University Environmental Leader Program, Strategic Energy and Resource Management and Sustainable Solutions (SERMSS)

<http://www.kankyo.tohoku.ac.jp/sermss/en/index.html>

Aoba Foundation for the Promotion of Engineering

General Information

Date

September 8th (Sunday) – September 12th (Thursday), 2013

Venue

Montana Resort, Iwanuma

1-1 Kiritoushi, Kitahase-aza, Iwanuma-City, Miyagi, 989-2455, Japan

Tel: (+81) 223-24-4455

Fax: (+81) 223-24-4459

Conference Topics

- Chemical Technology
- Biomedical Technology
- Environmental Technology

Oral Presentation

- Speakers should send their presentation file by e-mail (iscebt2013@gmail.com) by 14:00 on September 7th (Sat.). We ask that you write your name in the message subject line as “Presentation number_last name” and attach your presentation file which should also be named “Presentation number_last name”. If it is impossible to send your file until the deadline, please bring and use your own computer as prevention to viruses. Submission of your presentation files through a USB memory stick is not available.
- We will set up a computer in which Microsoft Office 2013 is installed on, however, we cannot guarantee that videos can be correctly reproduced. If videos and special images are included in your presentation, we recommend that you bring and use your own computer.
- Presentation times are as follows:
 - Keynote speakers: 30 minutes (presentation 25 min. + discussion 5 min.)
 - Invited speakers: 25 minutes (presentation 20 min. + discussion 5 min.)
 - Students: 20 minutes (presentation 15 min. + discussion 5 min.)
- We will ring a bell twice: once when your presentation time is over, and a second time when the discussion time is over.
- An “Outstanding Student Presentation Award” will be granted to the students who

give wonderful presentations. All of the students' presentations are candidates without any application required.

Poster Presentation

- The recommended poster size is 841 mm width and 1189 mm height (A0). Please do not exceed this size.
- Hang your poster in the corresponding spot on the poster boards. We will provide tape for hanging the posters.
- Hang your poster during lunch time (12:00 – 13:00) on September 9th (Mon.), and remove your poster after the poster session is over.
- You should make an effort to be present at your poster and answer questions in front of your poster during the poster session (17:00 –18:00) on September 9th (Mon.).
- An “Outstanding Poster Award” will be granted to the students who prepare wonderful poster presentations. All of the posters are candidates without any application required.

Welcome Party

The welcome party will be held at Parler from 18:00 to 20:00 on September 8th (Sun.).

Banquet

Banquet will be held at Sengan & Matsukaze from 18:00 to 19:00 on September 9th (Mon.).

Dinner (BBQ)

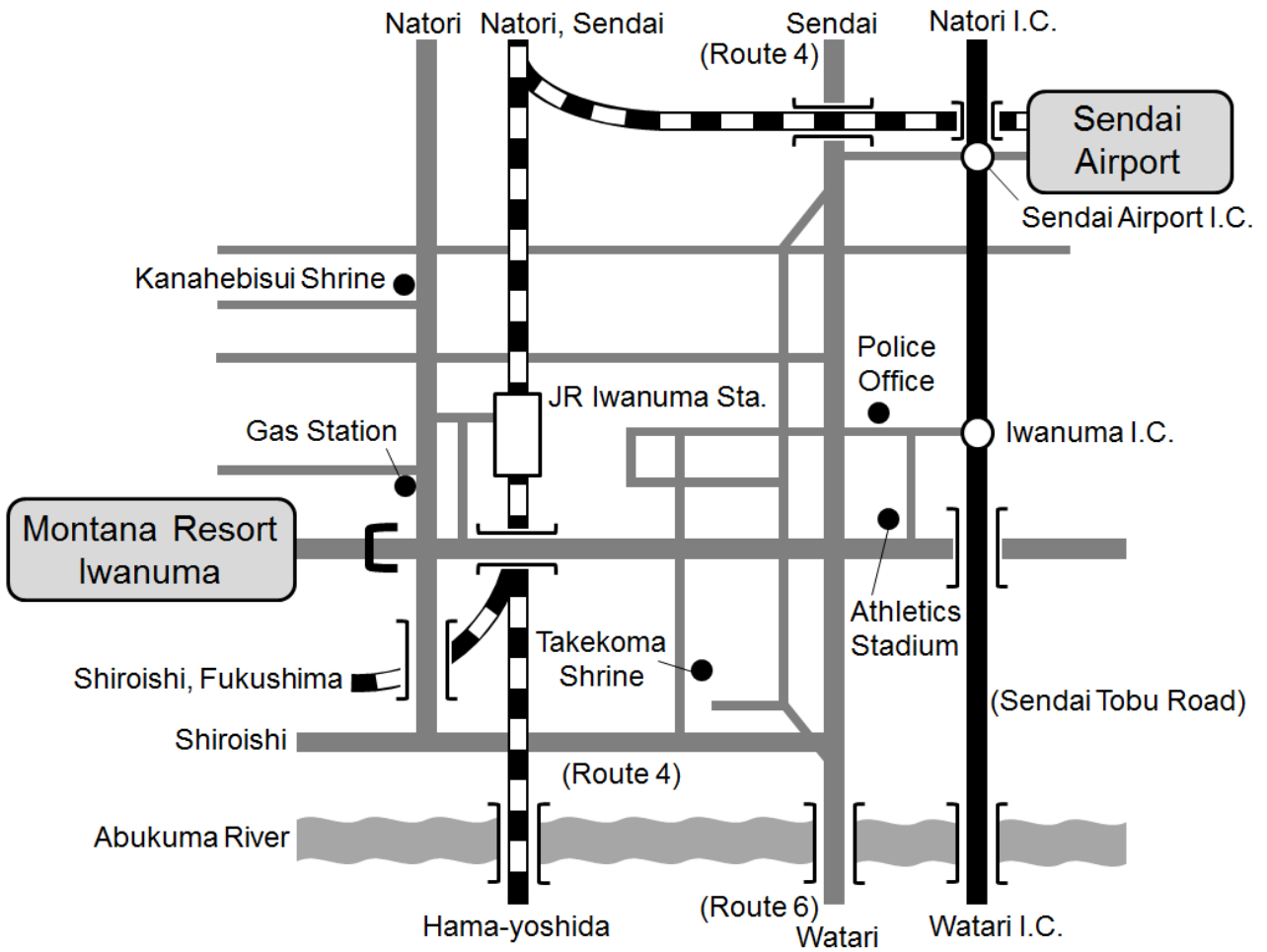
Barbecue (BBQ) party will be held outside of Azalea from 18:00 to 20:00 on September 10th (Tue.).

Breakfast & Lunch

Breakfast will be prepared at Sengan & Matsukaze from 7:00 to 9:00 on September 9th (Mon.) and 10th (Tue.), from 7:00 to 8:00 on September 11th (Wed.) and 12th (Thu.).

Lunch will be prepared at Botan from 11:55 to 12:55 on September 9th (Mon.), and Sengan & Matsukaze from 12:00 to 13:00 on September 10th (Tue.).

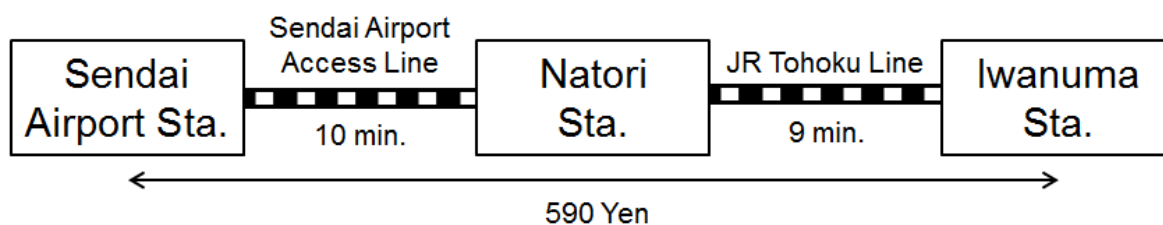
Access Map to Montana Resort, Iwanuma



Traffic Information

We will go and pick you up at the Sendai Airport and Tohoku University (Aobayama campus) by bus on September 8th (Sun.). Likewise, we will take you to the Sendai Airport and Tohoku University (Aobayama campus) by bus on September 12th (Thu.). Participants do not need to be concerned about transportation to Montana Resort Iwanuma. However, if for some reason you travel to Montana Resort Iwanuma by yourself, the following transportation options are available.

By train



You can buy a train ticket (590 Yen) and board a train bound for Sendai at the Sendai Airport station. The Sendai Airport Access line will take you to Natori station in 10 min. Then, you change trains at Natori station. You can use any trains bound for Hama-yoshida, Shiroishi, Fukushima, Iwanuma, Koriyama, Yanagawa, Matsukawa or Ogawara. Please get off the train at Iwanuma station.

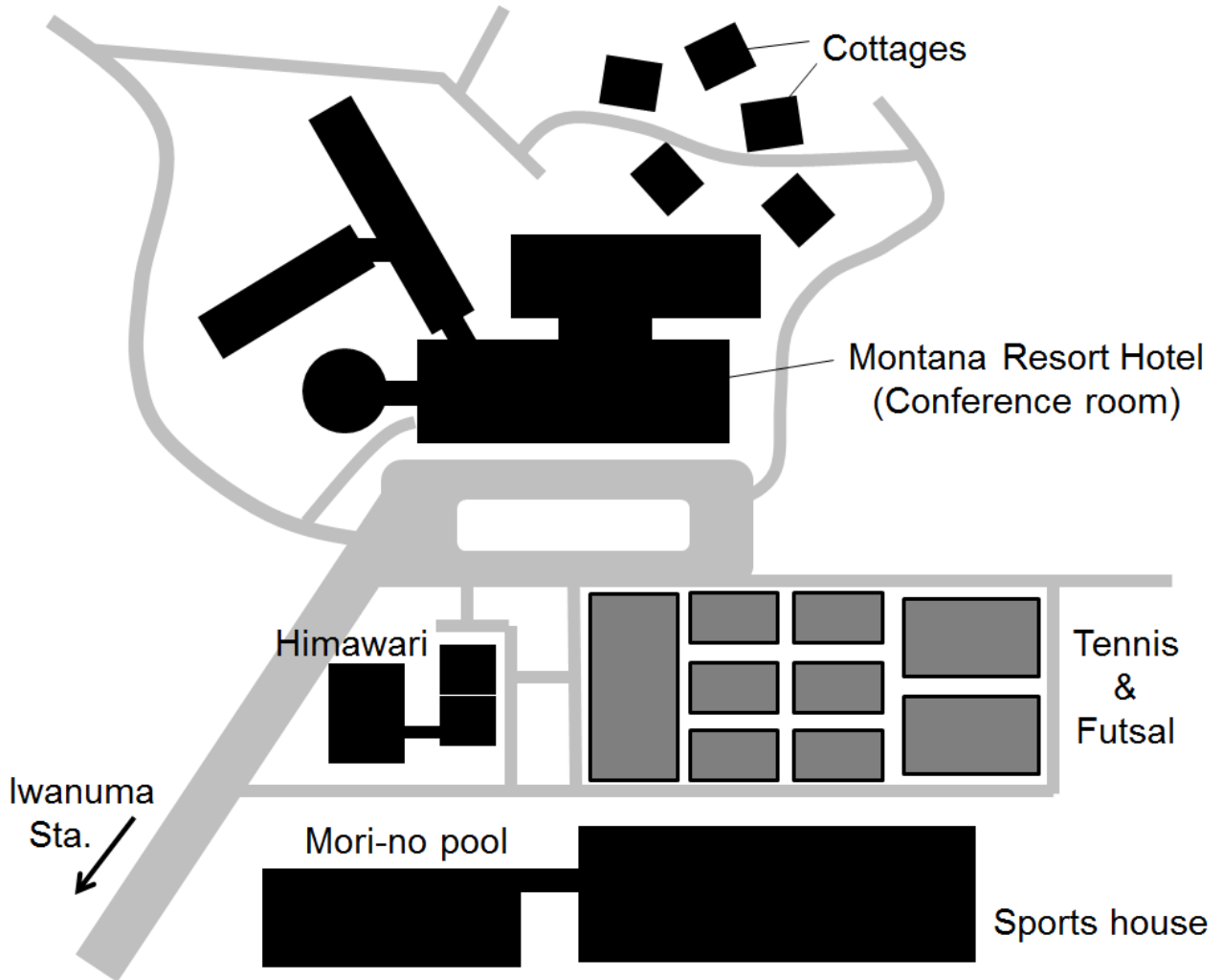
To go from Iwanuma station to Montana Resort, the best way is to take a hotel bus. You can use the hotel bus for free. You can also choose to go by taxi or city bus. If you use a taxi, it will take 5 min and the fee is about 700 Yen. The city bus will part from the west side of the station, and you should get on the bus bound for Shimin-kaikanmae. The bus will take you to 'Greenpia' in 15 min and the fee is 200 Yen.

By car

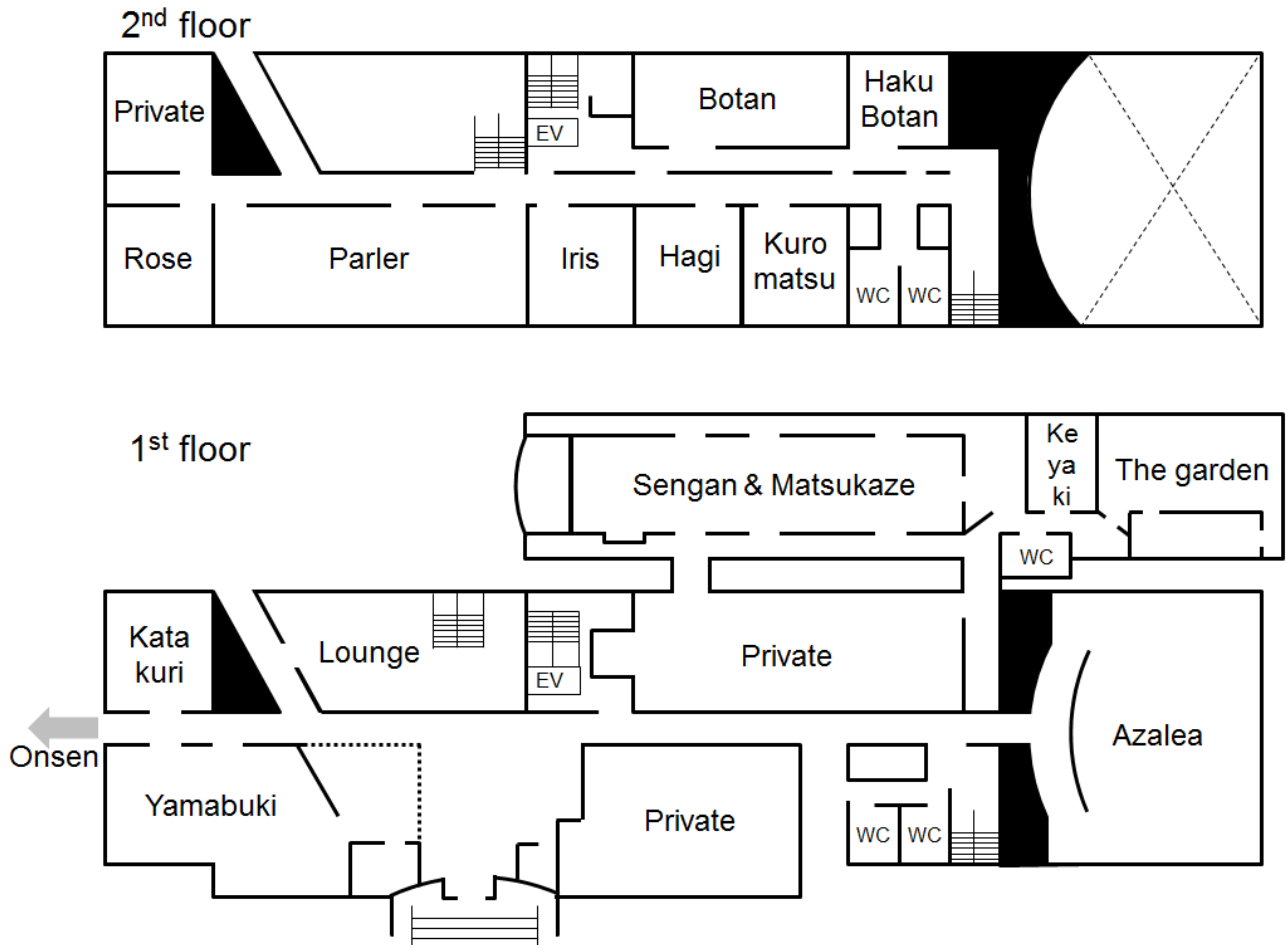
From Sendai Airport, taxi will take you to Montana Resort Iwanuma about 20 min. The fare is about 2800 Yen.

Map of Montana Resort, Iwanuma

Outside view



Inside of the Hotel



You can come and go to the cottages in which you stay at any time. On the other hand, the hotel will close at 0:00, and open at 6:00.

Program Overview

	9/8 (Sun.)	9/9 (Mon.)	9/10 (Tue.)	9/11 (Wed.)	9/12 (Thu.)
7:00 AM		Breakfast (Sengan & Matsukaze)	Breakfast (Sengan & Matsukaze)	Breakfast (Sengan&Matsukaze)	Breakfast (Sengan&Matsukaze)
8:00					
9:00		Oral Session (Azalea)	Oral Session (Azalea)	Technical & Cultural Meeting	Field Work (Higashi- Matsushima & Inside of Matsushima Bay)
10:00					
11:00					
12:00 PM		Lunch (Botan)	Lunch (Sengan&Matsukaze)		
13:00		Oral Session (Azalea)	Oral Session (Azalea)		
14:00					
15:00			International Exchange (Outside)		
16:00					
17:00	Registration (Front lobby)	Poster Session (Parler)			
18:00	Welcome Party (Parler)	Banquet (Sengan & Matsukaze)	BBQ Dinner (Azalea)		
19:00					
20:00					
21:00					

Scientific Program

September 9 th (Mon.)	
8:40 AM	<p>Opening Remarks</p> <p>Nobuyuki Uozumi <i>Tohoku University, Japan</i></p>
8:50	<p>O-13 Keynote</p> <p>Programmable Particle Manipulation with an Optoelectrokinetic Method</p> <p>Kuan-Chih Wang¹, Alope Kumar³, <u>Han-Sheng Chuang</u>^{1,2*}</p> <p>¹<i>Department of Biomedical Engineering, National Cheng Kung University, Taiwan</i> ²<i>Medical Device Innovation Center, National Cheng Kung University, Taiwan</i> ³<i>Department of Mechanical Engineering, University of Alberta, Canada</i></p>
9:40	<p>OS-01</p> <p>Investigation on the Carcinoembryonic Antigen Using Functionalized Silicon Nanowire Field Effect Transistors</p> <p><u>Hsu Chun-Chun</u> <i>Graduate Institute of Biomedical Engineering, Chung Hsing University, Taiwan</i></p>
10:00	<p>OS-02</p> <p>Study on Adsorption and Oxidation of Glycine Based on Surface-Enhanced ATR-IR Spectroscopy</p> <p><u>Yu-Chen Chang</u>, Li-Chia Chen, Hsien-Chang Chang <i>Department of Material Science and Engineering, National Cheng Kung University, Tainan</i></p>
10:20	Break
10:35	<p>OS-03</p> <p>The Passive and Continuous Separation of Bioparticles based on Gray-scale Light-Induced Dielectrophoresis</p> <p><u>Chun-Kai Chiang</u>¹, I-Fang Cheng^{2*}, Hsien-Chang Chang^{1*}</p> <p>¹<i>Department of Biomedical Engineering, National Cheng Kung University, Tainan</i> ²<i>National Nano Device Laboratory</i></p>
10:55	<p>OS-04</p> <p>A label-free and Sensitive Method for Rapid Discrimination of Cancer Cell Based on Electrorotation (ROT) Spectroscopy</p> <p><u>Che-Hua Wu</u>¹, I-Fang Chang², Wei-Lun Huang³, Wu-Chou Su³, Hsien-Chang Chang^{1*}</p> <p>¹<i>Department of Biomedical Engineering, National Cheng Kung University, Taiwan</i> ²<i>National Nano Device Laboratories, NDL</i> ³<i>Institute of Basic Medical Sciences, College of Medicine, National Cheng Kung University, Taiwan</i></p>

11:15	<p>OS-05</p> <p>Graphene-Enzyme-Immobilized Screen-Printed Electrode for Histamine detection in Food</p> <p><u>Cheng-Hui Chen</u>, Li-Chia Chen, Hsien-Chang Chang</p> <p><i>Department of Biomedical Engineering, National Cheng Kung University, Tainan</i></p>
11:35	<p>OS-06</p> <p>Mesenchymal Stem Cells as Cellular Vehicles for Brain Tumor-Targeted Delivery of Diagnostic and Therapeutic Agents</p> <p><u>Yuan-Chung Tsai</u>, Wen-Chia Huang, Hsin-Cheng Chiu</p> <p><i>Department of Biomedical Engineering and Environmental Sciences, National Tsing Hua University, Taiwan</i></p>
11:55	Lunch
12:55	<p>OS-08</p> <p>Studying the Effect of Blood Viscosity on Cardiovascular Diseases Using μPIV Diffusometry</p> <p><u>Chia-Hao Hsu</u>¹, Dar-Bin Shieh², Han-Sheng Chuang^{1,3}</p> <p>¹<i>Department of Biomedical Engineering, National Cheng Kung University, Taiwan</i></p> <p>²<i>Biochemistry and Molecular Biology, National Cheng Kung University, Taiwan</i></p> <p>³<i>Medical Device Innovation Center, National Cheng Kung University, Taiwan</i></p>
13:15	<p>OS-13</p> <p>Immobilization of Biomolecule on Field Effect Device (FED) by New Amino Group Functionalization</p> <p><u>Lin Yi-Ting</u></p> <p><i>Department of Electronic Engineering, Chang Gung University, Taiwan</i></p>
13:35	<p>OS-14</p> <p>Study of Lipofuscin Accumulation in <i>C. elegans</i> and Heat Shock Treatments Based on an Optoelectric Device</p> <p><u>Hsiang-Yu Chen</u>¹, Chang-Shi Chen², Wen-Tai Chiu¹, Han-Sheng Chuang^{1,3}</p> <p>¹<i>Department of Biomedical Engineering, National Cheng Kung University, Taiwan</i></p> <p>²<i>Biochemistry and Molecular Biology, National Cheng Kung University, Taiwan</i></p> <p>³<i>Medical Device Innovation Center, National Cheng Kung University, Taiwan</i></p>
13:55	Break
14:10	<p>OS-15</p> <p>Development of 2nd Generation Bio-LSI System for Real Time Bio-imaging</p> <p><u>Masanori Nakano</u>¹, Kumi Y. Inoue², Reyushi Kubo¹, Ryota Kunikata³, Atsushi Suda³, Masaaki Matsudaira², Kosuke Ino¹, Hitoshi Shiku¹, Tomokazu Matsue^{1,2,4}</p> <p>¹<i>Graduate School of Environmental Study</i></p>

	<p>²<i>Micro Systems Integration Center (μSIC)</i></p> <p>³<i>Japan Aviation Electronics Industry, Ltd.</i></p> <p>⁴<i>The World Premier International Research Center Advanced Institute for Materials Research (WPI-AIMR); Tohoku University, Japan</i></p>
14:30	<p>OS-16</p> <p>Development of Nano-Pt Electrode toward the Mapping of Dopamine Release Sites</p> <p><u>X. Wang</u>¹, Y. Takahashi², Y. Matsumae¹, K. Ino¹, H. Shiku¹, T. Matsue^{1,2}</p> <p>¹<i>Graduate School of Environmental Studies</i></p> <p>²<i>WPI-AIMR; Tohoku University, Japan</i></p>
14:50	<p>OS-17</p> <p>Effect of Surface Treatment on the Electrochemical Properties of Screen Printed Carbon Electrodes</p> <p><u>Ming-Jay Lin</u>, Ching-Chou Wu*</p> <p>¹<i>Department of Bio-industrial Mechatronics Engineering, National Chung Hsing University, Taiwan</i></p>
15:10	Break
15:25	<p>OS-10</p> <p>The Study of Hydrogen Generation from Hydrolysis of Ammonia Borane in The Presence of Ni-Co/r-GO Catalysts</p> <p><u>Chang-Chen Chou</u>, Bing-Hung Chen</p> <p>¹<i>Department of Chemical Engineering, National Cheng Kung University, Taiwan</i></p>
15:45	<p>OS-20</p> <p>Effect of Film Thickness on the Optical Energy Band Gap and Threshold Voltage for Micro Sensor Performance</p> <p><u>Nurul Farhanah Ab. Halim</u>, Mohd Noor Ahmad</p> <p><i>Centre of Excellence for Advanced Sensor Technology (CEASTech), Universiti Malaysia Perlis (UniMAP)</i></p>
16:05	<p>O-04</p> <p>Biodiesel Production from Transesterification of Vegetable Oils over Zeolite-like Catalysts Synthesized from Siliceous Clay</p> <p><u>Chen Bing-Hung</u></p> <p>¹<i>Department of Chemical Engineering, National Cheng Kung University, Taiwan</i></p>
16:30	<p>O-12</p> <p>Neutron Radiography and Numerical Simulation on Mixing Behavior in a Tubular Flow Reactor for Supercritical Hydrothermal Synthesis of Nanoparticles</p>

	<u>Takao Tsukada</u> <i>Department of Chemical Engineering, Tohoku University, Japan</i>
17:00	Poster Session
18:00	Banquet

September 10 th (Tue.)	
9:00 AM	<p>O-10</p> <p>Integrating Study of High Effective Biofuel Energy Recovery with Multistage Biorefinary Process</p> <p><u>Sheng-Shung Cheng</u></p> <p><i>Department of Environmental Engineering, National Cheng Kung University, Taiwan</i></p>
9:25	<p>OS-07</p> <p>Atmospheric Dry and Wet Depositions of Mercury</p> <p><u>Chia-Wei Lin</u></p> <p><i>¹Department of Environmental Engineering, National Cheng Kung University, Taiwan</i></p>
9:45	<p>OS-09</p> <p>Thermal Decomposition of Printed-Circuit Boards Based on Thermoset Resin</p> <p><u>Shogo Kumagai</u>^{1,2}, Guido Grause¹, Tomohito Kameda¹, Toshiaki Yoshioka¹</p> <p><i>¹Graduate School of Environmental Studies, Tohoku University</i></p> <p><i>²Research Fellow of the Japan Society for the Promotion of Science</i></p>
10:05	<p>OS-11</p> <p>Simultaneous Nitritation/Anammox in a Partial Aeration Biofilm Reactor for Treating Secondary Effluent from a Petrochemical Industrial Park</p> <p><u>Han-Lin Lin</u>, Hsiang-Wei Tsao, Yu-Wen Huang, Keng-Hao Yang, Ya-Fei Yang, Sheng-Shung Cheng</p> <p><i>Department of Environmental Engineering, National Cheng Kung University, Taiwan</i></p>
10:25	Break
10:40	<p>OS-19</p> <p>Bioaugmented Anaerobes Digest Kitchen Waste to Promote Cellulose Hydrolysis and Hydrogen Generation with Anaerobic Fluidized Bed Process</p> <p><u>Yu-Min Tien</u></p> <p><i>Department of Environmental Engineering, National Cheng Kung University, Taiwan</i></p>
11:00	<p>OS-21</p> <p>Long-term Competition between Sulfate-reducing Bacteria and Methane-producing Archaea in a UASB Reactor</p> <p><u>Yong Hu</u>, Yuta Sudo, Toshimasa Hojo, Yu-You Li</p> <p><i>Graduate School of Environmental Studies, Tohoku University, Japan</i></p>
11:20	<p>OS-22</p> <p>Continuous Thermophilic Hydrogen Fermentation of Cellulose by Mixed-culture</p>

	<p><u>Hongyu Jiang</u>, S. I. Gadow, Y. Y. Li <i>Graduate School of Environmental Studies, Tohoku University, Japan</i></p>
11:40	<p>O-18 Twenty-Second-Temporal-Resolution Monitoring of Trace Metal Ions in Living Rat Brain Using Microdialysis Sampling, Online Sequential/Segmented Solid Phase Extraction Device, and ICP-MS <u>Sheng-Chieh Hsia</u>, Cheng-Kuan Su, Yuh-Chang Sun* <i>Department of Biomedical Engineering and Environmental Sciences, National Tsing-Hua University, Taiwan</i></p>
12:00	Break
13:00	<p>O-11 Low CO Generation on Tunable Oxygen Vacancies of Non-noble Metallic Cu/ZnO Catalysts for Partial Oxidation of Methanol Reaction <u>Yuh-Jeen Huang</u> <i>Department of Biomedical Engineering and Environmental Sciences, National Tsing Hua University, Taiwan</i></p>
13:25	<p>O-14 Keynote Channeling the Forces of Nature for the Creation of Innovative Manufacturing and the Lifestyle Emile H. Ishida <i>Graduate School of Environmental Studies, Tohoku University, Japan</i></p>
14:15	Break
14:30	<p>O-01 Observation of Cell Growth on the Nanostructure Surface <u>Shu-Ping Lin</u> <i>Graduate Institute of Biomedical Engineering, National Chung Hsing University, Taiwan</i></p>
14:55	<p>O-02 Fast and Sensitive Impedimetric DNA Sensing Chips Integrated with An AC Electroosmotic Vortex <u>Ching-Chou Wu</u> <i>Department of Bio-industrial Mechatronics Engineering, National Chung Hsing University, Taiwan</i></p>
15:20	<p>O-03 Optical Thermophoresis for Interferon-gamma Detection using Aptamers <u>Yih-Fan Chen</u></p>

	<i>Department of Biomedical Engineering, National Cheng Kung University, Taiwan</i>
15:45	Break
16:00	<p>O-05</p> <p>Screening of Antibiotic Susceptibility to β-Lactam-Induced Elongation of Gram-Negative Bacteria Based on Dielectrophoresis</p> <p><u>Hsien-Chang Chang</u>, Cheng-Che Chung, I-Fang Cheng</p> <p><i>Department of Biomedical Engineering, National Cheng Kung University, Taiwan</i></p>
16:25	<p>O-06</p> <p>Microwave Nanosensor using Graphene-based Nanoantenna for Biomarker/Protein Detection</p> <p><u>Mohd Noor Ahmad</u>¹, Mohd. Faizal Jamlos², Nurul Farhanah Ab. Halim¹</p> <p>¹<i>School of Material Engineering, Universiti Malaysia Perlis (UniMAP)</i></p> <p>²<i>Advanced Communication Engineering Centre (ACE), School of Computer & Communication Engineering, Universiti Malaysia Perlis (UniMAP)</i></p>
16:50	<p>O-08</p> <p>Radioactive Gold Nanoparticle (198Au-GNP) for Brain Tumor Therapy</p> <p><u>Jen-Kun Chen</u></p> <p><i>Center for Nanomedicine Research, National Health Research Institutes, Taiwan</i></p>
17:15	Closing Remarks
18:00	BBQ dinner

O13 (Keynote)

Programmable Particle Manipulation with an Optoelectrokinetic Method

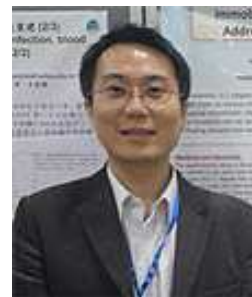
Kuan-Chih Wang¹, Alope Kumar³, and Han-Sheng Chuang^{1, 2 *}

¹ Department of Biomedical Engineering, National Cheng Kung University, TAIWAN

² Medical Device Innovation Center, National Cheng Kung University, TAIWAN

³ Department of Mechanical Engineering, University of Alberta, CANADA.

*oswaldchuang@mail.ncku.edu.tw



Abstract

Particle manipulation is essential yet challenging in numerous biochemical assays. For example, an effective concentration may enhance detection of low-abundance biological molecules that can serve as early diagnostic biomarkers. Among various technologies, electrokinetic and optical methods draw considerable attention due to their high efficiency, non-invasiveness, quick response, and ease of integration with other devices. Bown et al.[1] demonstrated DNA concentration by deliberately balancing the forces between AC electroosmotic flow and dielectrophoresis. Kühn et al.[2] achieved 1 μm particle aggregation in a microchannel coupled with an optical waveguide by utilizing two 125 mW IR laser beams. However, current optical or electrokinetic devices are limited either in their throughput or have fixed configurations. Taking into consideration that a platform enabling user-defined manipulation would be an important step forward, we therefore fulfilled the concept by developing an programmable optoelectric technique, Rapid Electrokinetic Patterning (REP)[3] (Fig.1). To showcase the REP enabled manipulation, a particle suspension (3 μm , Thermo Scientific) was sandwiched between an ITO glass cover (top) and a glass slide coated with a golden film (bottom). Successful particle trapping occurred only when the three forces, electrothermal flow, particle-particle repulsion, and induced electrostatic attraction, came to an equilibrium state. The trapping effect was a function of particle size, electrical potential, electric frequency, light patterns, and light intensity. Rather than patterning substantial electrodes, the trapping site was dynamically created by a tunable IR beam (67 mW, 1064 nm). By programming a motorized mirror, we were able to concentrate particles and move the particle clump over the entire microchip (Fig.2). This maneuverability enables a large extent of operation and enhances signal response in bead-based biochemical reactions.

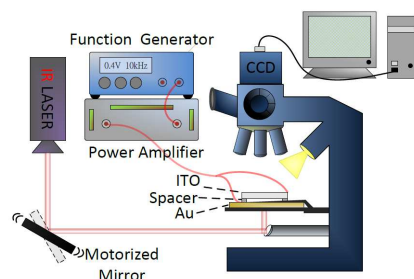


Figure 1: Schematic of the experimental setup of the optoelectric device under an inverted microscope.

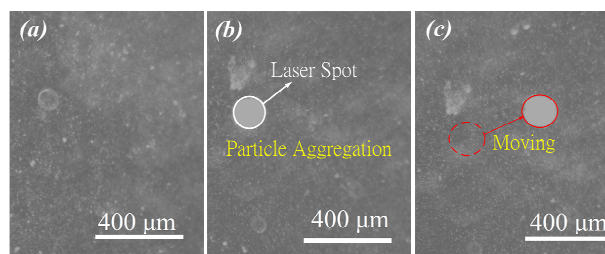


Figure 2: Top view of particle movement in the microchip (a) before and (b) after the optoelectric treatment is effective. (c) Particles are translated from dashed line circle to solid line circle.

Keywords: optoelectronics, particles, concentration, manipulation, biochemical assays

- 1) Bown, M.R. and C.D. Meinhart, *Microfluidics and Nanofluidics*, **2**, 513 (2006)
- 2) Kühn, S., E.J. Lunt, B.S. Phillips, A.R. Hawkins, and H. Schmidt, *Optics Letters*, **34**, 2306 (2009)
- 3) Williams, S.J., A. Kumar, and S.T. Wereley, *Lab Chip*, **8**, 1879 (2008)

O14 (Keynote)

“Channeling the Forces of Nature for the Creation of innovative manufacturing and the lifestyle”

Emile H. Ishida

Tohoku Univ. Graduate School of Environmental Studies, Japan



Abstract:

The Great East Japan Earthquake, which happened on March 11, 2011, made us aware once again that we had forgotten we were just one species within the great cycle of nature on earth, that we were allowed to survive only because of nature, and that the idea that we were somehow able to conquer the nature was simply an illusion.

Now, more than ever, is the time we must confront face-to-face the change from the underground resources type of civilization to one with a new way of life and technology that embraces a sense of nature. To do so, we must learn from nature that possesses the only sustainable society on earth and create technology which embraces such a view of nature.

We call technology, which cleverly revives nature’s greatness, Nature Technology, and we have completed fundamental consideration of the micro-wind generator using mechanism of the dragonfly’s wings, water free bath learning from bubbles, stain free surface learning from snail shell, electricity free air-conditioner and others.

We must now, in the midst of severe environmental restrictions, begin the great challenge of suspending and cutting back our escalating human activity, while living in a spiritually enriching way. How can we live in a spiritually fulfilling way on one planet? In order to find the form that this new way of life will take, we certainly need to adopt a backcasting point of view which starts with the prerequisite that we live on only one planet.

Resume:

Ishida served as a director and general manager of the headquarters for technology and was the chairman of both Environmental Strategy and Technological Strategy at INAX Corporation Japan. And now, he is a Professor of Graduate School of Environmental Studies and Eco-material Design & Process Engineering, Tohoku University since September, 2004 (PhD from Nagoya Institute of Tech. 1992). He is a representative of the Earth Village Research Laboratory, Nature Technology Research Consortium and many others. He is a Fellow of the American Ceramic Society. Has authored/coauthored 340 academic papers, 38 books, has 95 patents and 14 academic awards.



Lin, Shu-Ping Ph.D.

Assistant Professor
Graduate Institute of Biomedical
Engineering, National Chung Hsing
University, Taichung, 40227, Taiwan

Tel: 886-4-2284-0732 ext.302

Fax: 886-4-2285-2422

E-mail: splin@dragon.nchu.edu.tw

PRESENTATION: Observation of Cell Growth on the Nanostructure Surface

Nanotechnology had been drawn a lot of attentions in many biomedical aspects. In this study, we used unmodified and modified titania (TiO_2) surfaces to investigate the effect of nanostructure on cell morphological change and cell growth. First, the structure of TiO_2 nanotubes was prepared by anodization. After that, the nanostructures of TiO_2 were further modified by 3-aminopropyltrimethoxysilane (APTMS). X-ray diffraction (XRD) and scanning electron microscope (SEM) were used to analyze the structures of TiO_2 nanotubes. XRD showed the nanotubes consisted of TiO_2 . Those TiO_2 nanotubes were around 60.374 nm in diameter in SEM images. Electron spectroscopy for chemical analysis (ESCA) was used to characterize the original Ti web, unmodified TiO_2 , and APTMS modified TiO_2 . ESCA showed the successful surface modification with the specific amine ($-\text{NH}_2$) functional groups on the surface of APTMS modified TiO_2 ($-\text{NH}_2$ was at 399.8 eV and NH_3^+ was at around 401.5 eV). In order to investigate the effect of TiO_2 nanostructure on cell growth, 3T3 fibroblasts were independently cultured on the original Ti web, unmodified TiO_2 , and APTMS modified TiO_2 . Microscopy was used to examine the cells on the nanostructured TiO_2 substrates. SEM displayed the cell morphology on TiO_2 nanostructures. In addition, fluorescent images visualized the relative position of cells on TiO_2 nanostructures in Figure 1. Quantitative analyses of cell numbers exhibited APTMS modified TiO_2 effectively facilitated the cell proliferation with an increasingly cellular growth (Figure 2). We found APTMS modified TiO_2 improved the overall capability of cell growth up to 35.6 % in our *in-vitro* observation in comparison with Ti and unmodified TiO_2 substrates. Our study showed that APTMS modified TiO_2 increased cell growth and possessed better biocompatibility.

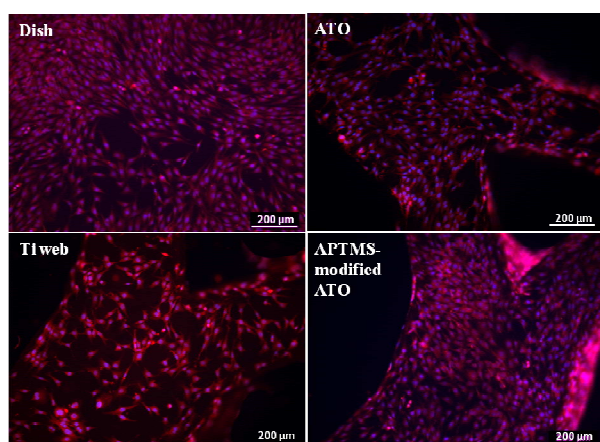


Figure 1 Observation of fluorescent images.

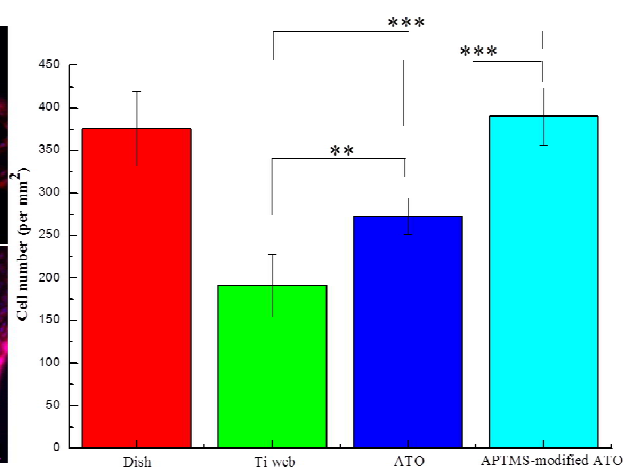


Figure 2 Statistic analyses of cell growth.

Keywords: nanostructure, titania, anodization, surface modification, cell growth

Fast and Sensitive Impedimetric DNA Sensing Chips Integrated with An AC Electroosmotic Vortex

Ching-Chou Wu

Department of Bio-industrial Mechatronics Engineering, National Chung
Hsing University, Taichung, Taiwan



Abstract

An AC electrokinetic flow such as AC electroosmosis (ACEO) or DC-biased ACEO and label-free electrochemical impedance spectroscopy are employed to increase the hybridization rate and specifically detect target DNA (tDNA) concentrations. The schematic of impedimetric DNA sensing chip integrated with the ACEO stirring in disk-ring dual electrodes is shown in Fig. 1(a). A low-ionic-strength solution, 6.1 $\mu\text{S}/\text{cm}$ 1 mM Tris (pH 9.3), was used to produce ACEO and DC-biased ACEO and proved the feasibility of hybridization. Adequate voltage parameters for the ACEO driving and DNA hybridization in the 1 mM Tris solution were 1.5 V_{pp} and 200 Hz. Moreover, an electrode set with a 1:4 ring width-to-disk diameter ratio exhibited a larger ACEO velocity above the disk electrode surface to improve collecting efficiency. The ACEO-integrated DNA sensing chips could reach 90% saturation hybridization within 117 s. The linear range and detection limit of the sensors was 10 aM–10 pM and 10 aM, respectively, as shown in Fig. 1(b). In addition, the DC-biased ACEO was also used in the similar chip to produce a vortex. The detection limit can be as low as 1 aM. The label-free impedimetric DNA sensing chips with integrated ACEO or DC-biased ACEO stirring can perform rapid hybridization and highly-sensitive detections to specifically measure tDNA concentrations.

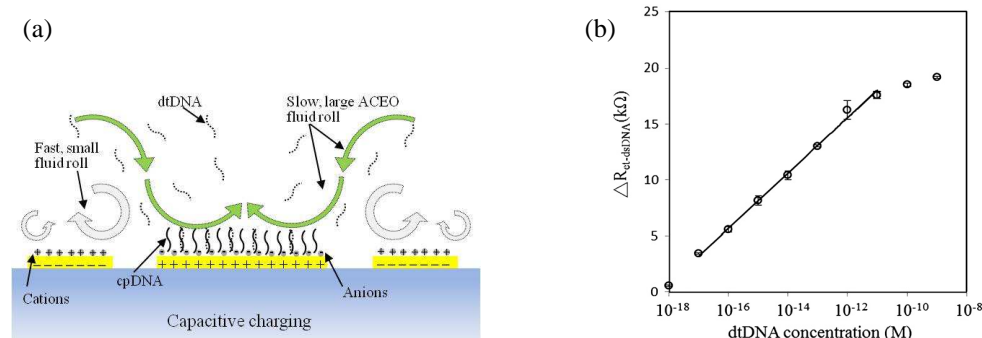


Figure 1 (a) Side-view schematic of rotating vortices induced by ACEO above the electrodes. (b) The $\Delta R_{\text{et-dsDNA}}$ value as a function of dtDNA concentration with 120 s ACEO stirring of 200Hz and 1.5 V_{pp} for each hybridization concentration

Keywords: Label-free, electrochemical impedance spectroscopy, AC electroosmosis, DNA sensor
1) Wu C.-C., Yang, D.-J. *Biosens. Bioelectron.*, **43**, 348(2013).

O03



Chen, Yih-Fan Assistant Professor

{ Ph.D., Univ. of Michigan, Ann Arbor
Assistant Prof. of the Department of
Biomedical Engineering, National Cheng
Kung Univ., Tainan, 70101, Taiwan, ROC
{ Tel: 886-6-2757575#63434
{ Fax: 886-6-2343270
{ E-mail: chenyf@mail.ncku.edu.tw

PRESENTATION: Optical thermophoresis for interferon-gamma detection using aptamers

Thermophoretic effects can be used to deplete or concentrate biomolecules in solution, and the difference in the thermophoretic motion among different molecules can be utilized for biosensing. In this study, aptamers were used to capture interferon-gamma for the detection of latent tuberculosis infection. The binding of aptamers to interferon-gamma results in changes in the charge and the size of the molecules. In addition, the binding disrupts some of the double-stranded parts of the aptamers. Since thermophoretic motion can be affected by charge, size and double-stranded parts of DNA, the concentration of interferon-gamma can be determined using thermophoresis. While thermophoresis usually drives molecules away from the hot region, it has been known that thermophoresis can be used to accumulate molecules such as DNA when polymers are added to the buffer solution. In this study investigate how to determine the concentration of interferon-gamma by measuring the changes in the level of thermophoretic accumulation.

Keywords: thermophoresis, interferon gamma, latent tuberculosis infection

References:

1. Duhr, S.; Braun, D. Proc. Natl. Acad. Sci. U.S.A. 2006, 103, 19678-19682.
2. Piazza, R. Soft Matter 2008, 4, 1740-1744.
3. Maeda, Y. T.; Buguin, A.; Libchaber, A. Phys. Rev. Lett. 2011, 107.



Chen, Bing-Hung (PhD)

Professor

Department of Chemical Engineering,
National Cheng Kung University

Tainan 70101, Taiwan

Tel: +886-6-275-7575 ext. 62695

Fax: +886-6-234-4496

E-mail: bkchen@mail.ncku.edu.tw

PRESENTATION: Biodiesel Production from Transesterification of Vegetable Oils over Zeolite-like Catalysts Synthesized from Siliceous Clay

Zeolite catalysts were prepared from natural siliceous clay (**Figure 1**) to catalyze transesterification of triglycerides/vegetable oils in excess methanol for biodiesel production. These effective catalysts were found to possess characteristics of zeolites (**Figure 2**). In a typical experiment, this zeolite-like material was obtained after aging a mixture of raw diatomite clay (**Figure 1**), sodium hydroxide, aluminum salt and deionized water for 0.5 h in ambient environment, followed by hydrothermal reaction at 220 °C for 12 h. Various instruments such as XRD, FT-IR, SEM, EDS, SS MNR and TGA were applied to characterize the *as*-synthesized catalyst. The obtained catalytic material was advantageous not only in easy preparation, but also as a low-cost solid catalyst that can effectively catalyze transesterification of triglycerides in excess methanol for production of methyl oleate and other fatty acid methyl esters as biodiesel. Over 95% of soybean oil transferred to biodiesel under optimal conditions of 63 °C and 2 h (**Figure 3**).

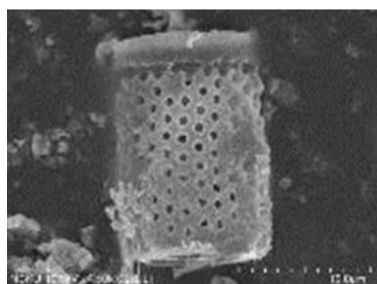


Figure 1

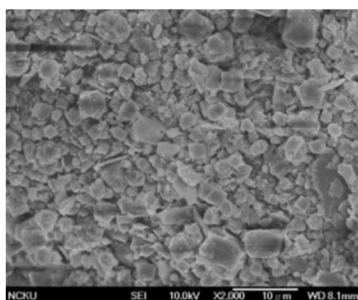


Figure 2

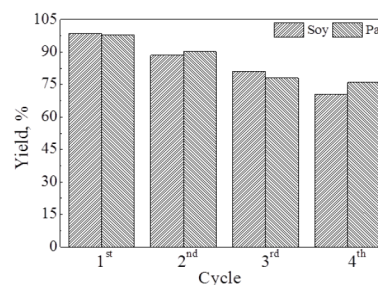


Figure 3

References:

- 1) T. H. Đặng, B.-H. Chen, D.-J. Lee, *Bioresource Tech.* **2013**
(<http://dx.doi.org/10.1016/j.biortech.2012.12.024>)

Keywords: Biodiesel, heterogeneous catalysts, kaolin, diatomite, vegetable oils, zeolite LTA, zeolite CAN.

Screening of Antibiotic Susceptibility to β -Lactam-Induced Elongation of Gram-Negative Bacteria Based on Dielectrophoresis

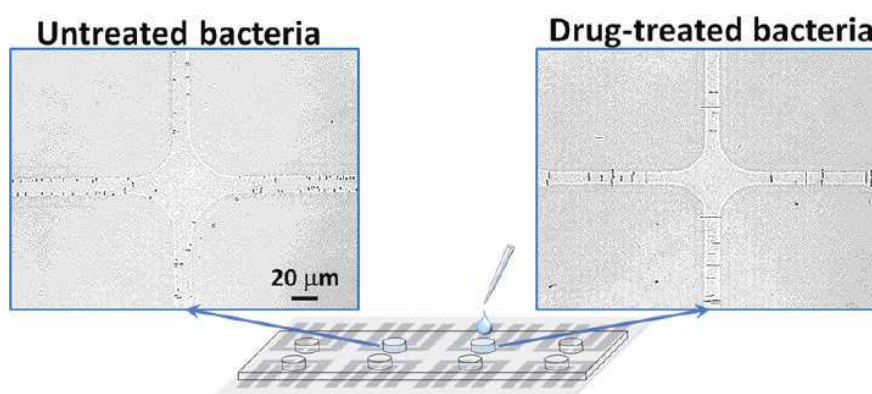
Hsien-Chang Chang*, Cheng-Che Chung and I-Fang Cheng

Department of Biomedical Engineering, National Cheng Kung University, Tainan, 70101, Taiwan

Abstract

We demonstrate a rapid antibiotic susceptibility test (AST) based on the changes in dielectrophoretic (DEP) behaviors related to the β -lactam-induced elongation of Gram-negative bacteria (GNB) on a quadruple electrode array (QEA). The minimum inhibitory concentration (MIC) can be determined within 2 h by observing the changes in the positive-DEP frequency (pdf) and cell length of GNB under the cefazolin (CEZ) treatment. *Escherichia coli* and *Klebsiella pneumoniae* and the CEZ are used as the sample bacteria and antibiotic respectively. The bacteria became filamentous due to the inhibition of cell wall synthesis and cell division and cell lysis occurred for the higher antibiotic dose. According to the results, the pdfs of wild type bacteria decrease to hundreds of kHz and the cell length is more than 10 μm when the bacterial growth is inhibited by the CEZ treatment. In addition, the growth of wild type bacteria and drug resistant bacteria differ significantly. There is an obvious decrease in the number of wild type bacteria but not in the number of drug resistant bacteria. Thus, the drug resistance of GNB to β -lactam antibiotics can be rapidly assessed. Furthermore, the MIC determined using dielectrophoresis-based AST (d-AST) was consistent with the results of the broth dilution method. Utilizing this approach could reduce the time needed for bacteria growth from days to hours, help physicians to administer appropriate antibiotic dosages, and reduce the possibility of the occurrence of multidrug resistant (MDR) bacteria.

Keywords: Dielectrophoresis, β -lactam antibiotics, antibiotic susceptibility test



1. C. -C. Chung, I-F. Cheng, W. -H. Yang, H. -C. Chang*, Antibiotic susceptibility test based on the dielectrophoretic behavior of elongated *Escherichia coli* with cephalixin treatment, *Biomicrofluidics*, 5(2011)021102.
2. C. -C Chung, I-F. Cheng, H. -M. Chen, H. -C. Kan, W. -H. Yang*, H. -C. Chang*, "Rapid screening of antibiotic susceptibility to β -lactam-induced elongation of gram-negative bacteria based on dielectrophoresis", *Analytical Chemistry*, 84(2012)3347-54.

Microwave Nanosensor using Graphene-based Nanoantenna for Biomarker/Protein Detection

Mohd Noor Ahmad¹, Mohd. Faizal Jamlos², Nurul Farhanah Ab. Halim¹

¹ School of Material Engineering, Universiti Malaysia Perlis (UniMAP), ²Advanced Communication Engineering Centre (ACE), School of Computer & Communication Engineering, Universiti Malaysia Perlis (UniMAP).



Abstract

Developing inverse scattering (IS) technique for characterization of biomarker/protein is very challenging because of its usefulness in many applications such as (stroke, breast cancer etc...). This presentation is to discuss inverse scattering (IS) technique for absorption of microwaves reflectance scattered signal depending on the impedance changes or scattered reflection signal when a microwave is propagated into the biomarkers'/proteins' protein. A graphene microwave radiator is a new platform for the creation of a new measurement approach called Microwave Inverse Scattering Nanomesh technique (MISN). MISN will fully absorb the unique scattered microwaves signal. These different forms of scattered microwave signals are the reflectance waves from different types of biomarker/protein that could lead to the detection cancerous or other diseases cells as the results of excitation/transmission wave that strike on them. Two-port microstrip-based signal processing method will be used to analyze the characteristic of unique absorbed scattered microwave signals extracted by graphene-based nanoantenna.

Keywords: graphene, nanoantenna, microwave nanosensor

1) Sergi Abadal. *et al.*, *Graphene 2011 Conference*, 1-2,(2011)



Chen, Jen-Kun Ph.D.

Assistant Principal Investigator
 Center for Nanomedicine Research,
 National Health Research Institutes
 Miaoli 35053, Taiwan
 Tel: 886-37-246166 ext 38117
 Fax: 886-37-586447
 E-mail: jkchen@nhri.org.tw

PRESENTATION: Radioactive Gold Nanoparticle (^{198}Au -GNP) for Brain Tumor Therapy

The challenges of brain tumor therapy are extremely stringent because of very poor prognosis and limited advances of therapeutics. Concurrent chemoradiotherapy (CCRT) has been employed for patients who have received maximal surgical resection to prohibit tumor recurrence. However, there is a non-therapeutic window between surgery and CCRT. A multiple function gold nanoparticle (GNP) presented in this study shows the merit of loco-regional treatment to complement current protocol of brain tumor therapy. The unique radioactive GNPs were prepared in a nuclear reactor without participation of reducing agents and radioactive precursors. For the concomitant radiation field of nuclear reactor, trivalent gold ions were reduced into GNP in which particular portion of natural gold atoms (^{197}Au) were simultaneously converted into radioactive ^{198}Au atoms through a one-pot/one-step reaction. The ^{198}Au -incorporated gold nanoparticle (^{198}Au -GNP) renders GNP extraordinary physical properties and provides multimodality to benefit patients bearing brain tumor. Firstly, the fluid ^{198}Au -GNP is feasible to be delivered through intracranial injection for interstitial radiotherapy. Furthermore, simultaneous emission of beta particles (E_{max} : 0.96 MeV) and gamma rays (412 keV) provide the niche for killing tumor cells and tracking ^{198}Au -GNP *in vivo*. The ^{198}Au -GNP also demonstrates striking property of X-ray contrast for computed tomography (CT), which is useful to demarcate the post-surgery tumor base for further treatments. We first report the application of ^{198}Au -GNP to effectively suppress orthotopic brain tumor using positron emission tomography (PET) imaging. Significant results give us an insight into harnessing nuclear energy for preparing multimodality GNP; and further, highlight its potential for brain tumor therapy.

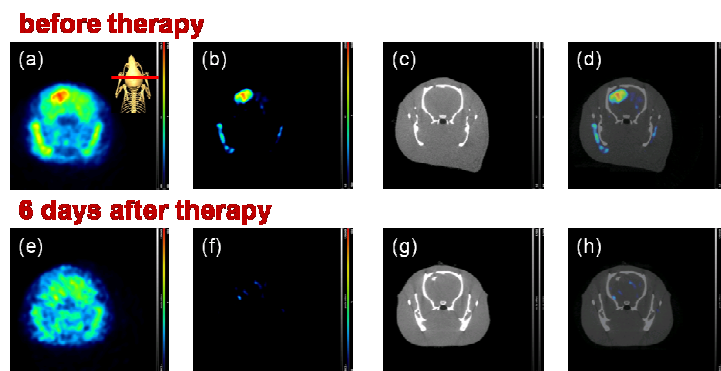


Figure 1

Keywords: radioactive gold nanoparticle (^{198}Au -GNP), interstitial radiotherapy, brain tumor, concurrent chemoradiotherapy (CCRT), positron emission tomography (PET) imaging



Cheng, Sheng-Shung Professor

{ PhD, Georgia Institute of Technology
 Prof. Of Department of Environmental
 Engineering, National Cheng Kung Univ.
 Tainan, 701-01, Taiwan, ROC
 { Tel: 886-6-2757575#65827
 { Fax: 886-6-2752790
 { E-mail: sscheng@mail.ncku.edu.tw

PRESENTATION: Integrating Study on High Effective Biofuel Energy Recovery with Multistage Biorefinery Process

Implementation of the circular economy for sustainable development of human being is a hot topic recently. Only when bio-based technologies producing food, fuel and chemicals were established can a circular economy be fulfilled. When the biomass is used for non-food products in the bio-based processes, concerns were raised for competing the land and resources with food crops. The biorefinery concept is proposed for producing food, fuel and valuable chemicals, which takes fully advantage of the biomass grows in the field. This research was sponsored by National Science Council in Taiwan from 2009 to 2012 and focused on biofuel production from non-food part of biomass converting by microbes. The research scope covered basic research on bioethanol and biobutanol production from cellulosic materials and the wholesome treatment process with biohydrogen and biomethane production. In order to improve the limiting step of hydrolyzing lipid and cellulosic materials, metagenomic study was conducted to clone innovative hydrolyzing enzymes. Eight cellulolytic sequences and five lipase sequences were obtained. Obtained sequences were ligated into pUC19 vector and further introduced to *E coli* strain MC1061 to produce cellulase and ligase. These hydrolyzing enzymes were secretory proteins so that can be produced without host cell emission. On the other hand, genetic engineering organisms were also evaluated to improve cellulolytic efficiency and butanol production ability by ordered gene assembly in *Bacillus subtilis*(OGAB) method. By OGAB techniques, functional gene sequences can be arranged in designed order and further controlled the expression level of each enzyme. Cellulosome forming genes from *Clostridium thermocellum* including CipA(Scaffoldin), CelK(exoglucanase), CelS(exoglucanase), CelR(endoglucanase), SdbA(cell-surface anchoring proteins), CelA(endoglucanase), XynC(xylanases), and XynZ(xylanases) were cloned and subsequently introduced in and translated by *Bacillus subtilis*. RT-QPCR and enzyme assays on endo-glucanase, exo-glucanase, and xylanase activities were also conducted and to monitor the cellulolytic ability of constructed host with different gene assemblages.

For the main stream to produce ethanol from cellulosic biomass, an innovative bioethanol reactor was designed and fed with straw or CMC as substrates. *Trichoderma reesei* and *Aspergillus niger* were co-immobilized on PU carrier to hydrolyze cellulosic materials and *Zymomonas mobilis* can further convert hydrolyzed saccharides into ethanol. However, as the growth stress increased through the fermentation, the ethanol concentration were only 1,051 mg/L and 577 mg/L with straw and CMC as substrate respectively. Because abundant organic residue left after the bioethanol process, post treatment for this fermented residues was also

proposed to recover more energy from the refractory residue. Because our scale in bio-alcohols was too small to provide enough biomass for this post treatment process. Accordingly, napiergrass was chosen as model substrate with kitchen waste as co-substrate in this post treatment process. In this integrated process, oxic leaching bed was presented for residue transformation in the 1st step. Refractory cellulosic material such as lignin can be converted by fungi to produce high concentration cellulolytic enzymes and mineralization of the organic residue simultaneously. We designed and upgraded the oxic leaching bed during the 3-year period to solve air block and substrate clog problems. Leachate hydraulic retention time from 0.08, 0.88, 8.95 days were tested and was found to be a crucial factor for cellulose degradation. 66% cellulose degradation efficiency can be achieved under 8.95 day leachate retention time. Diverse fungal species like *Rhizopus oryzae*, *Absidia corymbifera*, *Candida*, and *Fusarium* sp. were observed to be dominated in the oxic leaching bed. The 2nd and 3rd step was thermophilic biohydrogen and biomethane process to further convert the residue and recover hydrogen and methane gas. The result showed that though refractory biomass like oil & grease and cellulose cannot be converted in biohydrogen phase, the removal efficiency both achieved 90% in the biomethane phase. Total COD recovery can achieve 80% which was transformed into methane gas in this 2-stage process. The hydrogen/methane production rate achieved 1.2 L H₂/L-day and 1.2 L CH₄/L-day under the volumetric loading rate of 15 kg-COD/m³-d and 4 kg-COD/m³-d respectively. Pilot verification of 2-phased biohydrogen/methane process was conducted with 1 m³ biohydrogen tank and 4 m³ biomethane tank. Raw vegetable kitchen waste, which contained mainly the cellulosic biomass, and napiergrass were fed in this pilot plant. 0.73 L CH₄/L-day was obtained under VLR at 4 kg-COD/m³-d while little hydrogen accumulation in the biohydrogen phase due to hardware fault and biogas leakage. This project try to integrate the bio-alcohol production process with downstream residue utilizing process in a biorefinery way to get better use of non-food biomass. Further study in genomics and genetic modifying organism is necessary to bring the products' costs down and can show us a clue to the mechanism of hydrolysis of cellulosic biomass with greatly applicable potential.

Keywords: bioenergy, Biorefinery, OGAB method, Metagenomics, Multi-phased fermentation

References:

1. S. -S. Cheng*, M. -C. Chang, Y. -H. Wei, C. -C. Huang, W. -C. Kuo, Y. -C. Chao, "Integrating Study on High Effective Biofuel Energy Recovery with Multistage Biorefinery Process" The 9th International Workshop on Innovative Anaerobic Technologies, 12-13 June, 2013 Coex, Seoul, Korea.

O11

Low CO generation on tunable oxygen vacancies of non-noble metallic Cu/ZnO catalysts for partial oxidation of methanol reaction

Huang, Yuh-Jeen

Department of Biomedical Engineering and Environmental Sciences, National Tsing Hua University, Hsinchu, 30013, Taiwan



Abstract

A simple and very cheap method was created to modulate oxygen vacancies on the non-noble metallic CuZn-based catalysts surface. The identification and quantification of these oxygen vacancies on vZ (ZnO contain oxygen vacancies) and the catalytic activities of CvZ (Cu on ZnO contain oxygen vacancies, ca. 30 wt.% Cu and 70 wt.% Zn) during the partial oxidation of methanol (POM) reaction were studied. The vZ was calcined in nitrogen atmosphere at various temperatures (400°C, 450°C, 500°C and 550°C), and the catalytic activities of CvZ catalysts prepared in deposition precipitation (DP) and co-precipitation (CP) and CZr (Cu on ZrO, ca. 30 wt.% Cu and 70 wt.% Zr) catalysts were performed. Both CP-CvZ-450 and DP-CvZ-450 catalysts present excellent catalytic performance with 100% of C_{MeOH} , 5% of S_{H_2} at 250°C, and also maintained 70% of C_{MeOH} , 75% S_{H_2} at 150°C; especially, the S_{CO} was kept 2~5% at $T < 250^\circ C$ and outstanding stability for CP-CvZ-450 catalyst. These oxygen vacancies on the surface have the capability to adsorb POM reaction molecule which contain oxygen atoms at lower temperature as well as assist with the decomposition of intermediates species, and even can catalyze CO oxidation.

Keywords: tunable oxygen vacancies, non-noble metallic catalyst, POM

Neutron Radiography and Numerical Simulation on Mixing Behavior in a Tubular Flow Reactor for Supercritical Hydrothermal Synthesis of Nanoparticles



Seiichi Takami¹⁾, Ken-ichi Sugioka²⁾, Kyohei Ozawa²⁾,
Takao Tsukada²⁾, Tadafumi Adschiri³⁾, Katsumi Sugimoto⁴⁾,
Nobuyuki Takenaka⁴⁾, Yasushi Saito⁵⁾

1) IMRAM, Tohoku Univ., 2-1-1 Katahira, Aoba-ku, Sendai 980-8577, Japan

2) Dept. of Chemical Engineering, Tohoku Univ., 6-6-07 Aramaki, Aoba-ku, Sendai 980-8579, Japan

3) WPI-AIMR, Tohoku Univ., 2-1-1 Katahira, Aoba-ku, Sendai 980-8577, Japan

4) Dept. of Mechanical Engineering, Kobe Univ., 1-1 Rokkodai, Nada, Kobe 657-8501, Japan

5) RRI, Kyoto Univ., 2 Asashiro-Nishi, Kumatori-cho, Sennan-gun, Osaka 590-0494, Japan

Abstract

Hydrothermal synthesis at supercritical conditions is a useful method to produce metal oxide nanoparticles from metal salt aqueous solutions. The high reaction temperature and the properties of supercritical water as a reaction medium make the reaction rate quite fast and the solubility of dehydrated products extremely low. Consequently, a rapid increase in degree of supersaturation, very high nucleation rates and the mass production of nanoparticles can be achieved. In such a supercritical hydrothermal synthesis process, continuous flow reactors, in which two streams of metal salt aqueous solution and heated water are mixed at supercritical conditions, are commonly used. Rapid and uniform mixing of the streams is indispensable to produce metal oxide nanoparticles, and the size and its distributions of nanoparticles are strongly affected by how the reactants and supercritical water streams are mixed in the reactor. Therefore, it is important to understand the mixing behaviors of the streams, and the distributions of temperature and supersaturation in the reactor under supercritical conditions. However, the direct observation of the mixing behaviors in the reactor is difficult because the hydrothermal synthesis is performed at high pressure and high temperature in the reactor which is made of metal and consequently is opaque to visible light.

In this work, we have performed neutron radiography on a tubular flow reactor with a diameter of 1/8 inch which is commonly used for supercritical hydrothermal synthesis of metal oxide nanoparticles (J. Lu *et al.*, *ACS Appl. Mater. Interface*, **4** (2012) 351), and visualized the mixing behaviors of supercritical water and room-temperature water (corresponding to metal salt aqueous solution) and temperature distributions in the reactor. Here, hydrogen and water are opaque against neutrons, but heavier elements including iron, nickel, and chromium, i.e., the metal wall of the reactor, are more transparent. Moreover, since neutron attenuation coefficient of water depends on its density, the difference between the densities of supercritical water and room-temperature water in the reactor can be visualized by neutron radiography. In the experiments, a thermal neutron beam emitted from the B4 port of the KUR at the RRI, Kyoto University was used. The results demonstrated that the mixing behaviors, the distributions of water density and temperature in the reactor were clearly visualized by neutron radiography. In addition, numerical simulations have been carried out to investigate the flow patterns and temperature distributions in the reactor in detail using the commercial software FLUENT, and the numerical results could explain the experimental results obtained by neutron radiography well.

Keywords: neutron radiography, numerical simulation, temperature distributions, tubular flow reactor, supercritical hydrothermal synthesis

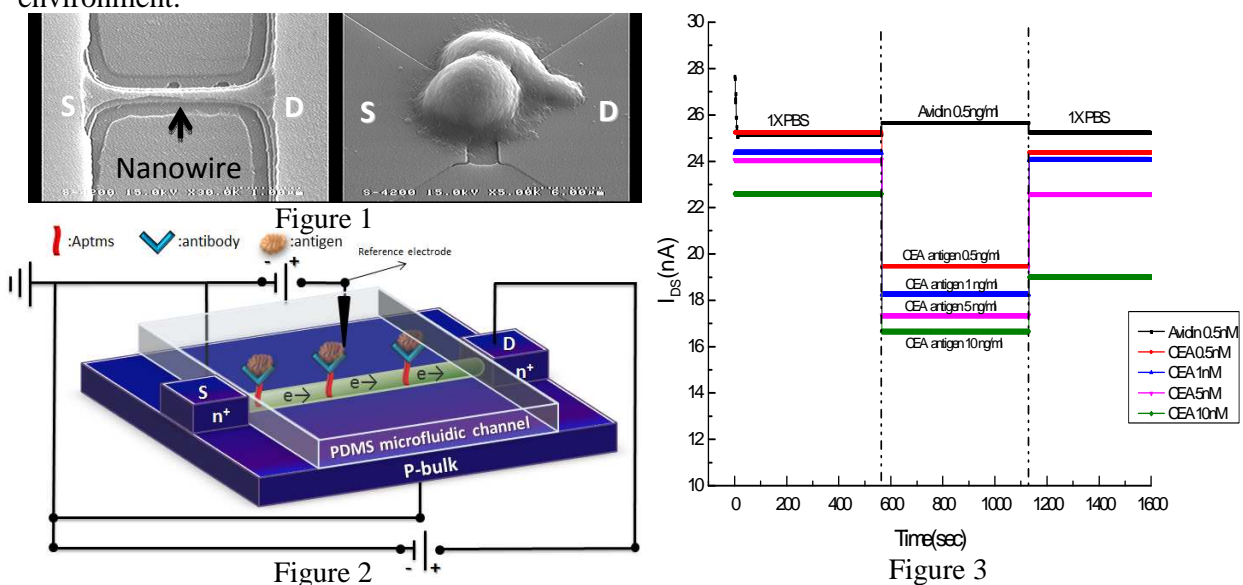


Hsu, Chun-Chun. MD

Master degree student
 Graduate Institute of Biomedical
 Engineering, Chung Hsing University,
 Taichung 40227, Taiwan
 Tel: +886-4-22840732 ext. 305
 Fax: +886-4-22852422
 E-mail: container0726@hotmail.com

PRESENTATION: Investigation on the Carcinoembryonic Antigen Using Functionalized Silicon Nanowire Field Effect Transistors

Silicon nanowire-based field-effect transistors (SiNW-FETs) have been demonstrated excellent sensitivity and stability after surface functionalization of nanowires. 3-aminopropyl trimethoxysilane (APTMS) self-assembled monolayer (SAM) were used to modify the surface of silicon NW-MOSFETs. After that, antibody against the carcinoembryonic antigen (CEA) was used to functionalize SiNWs. The functionalized NW-MOSFETs gave the ability to detect corresponding CEA in environment. In this study, the functionalized NW-MOSFETs was used to detect the known concentration of CEA (0.5, 1, 5, and 10 ng/ml, respectively) as well as the unknown concentration in the milieu of growth of human breast cancer cells, MCF-7. Scanning electron microscopy (SEM) was applied to characterize the structure of silicon NW and the relative position between cells and NW (Figure 1). Figure 2 shows our electrical measuring system integrated with microfluidic channel was used to dynamically sensing chemical molecules and analytes. Figure 3 shows increasing electrical responses of sensing higher corresponding CEA on CEA-antibody functionalized NW-MOSFETs. In addition, our functionalized NW-MOSFETs showed specificity in sensing CEA other than other molecule, such as avidin. Moreover, the increasing electrical responses were proportional to the population of MCF-7. Our results infer our setup has a potential to quantify the malicious cell population in dynamic environment.



Keywords: MOSFET; Surface Modification; CEA antigen; Cells on Chip

OS02

Study on Adsorption and Oxidation of Glycine Based on Surface-Enhanced ATR-IR Spectroscopy

Yu-Chen Chang, Li-Chia Chen, Hsien-Chang Chang

Department of Material Science and Engineering, National Cheng Kung University, Tainan, Taiwan



Abstract

There has been an intense interest in electrochemical biosensor with the development of biotechnology. However, most of these researches emphasize the performance of their device and still work by trial and error. There is a lack of fundamental information to support the strategies used for electrode design. Recently, an exciting development in the researching field called *Electrochemical Surface Science* has received much attention to provide *in-situ* measurement for electrode surface condition. Surface enhanced infrared spectroscopy in an attenuated total reflection configuration (ATR-SEIRAS) has been successfully used to a number of electrode reaction systems owing to its high signal sensitivity, simple surface selection rule, and negligible interference from bulk solution signals.

In this study, the electrochemical characteristic of glycine on Au surface was studied in a phosphate buffer solution by cyclic voltammetry experiments combined with ATR-SEIRAS. Infrared spectra confirm that an ordered orientation of glycinate anion adsorbs in a bridge-bonded configuration via two oxygen atoms of the carboxylate group with the C α -C bond perpendicular to the Au surface. The oxidation of glycine occurs at the potential (0.6 V) below the onset for surface oxidation, followed by another contribution in the Au surface-oxide region. The cleavage of C α -C bond is the first step in glycine oxidative decomposition to form a methylamine intermediate. The hydroxyl molecules on the Au surface would induce the dehydrogenation of the methylamine intermediate to form a cyanide, which can be detected only in the negative direction at E<0.4 V. At high potential, cyanide species is absent because of the oxidation to cyanate (OCN $^-$). Partial oxidation channel exists at high potential region leading to the production of NH $_4^+$ and OCN $^-$, called Wöhler synthesis, make the formation of urea. In spite of the probability of other products deriving from glycine oxidation, we believe that the reaction mechanism based on our SEIRA spectra is more reliable.

Keywords: Surface Enhanced Infrared Spectroscopy, Surface Science, Glycine, Adsorption, Oxidation, Wöhler synthesis

References:

1) Li-Chia Chen et al, *Electrochemistry Communications* (2013), doi:10.1016/j.elecom.2013.05.016

The Passive and Continuous Separation of Bioparticles based on Gray-scale Light-Induced Dielectrophoresis

Chun-Kai Chiang¹, I-Fang Cheng^{2*}, Hsien-Chang Chang^{1*}

¹Dept. of Biomedical Engineering, National Cheng Kung University

²National Nano Device Laboratory



Abstract

This article presents a gray-scale light-induced dielectrophoresis (GS-LIDEP) method that induces the lateral displacements normal to the through-flow for continuous and passive separation of microparticles (1). In general, DEP force only can affect the particles within very local areas due to the electric field is exponentially decayed by the distance away from the electrodes. Unlike with conventional LIDEP (2), a broad-ranged electrical field gradient can easily be created by GS pattern illumination, which induces DEP forces with two directions for continuous separation of particles to their specific sub-channels. *Candida albicans* were effectively guided to the specific outlet with the efficiency of 90% to increase the concentration of the sample below the flow rate of 0.6 $\mu\text{l}/\text{min}$. 2 and 10 μm polystyrene particles can also be passively and well separated using the multi-step GS pattern through positive and negative DEP forces, respectively, under an applied voltage of 36 V_{p-p} at the frequency of 10 kHz.

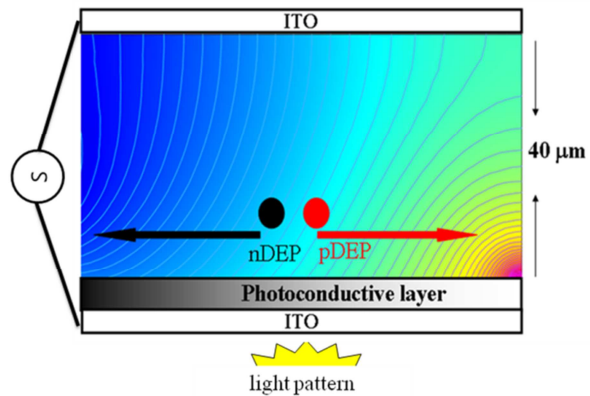


Fig.1 Illustration of GS-LIDEP.

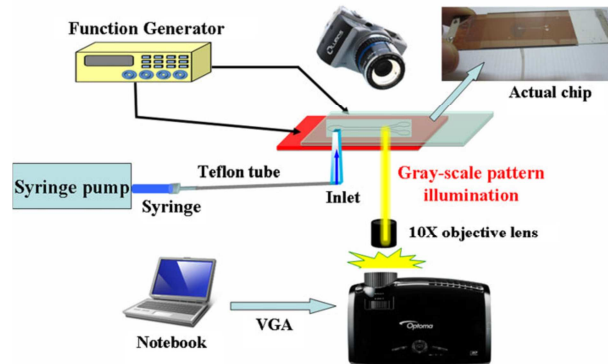


Fig.2 The LIDEP system configuration.

Keywords:

Gray-scale . Light-induced dielectrophoresis. Continuous and passive separation.

References:

- 1) Cheng IF, Froude VE, Zhu YX, Chang HC, Chang HC (2009), Lab Chip 9:3193–3201
- 2) Zhu X, Yi H, Ni Z (2010), Biomicrofluidics 4:013202

OS04

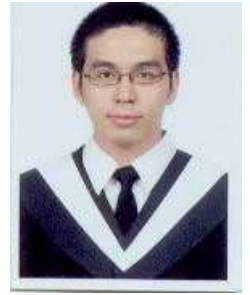
A label-free and sensitive method for rapid discrimination of cancer cell based on electrorotation (ROT) spectroscopy

Che-Hua Wu¹, I-Fang Chang², Wei-Lun Huang³, Wu-Chou Su³, Hsien-Chang Chang^{1*}

¹Department of Biomedical Engineering, National Cheng Kung University

²National Nano Device Laboratories, NDL

³Institute of Basic Medical Sciences, College of Medicine, National Cheng Kung University



Abstract

Conventional techniques for estimation of cancer cell use huge instruments, Western blot, and ELISA kits that are high cost and long time consuming. This study reports a label-free, rapid and sensitive approach that combines dielectrophoresis (DEP) and electrorotation (ROT) [1] for rapid discrimination of the transgenic lung cancer cells (AS2, S3C and S3D) [2]. DEP manipulate the cancer cells to detection zone, and the cells can be discriminated the difference of those transgenic lung cancer cells in a three-dimensional (3D) rotating field. As shown in the measured ROT spectra (Fig. 2), the frequency of the maximum rotation is 100 kHz. The data show that cancer cells with different treatments can be determined by their induced rotation speeds when applying 9 V_{pp} at an optimal frequency of 100 kHz, . The S3C cells transfected with constitutively-activated Stat3 showed a higher rotating speed than the parental AS2 cell. In contrast, the S3D cells transfected with dominant-negative Stat3 showed a lower rotating speed than the AS2 cell. The results taken by ROT are very agreement with the conventional results taken by Western blot.

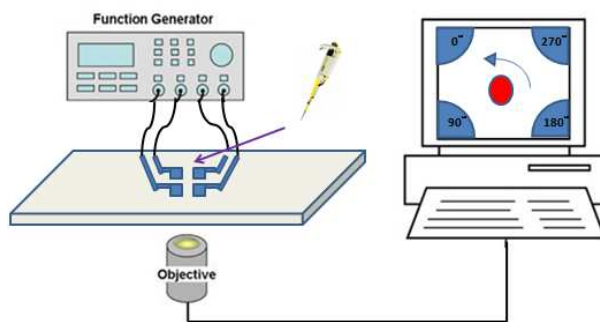


Fig. 1 Detection platform

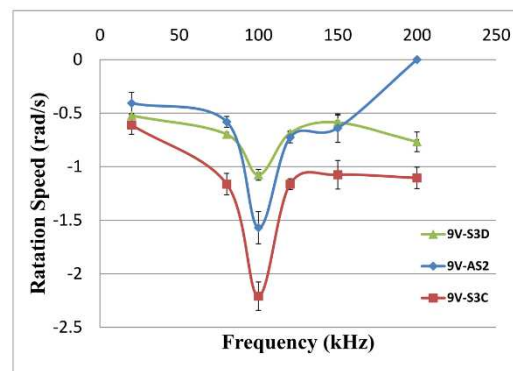


Fig. 2 The ROT result of the transfected lung cancer cells by applied 9 V_{pp} AC condition.

Keywords: electrorotation; dielectrophoresis; lung cancer cell

- 1) Massimo Cristofanilli, Giovanni De Gasperis, Lisha Zhang, et al, February 2002, Clin Cancer Res, Vol. 8, 615–619.
- 2) Hua Yu and Richard Jove, February 2004, NATURE REVIEWS, Vol. 4, 97–105.

Graphene-Enzyme-Immobilized Screen-Printed Electrode for Histamine detection in Food

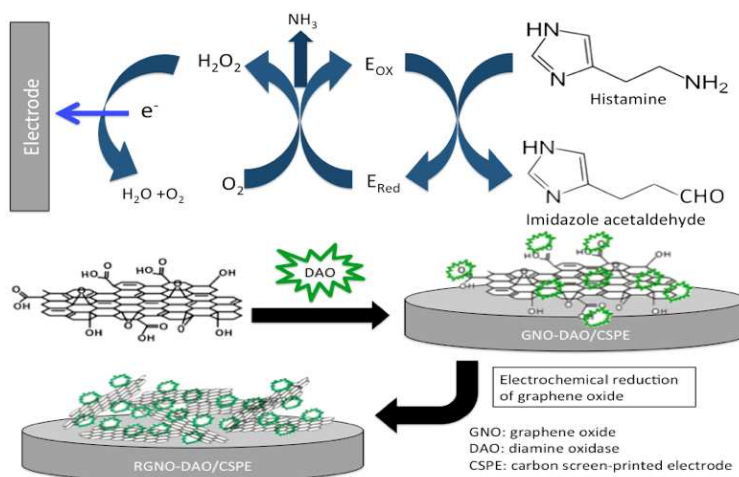
Cheng-Hui Chen¹, Li-Chia Chen¹, Hsien-Chang Chang¹

¹Department of Biomedical Engineering, National Cheng Kung
University, Tainan, Taiwan



Abstract

Histamine is one of the biogenic amines that would cause acute allergy-alike food poisoning and may cause symptoms such as headache, stomach ache, cramps, vomiting, hypertension, flushing, and so on. Foods containing more than 500 ppm histamine are considered as a health hazard to human body. Standard method for food histamine detection is high performance liquid chromatography (HPLC), which is a sensitive but expensive, not portable and not easy-to-use device. This study is aim to develop an amperometric enzyme-based biosensor to build a simple, reliable, low cost and disposable device for histamine detection in food samples. Graphene is a cheap nanomaterial with good electrical and mechanical properties that can enhance electron transfer and improve enzyme stability. Diamine oxidase (DAO) was mixed with graphene oxide and then immobilized on the screen-printed electrode. After immobilization, graphene oxide was electrochemically reduced into graphene for histamine sample detection. Optimal parameters of pH value, graphene oxide/DAO mixing ratio, reduction condition of graphene oxide, and detection voltage were measured and applied to the following measurements of histamine samples.



Keywords: Graphene, screen-printed electrode, food histamine detection

- 1) B. Unnikrishnan, S. Palanisamy, S. M. Chen, *Biosens. Bioelectron.*, **2013**, 39: 70-75.
- 2) C. M. Keow, F. A. Bakar, A. B. Salleh, L. Y. Heng, R. Wagiran, S. Siddiquee, *Int. J. Electrochem. Sci.*, **2012**, 7: 4702- 4715.

Mesenchymal Stem Cells as Cellular Vehicles for Brain Tumor-Targeted Delivery of Diagnostic and Therapeutic Agents

Yuan-Chung Tsai, Wen-Chia Huang, Hsin-Cheng Chiu

Department of Biomedical Engineering and Environmental Sciences,
National Tsing Hua University, Hsinchu, Taiwan



Abstract

Glioblastoma multiforme (GBM) is the most common type of primary brain tumor in humans. Despite advances in interventional techniques, the median survival duration of patients with GBM still is less than 15 months because of the limitation of transporting therapeutic agents across blood-brain barrier (BBB) [1]. To achieve effective transport of therapeutic agents to malignant brain tumor for improving the therapeutic efficacy, various active brain-targeting strategies to cross BBB have been extensively proposed and investigated.

In this study, Mesenchymal stem cells (MSCs) capable of migrating toward brain tumors were utilized as cellular vehicles to delivery Paclitaxel (PTX)/superparamagnetic iron oxide nanoparticle (SPION)-loaded poly(lactic-co-glycolic acid) (PLGA)-based nanohybrids to brain tumors [2]. The preliminary result showed that the drug release of PTX/SPION-loaded nanohybrids was well regulated by remote-controlled alternating magnetic field (**Figure 1**). As a result, it is expected that the efficient liberation of PTX from payload-containing MSCs within brain tumors could be achieved by external stimulus to improve the therapeutic outcomes of brain tumors.

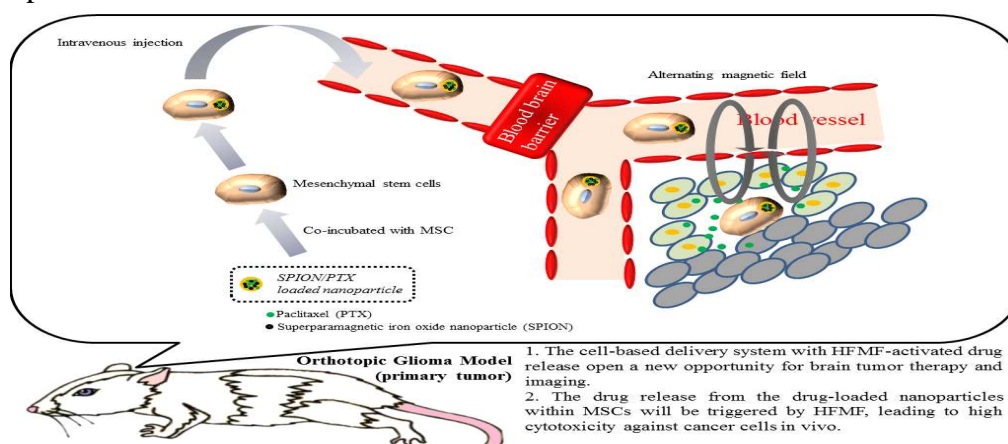


Figure 1. Illustration of HFMF-triggered PTX release from the nanoparticles.

Keywords: glioblastoma, nanoparticle, drug delivery

1) Juillerat-Jeanneret, L. et al., Drug Discov Today. 2008, Dec; 13: 1099-106.

2) Moniri MR et al., Cancer Gene Ther. 2012, Sep; 19: 652-8



Chia-Wei Lin -----

{ Bachelor degree student
 Department of Environmental
 Engineering, National Cheng Kung
 University
 Tainan, 701, Taiwan
 { Tel: 06-2757575#65831
 { Fax: 06-2752790
 E-mail: f54981715@gmail.com

PRESENTATION: Atmospheric Dry and Wet Depositions of Mercury

Mercury (Hg) is one of the major toxic heavy metal found in various media in the Environment. Mercury can exist in three oxidation states: Hg^0 (metallic), Hg^{2+} (mercurous), and Hg_2^{+2} (mercuric-Hg(II)). This study focused on the atmospheric Mercury concentration, dry and wet depositions, and the Hg distribution around Chiayi County. There were eight sampling sites, standing for upwind and downwind of both industrial and human activities. The sample was collected by PS-1 high volume sampler from each site, pretreated by digestion, and further analyzed with CVAFS. Results shows that the total Mercury deposition flux of each month ranged 229-942 $\text{ng/m}^2 \cdot \text{month}$ in Chiayi County. The seasonal variation of total Hg deposition flux was not significant, resulted from pooling the dry deposition and wet scavenging together. Thus, about 70% of the variance of mercury wet deposition in Taiwan is explained by precipitation amount. This is probably because mercury wet deposition is dominated by the scavenging of reactive gaseous mercury (RGM) by precipitation via oxidation of gaseous elemental mercury (Hg^0) in the gas and aqueous phases.

References:

- 1) Masahiro Sakata, Kazuo Asakura (2007) Atmospheric Environment 41, 1669–1680
- 2) Christian Seigneur, Kristen Lohman, Krish Vijayaraghavan, Run-Lie Shia (2003) Environmental Pollution 123, 365–373
- 3) Noelle E. Selin, Daniel J. Jacob, Rokjin J. Park, Robert M. Yantosca, Sarah Strode, Lyatt Jaegle, and Daniel Jaffe (2007) Journal of Geophysical Research 112, 450-486

Keywords:

Mercury, dry deposition, wet deposition

OS08

Studying the effect of blood viscosity on cardiovascular diseases using μ PIV Diffusometry

Chia-Hao Hsu^{1, 1}, Dar-Bin Shieh², Han-Sheng Chuang^{1,3}

¹ Department of Biomedical Engineering, National Cheng Kung University, Taiwan

² Biochemistry and Molecular Biology, National Cheng Kung University, Taiwan

³ Medical Device Innovation Center, National Cheng Kung University, Taiwan



Blood viscosity can provide plenty of pathological information, such as hypertension, multiple myeloma, diabetes, and so forth. Conventionally, capillary viscometers and rotary viscometers are most widely used for viscosity measurements.¹ However, capillary viscometers are easy to incur human errors while rotary viscometers are limited to working ranges causing inconvenience in cross-scale measurements. In addition, both are sample consuming and wasteful. To solve the problems, this study developed a micro-volume viscosity measurement technique based on the μ PIV diffusometry.

Brownian motion is known as random movement of particles suspended in a fluid. The relationship between the random movement and viscosity is expressed in the Stoke-Einstein equation. The whole measurement system (as shown in Fig. 1) comprised an epi-fluorescent microscope, a microchip, a high-speed camera, and a computer. Fluorescent polystyrene particles ($d_p=1 \mu\text{m}$, Ex:541/Em:611, Thermo Fisher) were filled in polydimethylsiloxane wells (PDMS, Sylgar 184, Ellsworth Adhesives), 2 mm in diameter and 40 μm in depth, and covered with a glass slide to achieve a stationary environment. A PIV analysis software (EDPIV) was used to analyze the Brownian motion. The viscosity could be expressed by the relationship of correlation peak width versus time (Fig. 2). Typically, a steep slope implies high viscosity while a mild slope links to low viscosity. A correction factor was employed to mitigate deviations. The factor was obtained by comparing the measurement with the reference value. A general calibration curve was eventually obtained from three glycerol solutions (0%, 65%, and 91.5%), which covered nearly three orders of magnitude (Fig. 3). This technique features a measurement volume of less than 1 μL and a broad range of viscosity measurement.

In the preliminary study, the viscosity of Bovine Serum Albumin (BSA) was investigated. The test sample was 10 fold diluted from an original concentration of approximately 50 mg/mL. A comparison of the measurement and the prior research is shown in Fig. 4. The experimental result shows a good agreement with the actual

value², which bolsters the practicability of the technique. to the follow-up work will be focused on measuring the blood viscosity of guinea pigs separately fed with a high cholesterol diet and a normal diet. Subsequent diseases resulting from the difference of blood viscosity will be further investigated.

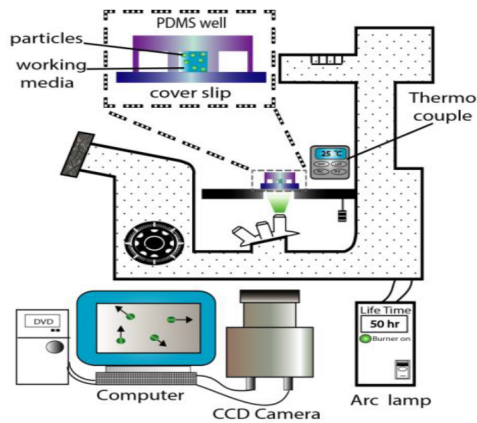


Fig1. The schematic diagram of the experimental setup.

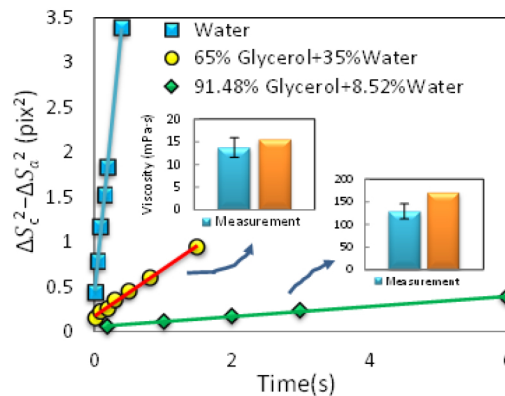


Fig2. Relationship between the peak width and the time interval (n = 5). A high slope implies low viscosity and vice versa.

References :

- 1 Steven A. Bogen, and Robert Rosencranz, 'Clinical Laboratory Measurement of Serum, Plasma, and Blood Viscosity', *Pathology Patterns Reviews*, 125 (2006), S78-S86.
- 2 S. Yadav, S. J. Shire, and D. S. Kalonia, 'Viscosity Analysis of High Concentration Bovine Serum Albumin Aqueous Solutions', *Pharm Res*, 28 (2011), 1973-83.

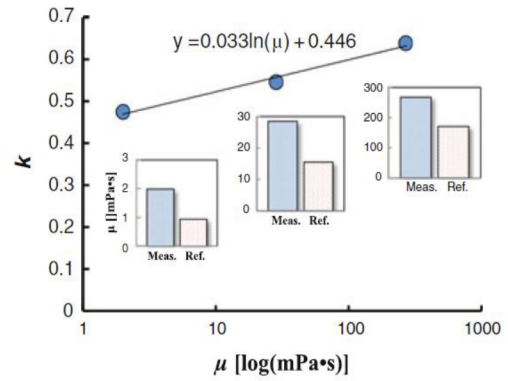


Fig 3. A calibration curve derived from the correction factors at three viscosity values of glycerol.

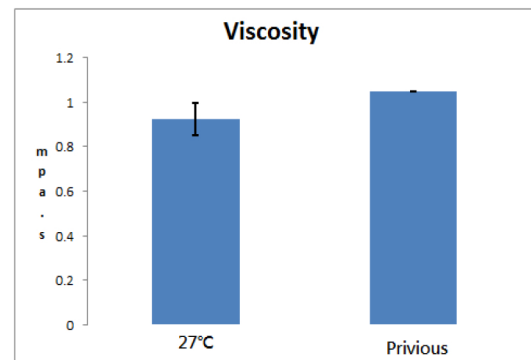


Fig 4 : A comparison of the measured viscosity of BSA (27) and the predicted value.

Thermal Decomposition of Printed-Circuit Boards Based on Thermoset Resin

Shogo Kumagai^{1,2}, Guido Grause¹, Tomohito Kameda¹ and
Toshiaki Yoshioka¹

¹Graduate School of Environmental Studies, Tohoku University

²Research Fellow of the Japan Society for the Promotion of Science



Abstract

Plastics are widely used in our daily life and they are often combined with metals when used for electronic products. Thermosetting resins are often used as metal carrier materials, and these metals are often of economic interest. However, for the sake of environmental conservation, the organic matrix should be considered as a resource as well. Pyrolysis is one of the methods of conversion of plastics into organic feedstock, allowing the simultaneous removal of inorganic matter. In this work, the degradation behavior of paper-laminated printed circuit boards (PCB) based on phenol and epoxy resins was investigated by thermogravimetric analysis coupled with mass spectrometry (TG-MS). The resins were decomposed using a fixed-bed reactor and both organic and inorganic products were recovered.

The obtained TG curves and selected MS spectra are summarized in Fig. 1. Multistep degradation of PCB was observed as a result of the simultaneous decomposition of paper, resin, and flame retardant (tetrabromo bisphenol A (TBBPA)). Bromophenols were produced by both the decomposition of TBBPA and the reaction between phenol (derived from PCB) and HBr (derived from TBBPA). The obtained oil mainly consisted in phenol and phenol derivatives, which also contained brominated compounds. However, bromine content in the oil was drastically decreased in the calcium hydroxide ($\text{Ca}(\text{OH})_2$) since the produced HBr was absorbed to $\text{Ca}(\text{OH})_2$. Furthermore, metal recovery rate was also improved in the presence of $\text{Ca}(\text{OH})_2$ due to the reduction of metal volatilization via metal bromination reaction.

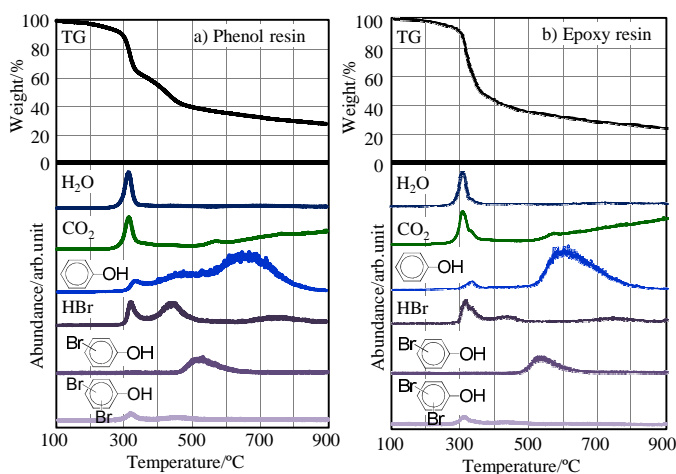


Fig.1 TG curves and extracted ion chromatograms obtained by TG-MS analysis of PCB based on a) Phenol resin and b) Epoxy resin.

Keywords: plastics, feedstock recycling, printed-circuit board, pyrolysis.

OS10

The Study of Hydrogen Generation from Hydrolysis of Ammonia Borane in The Presence of Ni-Co/r-GO Catalysts

Chang-Chen Chou¹, Bing-Hung Chen¹

¹Department of Chemical Engineering, National Cheng Kung University,
Tainan 70101, Taiwan



Abstract

Recently, the energy consumption and the emission of CO₂ increase which causes global warming and climate change in the worldwide. Research of renewable energy attract more and more attention. Among green energies, hydrogen is considered as one of promising candidates because the main product is non-toxic water. Proton exchange membrane fuel cells (PEMFCs) are widely studied due to its lower operating temperature, higher efficiency, higher power density, more rapid startup and so on. Therefore, the supplement of hydrogen to PEMFCs need to be considered.

Among several hydrogen storage methods, chemical hydrides have higher content of hydrogen. Hydrogen can be released from hydrolysis reaction of chemical hydrides in the presence of catalysts. Ammonia borane (NH₃BH₃) is a prospective compounds due to its non-flammable, rarely toxic and higher hydrogen content (19.6 wt%).

Graphene oxide (GO), one of carbon derivative, which has high surface area (theoretically 2600 m² g⁻¹) was selected to be the support for the catalysts. Electroless deposition method was utilized to synthesize Ni-Co particles on reduced graphene oxide (denoted Ni-Co/r-GO). Ni-Co/r-GO catalysts were then sent for instrument analysis: XRD (**Figure 1**), TEM (**Figure 2**), SEM, EDS, VSM and ICP-OES.

In this study, NH₃BH₃ and Ni-Co/r-GO catalysts were pulverized by using high energy ball milling machine. Adequate water was added to initiate the hydrolysis reaction of AB composite by a syringe. Hydrogen profiles were recorded by a mass flow meter (MFM) and temperature profiles could be observed by a thermocouple at the same time. Various parameters such as the amount of water dosage, loading of catalysts and injection rate will be discussed.

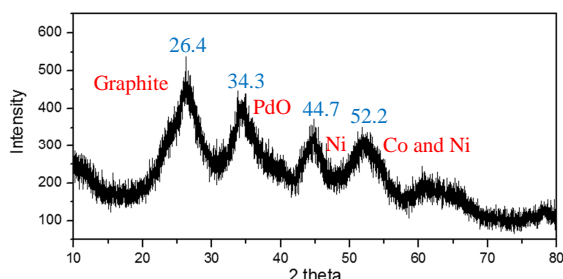


Figure 1. XRD pattern of Ni-Co /r-GO

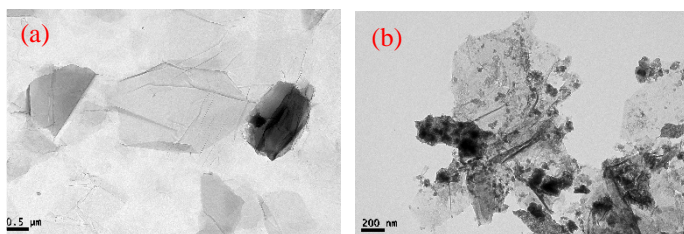


Figure 2. TEM images of (a) GO (b) Ni-Co/r-GO catalysts

Keywords: Electroless deposition, graphene oxide, ammonia borane, hydrolysis reaction.

1) Chou C.C. *et al.*, *Int. J. Hydrogen Energy*, **37**, 15681-15690(2012)

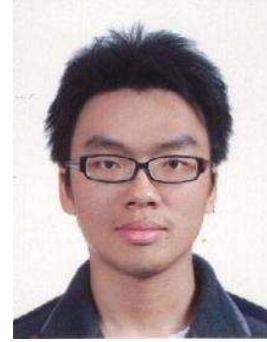
2) Wang Y. *et al.*, *Appl. Surf. Sci.*, **258**,8603-8608(2012)

OS11

Simultaneous nitrification/anammox in a partial aeration biofilm reactor for treating secondary effluent from a petrochemical industrial park

Han-Lin Lin, Hsiang-Wei Tsao, Yu-Wen Huang, Keng-Hao Yang, Ya-Fei Yang, and Sheng-Shung Cheng

Department of Environmental Engineering, National Cheng Kung University



Abstract

This study investigated the removal efficiency of simultaneous nitrification/anammox process in single reactor for treating secondary effluent from a petrochemical industrial park. A partial aeration biofilm reactor (10 L) was run to study the competition for nitrite between nitrite oxidizing bacteria (NOB) and anoxic ammonium oxidizing bacteria (anammox). A separating plate was inserted into the reactor, thus subdividing the reactor into the aerobic and anoxic compartment. Over 8 months of operating data showed that the dissolved oxygen (DO) in the aerobic compartment was a key factor affecting the nitrogen removal of the whole reactor. The optimal nitrogen removal rate (NRR) and efficiency (NRE) were $0.2 \text{ kg N L}^{-1} \text{ d}^{-1}$ and 70% with DO controlled at $1.0 \pm 0.2 \text{ mg O}_2 \text{ L}^{-1}$ in the aerobic compartment. The residual DO in the anoxic compartment was only $0.2 \pm 0.1 \text{ mg O}_2 \text{ L}^{-1}$ under this operating condition. The cluster of ANAMMOX bacteria, *Kuenenia stuttgartiensis*, was identified based on the 16S rRNA clone library.

Keywords: anammox, biofilm, carrier, single-stage reactor, petrochemical industries

- 1) Strous M. *et al.*, *Appl. Microbiol. Biotechnol.* **50**(5), 589-96. (1998)
- 2) van der Star W. R. L *et al.*, *Water Res.* **41**(18), 4149-63. (2007)

**Lin, Yi-Ting**

Ph.D Student
Department of Electronic Engineering,
Chang Gung University Tao-Yuan 333,
Taiwan
Tel: 886-3-2118800 ext 5786
Cell phone: 886-911-972-288
E-mail: linyiting0612@gmail.com

Title: Immobilization of biomolecule on field effect device (FED) by new amino group functionalization

In this study, we demonstrated ammonia (NH_3) plasma treatment to form functional amino groups on the various sensing membrane for application of biomolecule detection. NH_3 plasma treatment is compatible with standard CMOS technique and its stability and reproducibility can be better than chemical APTES silanization for SAM modification. As shown in Fig. 1, the output voltage of the EIS structure with plasma treatment is similar to the response of the samples with APTES silanization, where the urea sensitivity are 105 and 117 mV/p C_{urea} , respectively. The surface functionalization for urease immobilization is successfully replaced by NH_3 plasma treatment. Fig. 2 shows the urea responses of ITO/PET films with NH_3 plasma treatment at 100 W for 3, 6, and 9 min were 21.2, 49.7 and 62.4 mV/p C_{urea} . The higher output signal was observed in the samples of longer time in plasma treatment. It suggests that the longer time of plasma treatment is beneficial for nitrogen incorporation into ITO film as amine binding group. Fig. 3(a) and Fig. 3(b) show the experimental results with APTES silanization and NH_3 plasma condition that delta voltage increased with the group with relative wild type DNA concentration in the range of $10^{-6} \sim 10^{-9}$ M. Samples with NH_3 plasma treatment, the stability and reproducibility are much better than chemical silianization process, which is suitable for biomedical sensing device with high confidence level in clinical diagnosis by reducing false detection.

An inorganic method of surface modification, NH_3 plasma treatment is successfully developed on application of biomedical detection to create the functional group on the surface for biomolecule immobilization in covalent bonding.

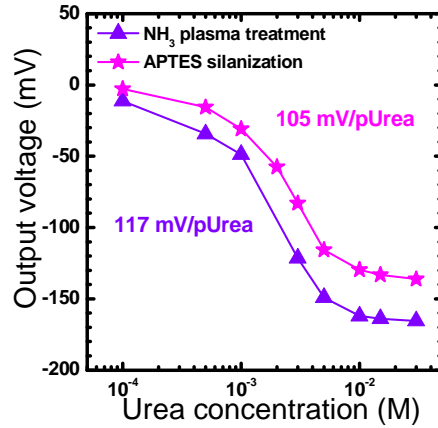


Fig. 3. The urea detection of EIS structure with chemical silanization and NH_3 plasma treatment.

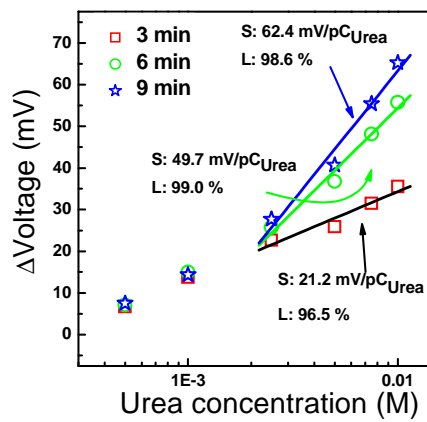


Fig. 2. Sensing responses by output voltage in different urea concentration of urea-enzyme-immobilized EGFET with ITO/PET electrode with different NH_3 plasma condition.

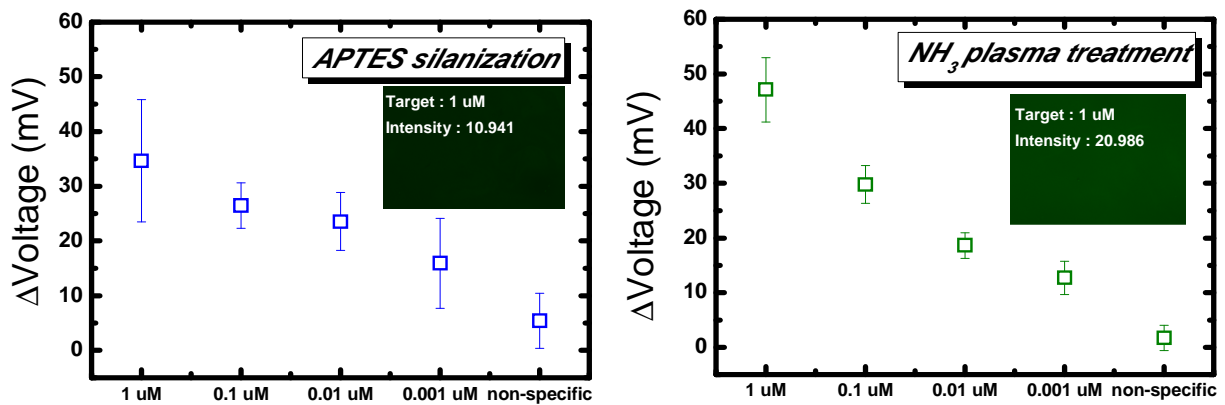


Fig.4. Electrical response with the logarithm of wild type DNA concentration in the range of $10^{-6} \sim 10^{-9}$ M for (a) the EIS structure with APTES silanization (b) the EIS structures with NH_3 plasma treatment.

OS14

Study of lipofuscin accumulation in *C. elegans* and heat shock treatments based on an optoelectric device

Hsiang-Yu Chen¹, Chang-Shi Chen², Wen-Tai Chiu¹, Han-Sheng Chuang^{1,3}

¹ Department of Biomedical Engineering, National Cheng Kung University, Taiwan

² Biochemistry and Molecular Biology, National Cheng Kung University, Taiwan

³ Medical Device Innovation Center, National Cheng Kung University, Taiwan



Abstract

C. elegans has been widely used as a model organism for fundamental biological research due to its potential in developmental biology, genetics and neuroscience. Compared with other model animals, the advantages of *C. elegans* include its small size (1 mm), short lifespan (about 3 weeks), fully sequence genome, simple neural network (302 neurons), ease of cultivation, and more than 60% genetic similarity with humans. Therefore, the study of *C. elegans* can bring great contribution to the preliminary understanding of numerous human diseases.

Lipofuscin (LF) is a membrane-bound cellular waste. It can be neither degraded nor ejected from the cell. LF is mainly composed of lipids, unfolded /damaged proteins and a small fraction of metals. In the human body, it can be found in the liver, kidney, heart muscle, adrenal, nerve cells and ganglion cells. The prior research has proven LF to be an age biomarker, because it significantly accumulates with age. Due to the toxicity of LF to cells, high concentration LF is very likely to result in degenerative diseases.

In this study, an addressable heating technique based on an optoelectric device was used to induce the heat shock proteins to scavenge the LF granules. The setup is shown in Fig. 1. Heat shock response is a protective mechanism typically induced by heat that helps animals to survive in harsh environments. For instance, small heat shock protein(HSP) family is collecting protein“garbage”and acting as“dustmen”of cells while the HSP-60 and HSP-70 family are assisting in protein folding and re-folding and so on. We reason the induction of HSPs may promote the treatments of the degenerative diseases resulting from LF, and therefore extend the lifespan of *C. elegans*. A preliminary study shows that LF accumulation in the worms underwent an optoelectric treatment significantly decreases (Fig. 2). For investigating the optimal conditions for inducing the heat shock response, the mutant strains, SJ4005 (*HSP-4::GFP*) and CL2070 (*HSP-16::GFP*), were treated with the optoelectric effect for 10 s, 20 s, 60 s and 120 s. The results show that only 10 s optoelectric treatment is adequate to induce equivalent heat shock response in a 30 min heat bath at 33°C (Fig. 3). Meanwhile, the maximum of HSP expression appears in head for HSP-16 but in tail for HSP-4 (Fig. 4).

To observe the effects of optoelectric treatment on the LF accumulation in *C. elegans*, treatments were applied to N2 strain worms starting at stage egg, L1, L2, L3, L4, and adult day 1, respectively. The LF fluorescence of all cases was measured at adult day 5 and day 10. In addition, lifespan, bag of worm and progeny were investigated to show the physiological variations. The results will provide valuable information treating and preventing degenerative diseases in the higher animals.

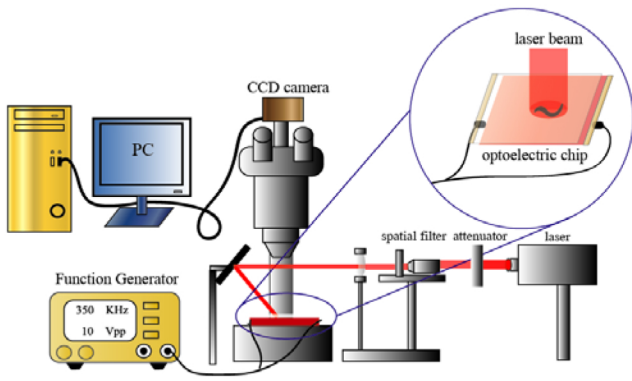


Fig. 1. Schematic of the experimental setup. The closeup shows the detailed configuration of the optoelectric device.

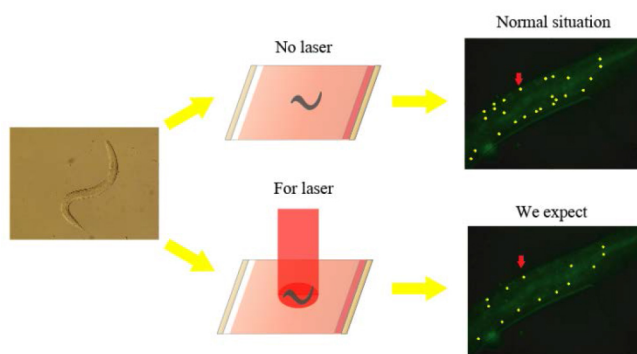


Fig. 2. Illustration of the LF accumulation in *C. elegans* with (bottom) and without (top) optoelectric treatment. The arrow indicates the LF granules.

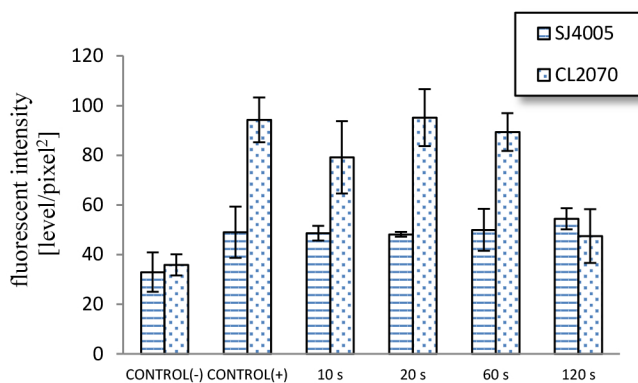


Fig. 3. Fluorescent intensity of LF on mutants CL2070 and SJ4005 subjected to different treatment conditions. Control (+) and control (-) are worms underwent and without heat bath, respectively. 10 s, 20 s, 60 s, and 120 s are laser exposure time intervals.

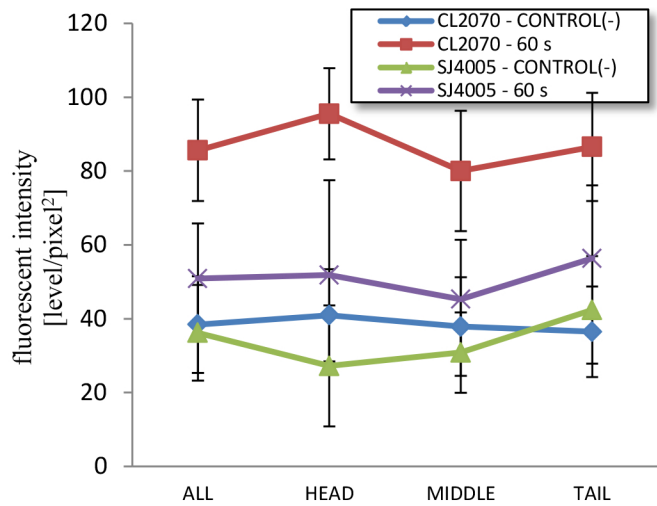


Fig. 4. Fluorescent intensity of LF captured from the head, middle, tail, and whole body of the mutant CL2070 (n=10) and SJ4005 (n=10). ◆ denotes CL2070 – CONTROL (-) treatment, ■ denotes CL2070 – 60 s, ▲ denotes SJ4005 – CONTROL (-) and × denotes SJ4005 – 60 s.

REFERENCE

1. Anders Olsen, Maithili C. Vantipalli, Gordon J. Lithgow (2006), Lifespan extension of *Caenorhabditis elegans* following repeated mild hormetic heat treatments. *Biogerontology* 7: 221–230
2. Alexei Terman and Ulf T. Brunk (1998), Lipofuscin: Mechanisms of formation and increase with age. *APMIS* 106: 265-276.

Development of 2nd Generation Bio-LSI System for Real Time Bio-imaging

Masanori Nakano¹, Kumi Y. Inoue², Reyushi Kubo¹,
Ryota Kunikata³, Atsushi Suda³, Masaaki Matsudaira²,
Kosuke Ino¹, Hitoshi Shiku¹, and Tomokazu Matsue^{1,2,4}

¹Graduate School of Environmental Study, ²Micro Systems Integration Center (μ SIC), ³Japan Aviation Electronics Industry, Ltd., ⁴The World Premier International Research Center Advanced Institute for Materials Research (WPI-AIMR); Tohoku University, Sendai, Japan



Abstract

We have developed Bio-LSI systems for highly sensitive and real-time amperometric bio-imaging platform with 400 sensor electrodes^{1,2}). In this study, we have estimated the improved functions of the 2nd generation Bio-LSI (Fig. 1). First, we checked the light shield effect of a top metal placed on a CMOS circuit to reduce a noise derived from a photocurrent. Only 800 fA of the photocurrent was produced even under the high intense (35000 lx) microscope light (below 1/100 of 1st generation). Next, we demonstrated a mode select function, which enables arbitrarily settings of the operation mode of the 400 electrodes individually from 4

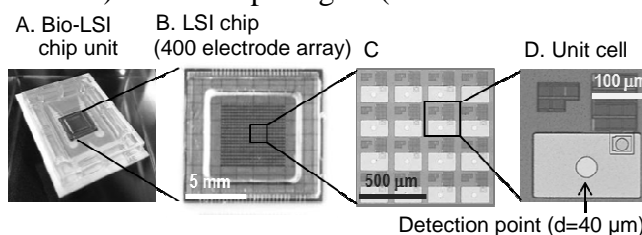


Fig. 1 Photographs of the 2nd generation Bio-LSI chip.

modes; off, electrometer, V1 or V2. First, we utilized this function to image the behaviour of 2 mM ferrocenemethanol (FcOH). The potential of the selected electrodes were stepped to +0.5 V, while the remaining electrodes were kept 0.0 V. The colour map indicating the current of 400 electrodes showed characters of “Bio LSI 2G” by oxidation of FcOH (Fig. 2). Next, we demonstrated the selective modification of electrodes by osmiumpolyvinylpyridine gel polymer containing horseradish peroxidase (Os-HRP). We successfully electrodeposited the Os-HRP on selected electrodes by cycling of the electrode potential from -0.4 V to 1.0 V. The Os-HRP deposited electrodes showed obvious chronoamperometric responses for successive addition of 10 μ M hydrogen peroxide (final concentration), while the non-deposited electrodes did not show any significant responses.

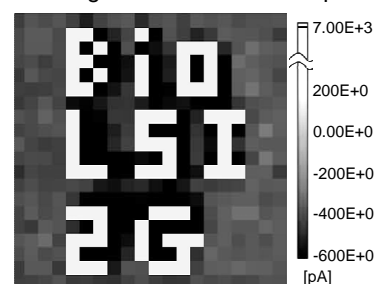


Fig. 2 Color map of the 400 electrodes obtained from the partial potential step in 2 mM FcOH (after 50 sec from the step). The electrodes indicating white color were stepped +0.5 V, while the remaining electrodes shown in gray were kept 0.0 V.

Keywords: electrochemistry, bio-imaging, multiassay

1) K.Y.Inoue *et al.*, *LabChip*, **12**,3481 (2012) 2) M.Şen *et al.*, *Biosens.Bioelectron.*, **18**,12(2013)

Development of nano-Pt electrode toward the mapping of dopamine release sites

X. Wang¹, Y. Takahashi², Y. Matsumae¹, K. Ino¹, H. Shiku¹, T. Matsue^{1,2}

¹Graduate School of Environmental Studies, ²WPI-AIMR; Tohoku University, Sendai, Japan



Abstract

Communication between cells is generally mediated by the neurotransmitter. And the release sites of neurotransmitters on cell membrane are not uniformly distributed. For example, differentiated PC12 cells (a pheochromocytoma of the rat adrenal medulla) are observed that the distribution of dopamine release sites is distinct from cell body to varicosity¹. To better understand this phenomenon, we plan to map release sites of differentiated PC12 cells and expect to make contribution to elucidation of neurotransmitter release mechanism. As the response of dopamine depend on the distance of the cell surface and the electrode tip in electrochemical detection², in this work, we developed a new type of nano-Pt electrode and use it to research on distance dependence of dopamine detection.

We used electroplating to form a platinum layer on the surface of the nano-carbon electrode (Fig(a)). Firstly, quartz tube (1.2 mm O.D; 0.90 mm I.D) was pulled by using a laser puller. Then, connect the rear of quartz tube with silicon tube and fill them with butane gas. Next, put the tip of the quartz tube into another quartz tube filling with nitrogen gas and bake carbon at the tip of quartz tube by heat under nitrogen atmosphere. At last, form a platinum layer out the carbon at the tip of quartz tube by electroplating in 2 mM H₂PtCl₆.

We detected dopamine with amperometric measurements under different distance from PC12 cell surface. Firstly, position electrode tip near the cell surface based on the decrease of oxygen reduction current. Next, induce cell to release dopamine by chemical or mechanical stimulation. Then, oxidize dopamine at the voltage of +650 mV under different distance. Fig (b) shows that the spikes of dopamine oxidation become less as the distance increases. Meantime, the value of i_{max} become smaller and the value of $t_{1/2}$ (half-height) become bigger. Furthermore, there is little spike at a certain distance (9 μ m at this data). It maybe because (1)With the diffusion of dopamine, the lower density of dopamine result smaller i_{max} and bigger $t_{1/2}$. (2)At a certain distance, the value of i_{max} become smaller than the noise of current so that it can't be detected.

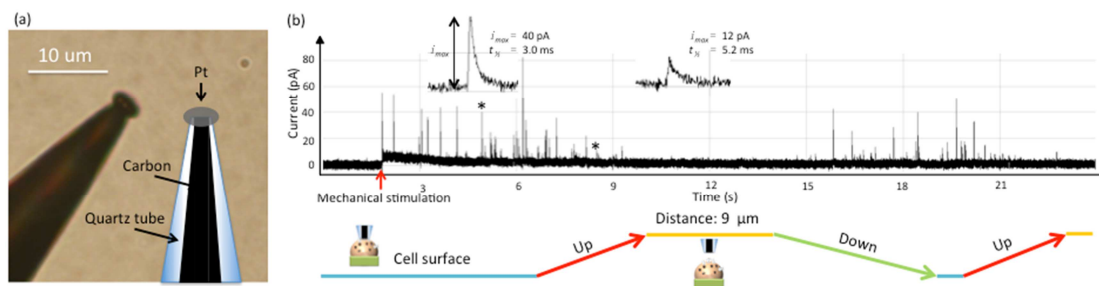


Figure (a) Optical micrographs of Pt electrode. Inset: schematic of forming platinum layer on the carbon electrode.

(b) Amperometric recordings at a single PC12 cells when the electrode moved between cell surface and 9 μ m distance.

Keywords: dopamine, nano-Pt electrode, distance dependence

1) S.E.Zerby, A.G.Ewing., *Brain Research* 712,1-10 (1996) 2) R.M.Wightman, et al., *Biophysical* 68,383-390 (1995)

Effect of Surface Treatment on The Electrochemical Properties of Screen Printed Carbon Electrodes

Ming-Jay Lin, Ching-Chou Wu*

Department of Bio-industrial Mechatronics Engineering, National Chung Hsing University, Taichung, Taiwan



Abstract

Screen printed carbon electrode (SPCE) is widely used in development of disposable blood glucose biosensor. To improve the electron transfer rate and the stability of SPCE is important for commercial glucose biosensor. In the study, SPCEs are preanodized in 0.1 M NaOH, PBS and H₂SO₄. Figure 1 shows that the preanodized SPCEs in NaOH (named SPCE[†]) and in PBS (named SPCE*) can effectively enhance the oxidative current density (I_{pa}) of Fe(CN)₆⁻³ mediator and reduce the over potential. Moreover, the SPCE* preanodized for 400 s obtained the maximum I_{pa}, but SPCE[†] preanodized for 300 s presented the better reproducibility and moderate I_{pa}. Especially, after modifying the SPCE[†]_{300s} by 3-aminopropyl-triethoxysilane (APTES) for 15 min, it exhibited a good stability with an I_{pa} decrement of only 13% after 30 days. The result proves that the preanodization process and the APTES modification can enhance the electron transfer rate and stability of SPCE.

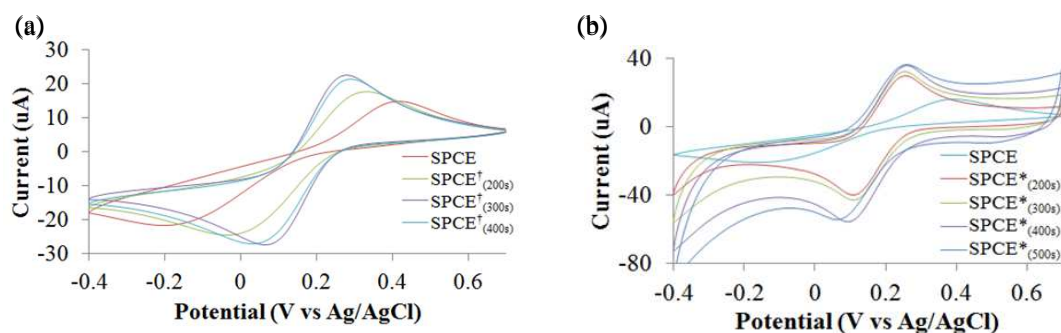


Figure 1 CV measured at (a) SPCE[†] and (b) SPCE* in 10 mM PBS containing 5 mM Fe(CN)₆⁻³ at a scanning rate of 50 mV s⁻¹.

Keywords: Surface treatment, preanodization, APTES, stability

1) Prasad K.S., Muthuraman G., Zen J.M., *Electrochem. Commun.* **10**, 559 (2008)

OS18

Twenty-Second-Temporal-Resolution Monitoring of Trace Metal Ions in Living Rat Brain Using Microdialysis Sampling, Online Sequential/Segmented Solid Phase Extraction Device, and ICP-MS



Sheng-Chieh Hsia, Cheng-Kuan Su, and Yuh-Chang Sun*

*Department of Biomedical Engineering and Environmental Sciences, National Tsing-Hua University,
30013 Hsinchu, Taiwan*

Abstract

To improve the analytical capability of the dynamic monitoring of the trace metal ions in living rat brain, the configuration of the online segmentation system incorporated into a solid phase extraction (SPE) device was the first time to be achieved. By means of using polymer-ion interactions, the non-functionalized poly(vinyl chloride) (PVC) tubing was predominately selected as an effective preconcentrator/interface to online bridge the in vivo microdialysis sampling and inductively coupled plasma mass spectrometry (ICP-MS) analysis. The streams of the rat brain microdialysate, the air to remove the residuals inside of the PVC tubing as well as the elution solution (0.2% nitric acid) to detach the retained analyte were sequentially segmented through the manipulation of a two-way selector valve. After optimizing this online analytical system and ICP-MS for analyzing metal ions in ultra-trace levels, the volume of the microdialysate was set to 833 nL, and the temporal resolution was available 20 s, corresponding to a sampling frequency of 3 min⁻¹. The system stability within 4-h continuous measurement ($n = 720$) and detection limits (based on three times the standard deviation of the baseline noise, $n = 13$) was 8%, 10%, 12% and 0.03 $\mu\text{g L}^{-1}$, 0.23 $\mu\text{g L}^{-1}$, 0.21 $\mu\text{g L}^{-1}$ for Mn, Zn and Cu, respectively. To further demonstrate the system's applicability, the spike analysis for the offline-collected brain microdialysate, and in vivo continuous monitoring of trace metal ions in living rat brains with a stimulus of perfusing high concentration of potassium ions were conducted.

Keywords: Solid phase extraction, temporal resolution, trace metal ion, stimulation

1) C. K. Su, T. W. Li, and Y. C. Sun *Anal. Chem.* **2008**, 80, 6959–6967

2) Meng Wang, Gregory T. Roman, Kristin Schultz, Colin Jennings, and Robert T. Kennedy *Anal. Chem.* **2008**, 80, 5607–5615

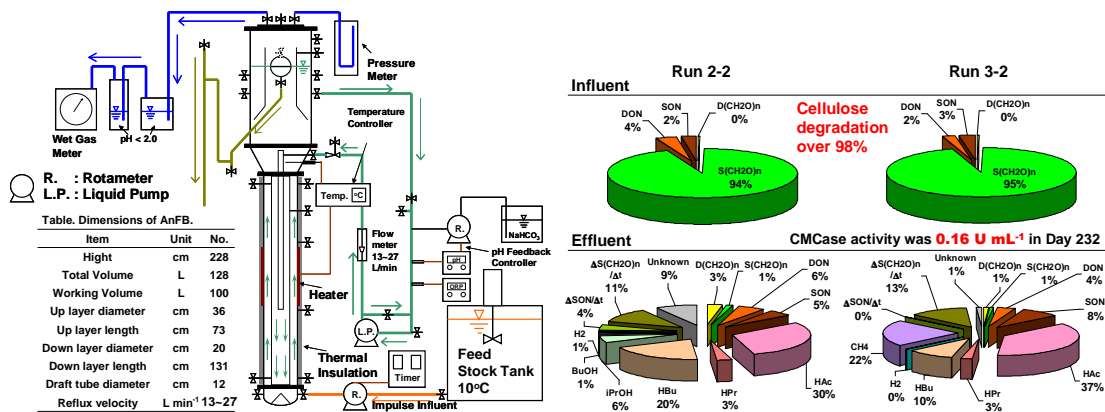


Yu-Min Tien MD

Master degree student
 Department of Environmental Engineering,
 National Cheng Kung University
 Tainan, 701, Taiwan
 Tel: 06-2757575#65827
 Fax:
 E-mail: tbs_617@yahoo.com.tw

PRESENTATION: Bioaugmented Anaerobes Digest Kitchen Waste to Promote Cellulose Hydrolysis and Hydrogen Generation with Anaerobic Fluidized Bed Process

The objective of this study is to construct a system that hydrolyzes cellulose and produces hydrogen simultaneously using anaerobic fluidized bed (AnFB) reactor. A thermophilophilic cellulolytic microbe, *Clostridium* sp. TCW1 was chosen as an inoculation for AnFB. There were three Runs in AnFB process operation. 1st Run was to start up this system and enrich biomass of cellulose hydrolyzing microbes, 2nd Run was to increase cellulose volumetric loading rate (VLR) to 1.16 g-COD/L/d, and 3rd Run was adding starch kitchen waste (SKW) to increase hydrogen production. In 1st Run, the hydrogen production rate was 0.02 ± 0.01 L-H₂/L/d, hydrogen yield was 0.77 ± 0.57 mmole-H₂/g-COD, and the total solid amount at Day 111 was 2,046 g SS. In 2nd Run, the hydrogen production rate was 0.004 L-H₂/L/d, hydrogen yield was 0.10 mmole-H₂/g-COD, and the total solid amount at Day 232 and Day 248 were 538 g SS and 206 g SS respectively, there were biomass washed out and degraded during 2nd Run. In 3rd Run, the hydrogen production rate is up to 1.0 L-H₂/L/d. The enzyme activity of Endo-β-1,4-glucanase (CMCase) of AnFB operation process at Day 232 in 2nd Run was 0.15 U/mL, it near the maximum activity 0.17 U/mL of batch culture though biomass content in AnFB was not enough (538 g); at Day 280 in 3rd Run, CMCase activity down to 0.02 U/mL when vegetable kitchen waste (VKW) was fed to AnFB, it seems VKW was not favored for cellulase production in this process operation.



References:

- 1) 陳怡傑. 2009. 以厭氧流體化床進行廚餘過篩液及狼尾草之氫醱酵程序研究. in: 環境工程學系, 國立成功大學. 台南.
- 2) 傅子寧. 2009. 牛糞肥中一株嗜熱厭氧纖維水解菌 *Clostridium* sp. TCW1 之分離鑑定及纖維素醱化特性研究. in: 環境科學與工程學系, 東海大學. 台中.

Keywords: Cellulose, *Clostridium* sp. TCW1, AnFB, hydrogen, CMCase

OS20

Effect of Film Thickness on the Optical Energy Band Gap and Threshold Voltage for Micro Sensor Performance.

Nurul Farhanah Ab. Halim¹, Mohd Noor Ahmad¹

¹ *Centre of Excellence for Advanced Sensor Technology (CEASTech),
Universiti Malaysia Perlis (UniMAP)*



Abstract

Sensor instability has been the hurdles to commercialization of organic electronics device. Through electrical and optical characterization, much progress have been made in understanding the dependence of organic thin film transistor (OTFT) performance with semiconductor (pentacene) thickness. We analyze the variation of the optical band gap and threshold voltage when the thickness of pentacene layer is increased. These factors (optical band gap & threshold voltage) are investigated to enable controllable and reproducible sensor device fabrication.

Keywords: optical band gap, threshold voltage

1) N.S. Das *et al.*, *J.Physica E.*, 2097-2102 (2010)

Long-term competition between sulfate-reducing bacteria and methane-producing archaea in a UASB reactor

Yong Hu¹, Yuta Sudo¹, Toshimasa Hojo¹, Yu-You Li¹

¹Graduate School of Environmental Studies, Tohoku University, Sendai, Japan



Abstract

Wastewater streams from chemical industry contain both high concentrations of sulfate and organic compounds¹). When this kind of wastewater is treated with anaerobic process, competition between sulfate reducing bacteria (SRB) and methane-producing archaea (MPA) for utilization of carbon sources often leads to decrease of methane production rate and even failure of treatment process²). However, little information is available about the effect of organic loading rate (OLR) on methane fermentation and sulfate reduction in sulfate-rich wastewater treatment.

This study investigated the effects of COD/SO₄²⁻ ratio on anaerobic treatment of synthetic chemical wastewater containing sulfate, acetate and ethanol using a UASB reactor. According to CH₄ and H₂S composition in biogas, as well as sulfide and residual COD in the effluent, COD and sulfate mass balance at different COD/SO₄²⁻ ratios were obtained according to stoichiometry. Experimental results show that more than half of the influent COD was converted into methane at all COD/SO₄²⁻ ratios applied. When COD/SO₄²⁻ ratio change from 20 to 0.5, the proportion of sulfate converted into aqueous sulfide dropped sharply. Most of the influent sulfate was unused at low COD/SO₄²⁻ ratio.

As shown in Fig. 1, the proportions of electrons utilized by MPA and SRB at various COD/SO₄²⁻ ratios were calculated. The percentage of electrons utilized by MPA was 96.5% with COD/SO₄²⁻ ratios of 20. Even at COD/SO₄²⁻ ratio of 0.5, around 80% of electrons were still utilized by MPA. With COD/SO₄²⁻ ratio in the range of 20-0.5, SRB accounted for 3.5-20.6% of electrons utilization. All of these results indicated that methane production was the main reaction in this experiment.

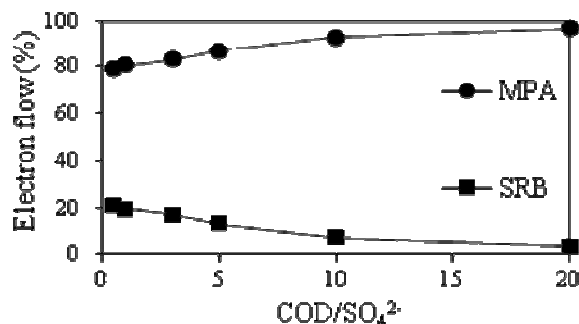


Fig. 1 Electron flow at various COD/SO₄²⁻ ratios

Keywords: anaerobic treatment, sulfate-reducing bacteria, methane-producing archaea

1) Lopes, S.I.C. *et al.*, *Water Res.*, **41**, 2379(2007) 2) Lehua, Z., *et al.*, *Water Res.*, **42**,1(2008)

Continuous thermophilic hydrogen fermentation of cellulose by mixed-culture

Hongyu Jiang, S. I. Gadow, Y. Y. Li

Graduate School of Environmental Studies, Tohoku University, Sendai, Japan



Abstract

Anaerobic dark fermentation is one promising method to produce renewable hydrogen from various organic wastes ¹⁾. A long-term continuous thermophilic cellulosic-hydrogen fermentation using a Continuous Stirred Tank Reactor (CSTR) by anaerobic mixed microflora was carried out in this experiment.

Anaerobic seed sludge was taken from a sewage sludge digester at the Sendai municipal sewage treatment plant. In order to inactivate hydrogen-consuming microorganisms and to harvest H₂-producing anaerobes, especially the spore-forming *Clostridia* bacteria, heat pretreatment has been done at 80°C for 30mins. The experiment apparatus was composed of a substrate tank and a CSTR with 6L effective volume. The reactor was operated under thermophilic temperature (55 ± 1°C). The experiment was conducted with an influent concentration of 10g/L cellulose at a HRT of 10 days.

The results show that the system reached a steady state condition after 60 days. A stable hydrogen yield of 10.9 ± 0.23mmol H₂/g cellulose was maintained for 190 days with acetate, butyrate and ethanol as main soluble byproducts. Analysis of 16S rRNA sequences showed that the cellulolytic bacteria were close to *Thermoanaerobacterium thermosaccharolyticum*, *Enterobacter cloacae*, *clostridium* sp. and *Pedobacter* sp.

In addition, twenty six batch experiments were conducted to investigate the activity of thermophilic H₂ producing mixed microflora to the temperature variation. The cellulosic-hydrogen producing bacteria were able to utilize the cellulose or glucose within a wide range of fermentation temperatures (35-65 °C) to produce hydrogen with maximum activity obtained at 55 °C. The activation energy for cellulose and glucose were estimated at 103 and 98.8 kJ/mol, respectively.

Keywords: biohydrogen; dark fermentation; cellulose; thermophilic; long-term; activity test

1) Guo X.M. *et al.*, *Int. J. Hydrogen Energy*, **35**,10660-10673(2010)

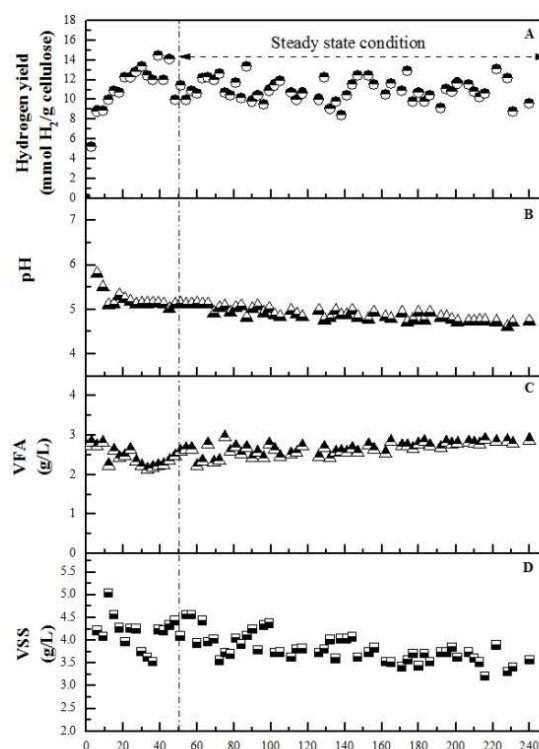


Fig. Time course of long-term performance

Poster Program

P01	<p>Investigation of Far Infrared Irradiation of Titania Nanotubes on the Growth of 3T3 Fibroblasts</p> <p><u>Shu-Yen Huang</u></p> <p><i>Graduate Institute of Biomedical Engineering, Chung Hsing University, Taiwan</i></p>
P02	<p>Study on a Ring-shaped Interdigitated Electrode Controlled by AC Electrokinetic for Concentrating Bio-particles</p> <p><u>Sheng-Kai Zhong</u>, Jyun-Hong Wang, Hsien-Chang Chang</p> <p><i>Department of Biomedical Engineering, National Cheng Kung University, Tainan</i></p>
P03	<p>Development of Albumin-based Carriers to Enhance Inhalation Therapy for COPD</p> <p><u>Ting-Yu Cheng</u>^{1, 2}, Ya-Ting Yang², Jiun-Yu Chen², Wei-Neng Liao², Jen-Kun Chen², Yuh-Chang Sun¹</p> <p>¹<i>Department of Biomedical Engineering and Environmental Sciences, National Tsing-Hua University, Taiwan</i></p> <p>²<i>Center for Nanomedicine research, National Health Research Institutes, Taiwan</i></p>
P04	<p>Effect of Electrolyte Cations on the Sensing Characteristic of Label Free impedimetric DNA Biosensors</p> <p><u>Hao-Yu Yen</u>, Ching-Chou Wu*</p> <p><i>Department of Bio-industrial Mechatronics Engineering, National Chung Hsing University, Taiwan</i></p>
P05	<p>Synthesis the Cu/Au@SiO₂ Yolk Shell Nanoparticles as the Partial Oxidation of Methanol Reaction Catalyst</p> <p><u>Yu-Yi Chuang</u>, Yuh-Jeen Huang*</p> <p><i>Department of Biomedical Engineering & Environmental Sciences, National Tsing Hua University, Taiwan</i></p>
P06	<p>Nanosize Titanium Dioxide Expression Related to Factors in Neurodegenerative Diseases</p> <p><u>Zia-Cheng Chang</u>, Yuh-Jeen Huang*</p> <p><i>Department of Biomedical Engineering and Environmental Sciences, National Tsing Hua University, Taiwan</i></p>
P07	<p>Uptake of Borate Ion from Aqueous Solution by Mg-Al oxide</p> <p><u>Jumpei Oba</u>, T. Kameda, T. Yoshioka</p> <p><i>Graduate School of Environmental Studies, Tohoku University, Japan</i></p>
P08	<p>Development of an AgCl/Al₂O₃ Membrane for the Removal of Chloride from Solutions of NaCl in Ethylene Glycol</p> <p><u>Kento Yamada</u>, Guido Grause, Tomohito Kameda, Toshiaki Yoshioka</p> <p><i>Graduate School of Environmental Studies, Tohoku University, Japan</i></p>

P09	Lead Removal from Cathode Ray Tube Glass in the Presence of PVC and Calcium Hydroxide <u>Kenshi Takahashi</u> , Guido Grause, Tomohito Kameda, Toshiaki Yoshioka <i>Graduate School of Environmental Studies, Tohoku University, Japan</i>
P10	Selective Adsorption of Substituted Phenols by Cu-Al Layered Double Hydroxide Intercalated with 1-Naphthol-3,8-disulfonate <u>Tomomi Uchiyama</u> , T. Kameda, T. Yoshioka <i>Graduate School of Environmental Studies, Tohoku University, Japan</i>
P11	Concentration of Cs⁺ using Perfluorooctanoic Acid and Nitrobenzene <u>Kotaro Hayashi</u> , G.Grause, T.Kameda, T.Yoshioka <i>Graduate School of Environmental Studies, Tohoku University, Japan</i>
P12	A Microfluidics for Real Time DNA Molecules Replication <u>Chia-Chin Ho</u> , M.-S Hung* <i>Department of Biomechatronic Engineering, National Chiayi University, Taiwan</i>
P13	Uptake of Nd³⁺ and Sr²⁺ from Aqueous Solution using Zn-Al Layered Double Hydroxide Intercalated with Aminocarboxylic Acid <u>Tetsu Shinmyo</u> , T.Kameda, T.Yoshioka <i>Graduate School of Environmental Studies, Tohoku University, Japan</i>
P14	Ultrahigh Surface Area Graphene Oxide Nanoribbons for Electrochemical Detection of Ascorbic Acid, Dopamine and Uric Acid <u>Chun-Yi Chiu</u> , Chun-Hao Su, Chia-Liang Sun <i>Department of Chemical and Materials Engineering, Chang Gung University, Taiwan</i>
P17	Laser-induced Heating for Rapid Targeted DNA Replication <u>Chih-Pin Chen</u> , M.-S Hung* <i>Department of Biomechatronic Engineering, National Chiayi University, Taiwan</i>
P18	Control of Selectivity by Solvent Permittivity in Inclusion of Methylamines with Crystals of Thiocalix[4]arene <u>Ikuko Miyoshi</u> , Y. Kitamoto, O. Shibata, N. Morohashi, T. Hattori <i>Graduate School of Engineering, Tohoku University, Japan</i>
P19	Removal of Heavy Metals in Solution by Fe²⁺ Doped Mg-Al Layered Double Hydroxides <u>Eisuke Kondo</u> , Tomohito Kameda, Toshiaki Yoshioka <i>Graduate School of Environmental Studies, Tohoku University, Japan</i>
P20	Simultaneous Hydrolytic and Thermal Decomposition of Poly(ethylene terephthalate) using ¹⁸O isotope-labeled Water <u>Y. Morohoshi</u> ¹ , S.Kumagai ^{1,2} , G. Grause ¹ , T. Kameda ¹ , T. Yoshioka ¹ ¹ <i>Graduate School of Environmental Studies, Tohoku University, Japan</i> ² <i>Research Fellow of the Japan Society for the Promotion of Science</i>

P22	<p>Influence of Various Factors on Spatial Structure of Nanoparticles in Polymer Nanocomposite Thin Films</p> <p><u>Yang Liu</u>¹, T. Fujii¹, M. Kubo¹, K. Sugioka¹, T. Tsukada¹, S. Takami², T. Adschiri³</p> <p>¹<i>Department of Chemical Engineering, Tohoku University, Japan</i></p> <p>²<i>Institute of Multidisciplinary Research for Advanced Materials, Tohoku University, Japan</i></p> <p>³<i>WPI Advanced Institute for Materials Research, Tohoku University, Japan</i></p>
P23	<p>Fundamental Study on Incubation and Condensation of Culture Medium for Extraction from Nannochloropsis Species</p> <p><u>Yuri Hamabe</u>, Masaki Ota, Yoshiyuki Sato, Hiroshi Inomata</p> <p><i>Research Center of Supercritical Fluid Technology, Graduate School of Engineering, Tohoku University, Japan</i></p>
P24	<p>Solid Acid Catalysts for Cellulose Hydrolysis in 1-Butyl-3-methylimidazolium Chloride ([Bmim][Cl])</p> <p><u>Shiho Matsuda</u>¹, M. Watanabe², T. M. Aida¹, R. L. Smith Jr.^{1,2}</p> <p>¹<i>Graduate School of Environmental Studies</i></p> <p>²<i>Research Center of Supercritical Fluid Technology, Tohoku University, Japan</i></p>
P25	<p>Numerical Simulations of SiGe Single Crystal Growth by TLZ Method in ISS</p> <p><u>Keita Abe</u>^{*1}, Sara Sumioka¹, Ken-ichi Sugioka¹, Masaki Kubo¹, Takao Tsukada¹, Kyoichi Kinoshita², Yasutomo Arai², Yuko Inatomi²</p> <p>¹<i>Department of Chemical Engineering, Tohoku University, Japan</i></p> <p>²<i>Institute of Space and Astronautical Science, Japan Aerospace Exploration Agency (JAXA), Japan</i></p>
P26	<p>Low-Invasive, Quantitative and Single Cell Level Evaluation of Differentiation State of Embryonic Stem Cells by SECM</p> <p><u>Yoshiharu Matsumae</u>¹, T. Arai¹, Y. Takahashi², K. Ino¹, H. Shiku¹, T. Matsue^{1,2}</p> <p>¹<i>Graduate School of Environmental Studies, Tohoku University, Japan</i></p> <p>²<i>Advanced Institute for Materials Research, Tohoku University, Japan</i></p>
P27	<p>Sorting, Culture and Functional Evaluation of Mouse Mesodermal Embryoid Bodies</p> <p><u>Y. Zhou</u>¹, T. Arai¹, S. Yamada¹, I. Fujisawa¹, K. Ino¹, H. Shiku¹, T. Matsue^{1,2}</p> <p>¹<i>Graduate School of Environmental Studies, Tohoku University, Japan</i></p> <p>²<i>WPI-AIMR</i></p>
P28	<p>Construction of Small Bispecific Antibody Mutants with Enhanced Anti-tumor Activity</p> <p><u>Katsuhiko Hosokawa</u>, R. Asano, S. Taki, M. Umetsu, I. Kumagai</p> <p><i>Department of Biomolecular Engineering, Graduate School of Engineering, Tohoku University, Japan</i></p>
P29	<p>In Vivo Assembly Design: Multivalent Antibody Generation</p> <p><u>Rui Todokoro</u>, Hikaru Nakazawa, Ryutaro Asano, Izumi Kumagai, Mitsuo Umetsu</p> <p><i>Department of Biomolecular Engineering, Graduate School of Engineering, Tohoku University,</i></p>

	<i>Japan</i>
P30	<p>Design of Bispecific Interface Molecules for Biosensor Utilizing Camel Antibody with Affinity for ZnO Surface</p> <p><u>Takuma Sujino</u>, Hikaru Nakazawa, Ryutaro Asano, Izumi Kumagai, Mitsuo Umetsu</p> <p><i>Department of Biomolecular Engineering, Graduate School of Engineering, Tohoku University, Japan</i></p>
P31	<p>Estimation Kamlet-Taft Solvatochromic Parameters and Solubility Parameter of Binary Solvent Mixtures for Nucleophilic Substitution and Homogeneous Reaction</p> <p><u>Alif Duereh</u>, Masaki Ota, Yoshiyuki Sato, Hiroshi Inomata</p> <p><i>Department of Chemical Engineering, Research Center of Supercritical Fluid Technology; Graduate School of Engineering, Tohoku University, Japan</i></p>
P32	<p>A Field Emission Lighting Device Employing Highly Crystalline Single-walled Carbon Nanotubes</p> <p><u>Sharon Marie Garrido</u>, Norihiro Shimoi, Adriana Ledezma Estrada, Toshimasa Hojo, Yasumitsu Tanaka, Kazuyuki Tohji</p> <p><i>Graduate School of Environmental Studies, Tohoku University, Japan</i></p>
P33	<p>Evaluation of Specific Strength of Ultimet Thin MWCNT Fiber Based on Uncertainty</p> <p><u>Hikaru Nishizaka</u>^{1,2}, Yoshinori Sato¹, Kenichi Motomiya¹, Kazuyuki Tohji¹</p> <p>¹<i>Graduate School of Environmental Studies, Tohoku University, Japan</i></p> <p>²<i>Research Fellow of the Japan Society for the Promotion of Science</i></p>
P34	<p>Microbial Community Dynamic and Process Performance on Chicken Manure Fermentation at a Wide Range of Ammonia Concentration</p> <p><u>Qigui Niu</u>¹, Wei Qiao¹, Toshimasa Hojo¹, Yu-You Li^{1,2}</p> <p>¹<i>Graduate School of Environmental Studies, Tohoku University, Japan</i></p> <p>²<i>Department of Civil and Environmental Engineering, Graduate School of Engineering, Tohoku University, Japan</i></p>
P35	<p>Evaluation of the steam assisted thermal dehydrochlorination of poly(vinyl chloride)</p> <p>Juan D. Fonseca, G. Grause, T. Kameda, T. Yoshioka</p> <p><i>Graduate School of Environmental Studies, Tohoku University, Japan</i></p>

P01

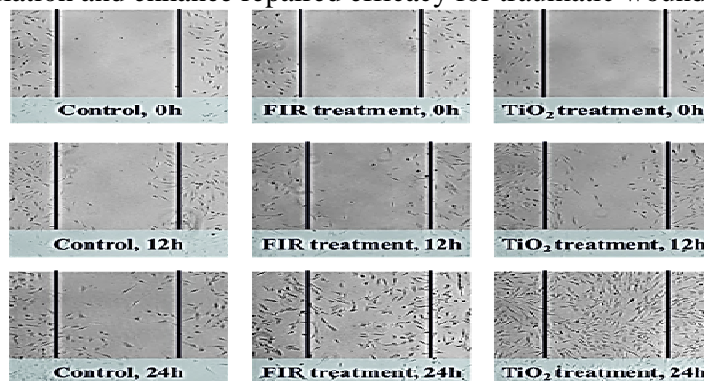


Huang, Shu-Yen MD

Master degree student
Graduate Institute of Biomedical
Engineering, Chung Hsing University,
Taichung 40227, Taiwan
Tel: +886-4-2284-0732 ext. 305
Fax: +886-4-2285-2422
E-mail: wraino690@gmail.com

PRESENTATION: Investigation of Far Infrared Irradiation of Titania Nanotubes on the Growth of 3T3 Fibroblasts

Far-infrared radiation (FIR) had been drawn a lot of attentions in many therapeutic aspects. In this study, we used 3T3 fibroblasts to investigate the effect of in-vitro FIR treatment on fibroblasts morphological change for implication of wound repair. The morphological structures of anodized titania nanotubes (ATOs), before and after specific washing by using deionized water, ethanol, and acetone, were independently observed by scanning electron microscope (SEM). The components of ATOs were analyzed and characterized by energy dispersive X-ray spectrometer (EDS), electron spectroscopy for chemical analysis (ESCA), and the crystallization of those was by X-ray diffraction (XRD). The specific IR wavelength irradiated from the self-made ATOs was detected at 10 μm by using the Fourier transform infrared spectrometer (FTIR). The in vitro artificial wound model was composed of fibroblast cells for observation cell growth and migration. The fibroblast cells were in vitro irradiated by using the commercial FIR substrates and the self-made ATOs. The results indicated that acetone-cleaned self-made ATO could facilitate the proliferation of fibroblast cells after 40-min irradiation. Our self-made ATOs and commercial FIR substrates could promote the fibroblast cells growth and migration in 24h. We proved that exposure to the FIR can enhance the overall capability of cell growth in our in-vitro observation. Our results showed FIR effectively facilitated the cell proliferation with an increasingly cellular growth to $1.04 \times 10^5 / \text{cm}^2$ on the 3rd day in 40-min FIR treated group. In addition, the pseudopodium-like and polygonal shape of 3T3 fibroblasts were observed in fluorescent images in FIR treated groups. Our study showed that FIR treatment for 40 min induced fibroblasts growth and further affected its cellular morphological change. Above all, a neat and organized nanotube-structure of our self-made acetone-cleaned ATOs can emit 10- μm thermal infrared radiation and enhance repaired efficacy for traumatic wounds.



Keywords: Far-infrared radiation, anodized titania nanotubes, cell growth and migration, proliferation

**Study on a Ring-shaped
Interdigitated Electrode Controlled by AC
Electrokinetic for Concentrating Bio-particles**

Sheng-Kai Zhong, Jyun-Hong Wang, Hsien-Chang Chang

*Department of Biomedical Engineering; National Cheng Kung University,
Tainan, Taiwan*



Abstract

In recent years, with the development of micro-nanotechnology, not only make advances in cell phone and tablet computers and other electronic components, but also extends to a variety of fields such as materials, chemicals, aerospace, medicine, medical laboratory, medical engineering. The problems of the traditional laboratory instruments such as occupying the space, carrying inconvenience reducing the required sample volume and detection time can be solved by components miniaturization. In general, the processes from sample pre-treatment to the detection are overly complicated and lengthy. Therefore, in this research, we design a micro-concentrator platform for medical combined micro electro mechanical systems (MEMS) and electrokinetic, then the sample in solution can be concentrated in few minutes.

When the AC voltage is applied to the electrode, the bacteria in the sample will be dragged to the center of the electrode by AC electroosmotic flow (ACEO). From the results, samples (~100 μ L) were dropped on the micro-concentrator platform, and applied an appropriate AC voltage and frequency. The *Escherichia coli* were dragged toward the center of the electrode and adsorbed on the electrode due to the interaction of AC electroosmotic flow and dielectrophoretic force. In the future, the platform may be applied to the low concentration detection, such as rapid test on urinary tract infection, etc.

Keywords: micro-concentrator, AC electroosmotic flow (ACEO), dielectrophoretic force

P03

Development of Albumin-based Carriers to Enhance Inhalation Therapy for COPD

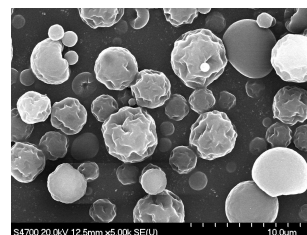
Ting-Yu Cheng^{1,2}, Ya-Ting Yang², Jiun-Yu Chen², Wei-Neng Liao², Jen-Kun Chen², Yuh-Chang Sun¹

¹Department of Biomedical Engineering and Environmental Sciences, National Tsing-Hua University, 30013 Hsinchu, Taiwan, ²Center for Nanomedicine research, National Health Research Institutes, 35053 Miaoli, Taiwan



Abstract

Chronic obstructive pulmonary disease (COPD) is the most important cause leading to gradual deterioration of lung function. The COPD has been ranked to one of the top 10 causes of death in Taiwan for more than a decade. To maintain long-term health care, inhalation of beta2-agonists, anticholinergics or corticosteroid are frequently used for patients. However, the deposition of various drugs in target region of lung are always less than 30%. An albumin-base carrier platform has been developed in present work to improve drug delivery and retention in small airway. There are three approaches, including desolvation, emulsion and spray dry, to prepare microspheres for this research. Desolvation and emulsion are convenient to synthesize microspheres in solution but show drawbacks of reproducibility and challenges of upscale production. In comparison, spray dry takes advantage of preparing uniform microspheres ($< 5\mu\text{m}$) at adequate throughput. Morphology and surface roughness of microsphere were inspected by scanning electron microscope (SEM) and atomic force microscope (AFM), respectively. Attempts of *in vivo* imaging technique were employed for evaluating delivery efficiency of the above-mentioned drug carrier. In addition to delivery efficiency, releasing properties of active ingredients from drug carriers should be critical to affect therapeutic efficacy and eliminate side effects. We try to adjust the composition of cross-linker in drug carrier to alter drug releasing profiles and pharmacokinetics, which can be successfully evaluated by liquid chromatography-electrospray ionization/mass spectrometry (LC-ESI/MS) analysis. The albumin-based drug carrier not only provides a biocompatible platform for COPD therapy but also show a niche to elevate loco-regional deposition rate along with ameliorate bioavailability for inhalation drug delivery.



Keyword: microspheres, COPD, pulmonary drug delivery

Fig.1 BSA microspheres

Effect of Electrolyte Cations on the Sensing Characteristic of Label Free impedimetric DNA Biosensors

Hao-Yu Yen, Ching-Chou Wu*

Department of Bio-industrial Mechatronics Engineering, National Chung Hsing University, Taichung, Taiwan



Abstract

Geminiviridae viruses are one of the most notorious pathogens causing serious damage to many important economic crops presently. Developing a sensitive, fast hybridized, portable and miniature sensing platform for the geminiviruse detection based on complementary nucleic acid is an important issue. This study explored the effect of electrolyte cations on the sensing characteristics of chip-type electrodes. The thin-film Au electrodes were sequentially cleaned by piranha and aqua regia before immobilizing DNA probes. 1 μM thiolated ssDNA was immobilized at the cleaned Au electrode for 2 h as the DNA probes (pDNA), and then 1 mM mercaptohexanol (MCH) was used for blocking the residual area of electrode. Lastly, 10 μl aliquot of 20-mers target DNA (tDNA) was dropped for 1 h for DNA hybridization, as shown in Fig. 1(a). The Nyquist plots were measured by the electrochemical impedance spectroscopy (EIS) in three kinds of cation-different buffers, such as PBS, Tris and TES, containing 1 mM $\text{Fe}(\text{CN})_6^{3-/4-}$ after hybridization, as shown in Fig. 1(b). Experimentally, the electron transfer resistance (R_{et}) obtained from equivalent circuit of EIS measurement was used as an indicator to probe the hybridization reaction. The results reveal that the R_{et} measured in TES buffer exhibited the largest R_{et} response after hybridizing the tDNA. Moreover, the linear range, $10^{-10} \sim 10^{-15}$ M, and the detection limit, 10^{-15} M, for tDNA measured in TES was superior to the linear range ($10^{-10} \sim 10^{-13}$ M) and the detection limit (10^{-13} M) measured in PBS. The label-free EIS-based DNA chip is beneficial for the integration of micro-fluidic system and has the advantages of portability and mass production.

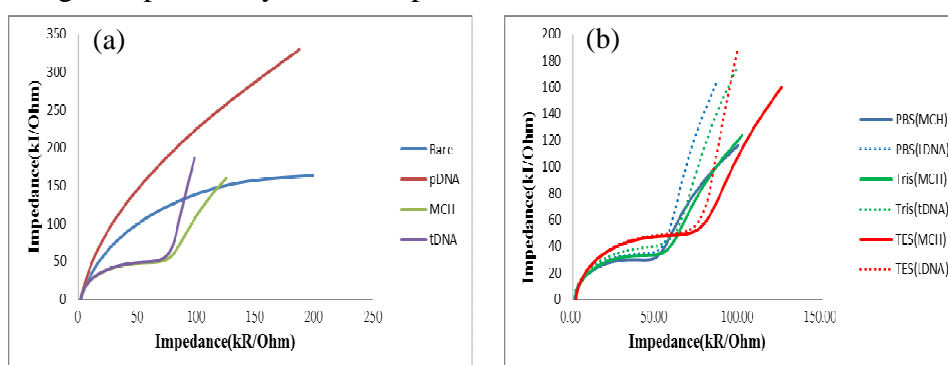


Figure 1 (a) Nyquist plots recorded at bare, pDNA-, MCH- and tDNA-modified Au electrode in TES. (b) Nyquist plots obtained in different buffers before and tDNA hybridization.

Keywords : Label free, impedance, DNA sensor, cations

P05



Synthesis the Cu/Au@SiO₂ Yolk Shell Nanoparticles as the Partial Oxidation of Methanol Reaction Catalyst

Yu-Yi Chuang, Yuh-Jeen Huang*

*Department of Biomedical Engineering & Environmental Sciences, National
Tsing Hua University, Hsinchu, Taiwan 30013*

Abstract

The copper-based catalysts have been well developed for partial oxidation of methanol (POM) reaction due to low cost, high activity and good selectivity for hydrogen. However, the sintering problem for copper-based catalysts during the temperature ($>250^{\circ}\text{C}$) should be concerned. Therefore, the yolk-shell with porous structure is induced into the catalysts.

In the previous work, we have found that CuZnO catalysts with gold promoter can reduce the CO selectivity [1]. Furthermore, copper and gold have the same face center cubic (fcc) crystal structure and similar lattice spacing, so they can form alloy very easily [2]. Thus, an CuAu@SiO₂ yolk shell with porous structure is synthesized by using co-reduction method for the CuAu core and stöber method [3] for the porous silica shell and characterized by Transmission Electron Microscope (TEM), X-ray Diffraction (XRD), X-ray photoelectron spectroscopy (XPS), Inductively coupled plasma mass spectrometry (ICP-MS). We hope this CuAu@SiO₂ yolk shell catalyst can prevent the sintering problems of the catalysts and decrease the CO selectivity in the POM reaction.

Reference

- 1) Yuh-Jeen Huang*, Ke Lun Ng, Hsiao-Yu Huang, international journal of hydrogen energy 36 (2011) 15203-15211
- 2) Xiaoyan Liu, Aiqin Wang, Tao Zhang*, Dang-Sheng Su, Chung-Yuan Mou*, Catalysis Today 160 (2011) 103–108
- 3) W. Stöber, A. Fink and E. Bohn, J. Colloid Interface Sci., 1968, 26, 62

key word: yolk shell 、 rattle type 、 POM 、 copper/gold alloy

P06

Nanosize Titanium Dioxide Expression Related to Factors in Neurodegenerative Diseases

Zia-Cheng Chang, and Yuh-Jeen Huang*

Department of Biomedical Engineering and Environmental Sciences, National Tsing Hua University, Hsinchu, 30013, Taiwan

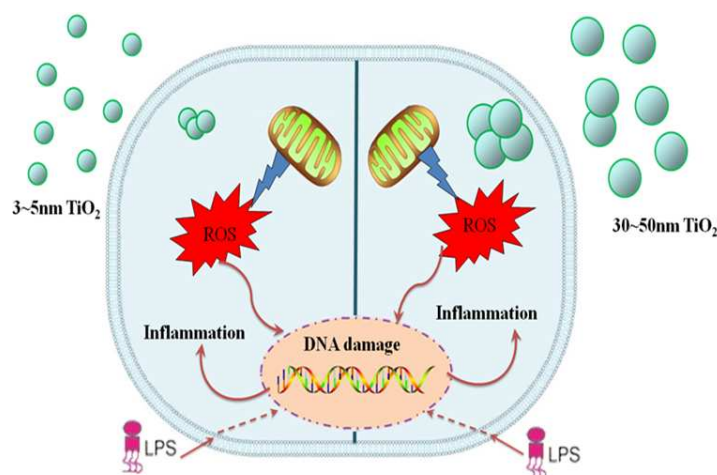


Abstract

With the development of nanotechnology, more and more nanomaterials have been produced. Titanium dioxide (TiO₂) nanoparticle (NP) is one of the most important nanoscale materials. Though titanium dioxide (TiO₂) nanoparticles (NPs) have been widely used in industry and biomedical field, they would have some potential risk to organism. Furthermore, some animals and cell experiments were found NPs seems to produce some biological effects of central nervous system, such as cell death, inflammation, and oxidative stress ... etc. Therefore, we investigated the neurotoxicity of TiO₂ NPs (5 nm and 30 nm) in vitro by using three neuro-cell lines of mouse: Neuro-2a cell line (N2A), microglial cell line (BV-2), and astrocytes (ALT).

First, the physicochemical characteristics of titanium dioxide nanoparticles were identified by Transmission Electron Microscope (TEM), X-ray Diffraction, Inductively Coupled Plasma - Optical Emission Spectrometer (ICP-OES), and Dynamic Laser Light Scattering (DLS). Cell cytotoxicity was evaluated by detecting cell viability (Alamar blue), inflammatory response (IL-1 β , IL-6, TNF- α , and MCP-1), cell uptake and induced reactive oxygen species (ROS).

The result showed that TiO₂ NPs have good distribution in DMEM medium. The cell viability analysis results show that there did not have statistical significant different with the control group in all cells except BV-2 cell with the addition of LPS. The inflammatory response (IL-1 β) shows that the smaller size TiO₂ NPs can induce more IL-1 β .



keywords: Titanium dioxide (TiO₂), Neurodegenerative diseases, IL-1 β , IL-6, TNF- α ,

nd MCP-1

Reference

- 1) BaoYong Sha , Wei Gao , ShuQi Wang , Feng Xu , TianJian Lu, Composites: Part B, **42** (2011)
2136 - 2144

Uptake of borate ion from aqueous solution by Mg-Al oxide

Jumppei Oba, T. Kameda, T. Yoshioka

Graduate School of Environmental Studies

Tohoku University, Sendai, Japan



Abstract

[Introduction] Mg-Al layered double hydroxides (LDHs) consist of positively charged metal hydroxide layers and anions in the interlayers. The LDHs decompose at 500 °C to become Mg-Al oxide (LDO) which rehydrates and reconstructs the original structure. While reconstructing, the LDO is able to intercalate anions hence this phenomenon can be utilized to remove anions from the water. Boron is normally present in the wastewater of e.g. glass factories, incineration plants and thermal power plants. In Japan, the standard of boron effluent is 10 mg/L. In this study, the uptake of boron from aqueous solution by LDO was studied.

[Experimental] The LDHs were prepared by co-precipitation method and calcined at 500 °C to obtain the LDO. The prepared 0.593 g of LDO at Al/B=1 was added to 0.5 L of 100 mg/L boric acid solution and the resulting suspension was kept at 30 °C under stirring. The suspension was extracted at different time intervals. After the uptake, the LDHs were added to 20mL of Na₂CO₃ solution for desorption. Afterwards, the LDHs were calcined and reused for the second time. The borate concentration was determined by ICP-AES.

[Results and discussion] Fig.1 shows the degree of boron uptake with respect to time. With the addition of twice stoichiometric LDO (Al/B=2), the concentration of borate ion was reduced to 3.0 mg/L, which is acceptable referring to borate standard effluent of Japan. Fig.2 shows the effect of Na₂CO₃ concentration on the desorption. The desorption changed only a bit with Na₂CO₃ concentration and 90.4 % of the borate ion was desorbed at 0.05 mol/L. The first uptake rate was 67.7 % while the recycled LDHs uptake rate was 38.0 % at 120 minutes. This reduction is caused by remaining borate ions and the collapse of the layered structure of the LDHs.

Keywords: boron, Mg-Al oxide, uptake

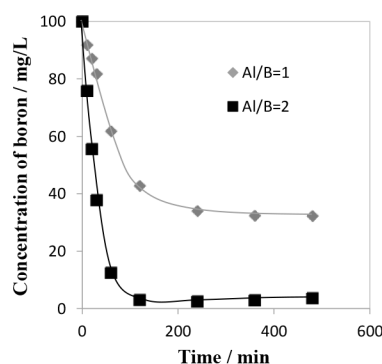


Fig.1 Uptake of borate ions with Al/B=1 and 2.

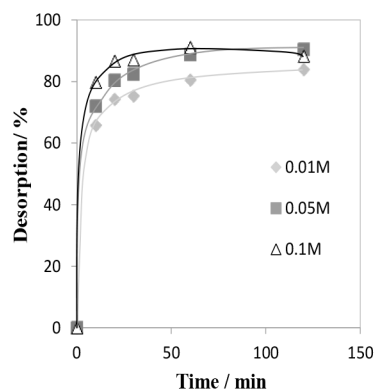


Fig.2 Desorption of borate ions with varied concentration.

Development of an AgCl/Al₂O₃ membrane for the removal of chloride from solutions of NaCl in ethylene glycol

Kento Yamada, Guido Grause, Tomohito Kameda,
Toshiaki Yoshioka

Graduate School of Environmental Studies; Tohoku University, Sendai, Japan



Abstract

Dechlorination of polyvinyl chloride (PVC) is necessary prior to its the thermal treatment. A high degree of dechlorination can be achieved in a solution of NaOH in ethylene glycol (NaOH_{EG})¹⁾, in which case, the solution is enriched in chloride. For the regeneration of NaOH_{EG}, chloride has to be removed – after recovery it might be reemployed in the PVC products, achieving “chlorine circulation”. In this work, we investigated the recovery of chloride from the EG solution by electrodialysis using an AgCl/Al₂O₃ membrane which is superior in mechanical strength and organic solvent tolerance.

AgCl was precipitated on the Al₂O₃ surface electrolytically. 180 ml of NaCl_{aq} (1 M) in the cathode cell, and 30 ml of AgNO₃_{aq} (1 M) in the anode cell was exposed to 4 V for 3 h. Cathode and anode were separated by either a CP2 membrane (Al₂O₃ 99%) or an S membrane (Al₂O₃ 69%, SiO₂ 28%).

Electrodialysis was conducted at 6 V for 5 h with 30 ml of NaCl_{EG} (5 wt %) in the cathode cell and 180 ml of ion-exchanged water in the anode cell.

Fig. 1 shows the transmission of Cl⁻ through Al₂O₃ and AgCl/Al₂O₃ membranes. The transmission of Cl⁻ decreased slightly in the presence of AgCl. Maximal transmission of Cl⁻ reached only 15% because of the high electrical resistance in the ion-exchanged water. Fig. 2 shows the transmission of EG. The presence of AgCl reduced the EG transmission by about 5%. Electrical resistance decreased when NaOH_{aq} was used instead of deionized water. The chloride ion recovery reached approximately 40%, while an increasing EG transmission was not observed. Therefore, the use of NaOH_{aq} can improve the efficiency of Cl⁻ recovery. The further reduction of the EG permeation is indispensable for the utilization of chloride.

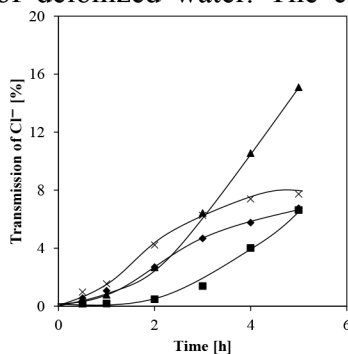


Fig.1 Transmission of Cl⁻

[▲:CP2, ×:CP2(AgCl-supported),
■:S, ◆:S(AgCl-supported)]

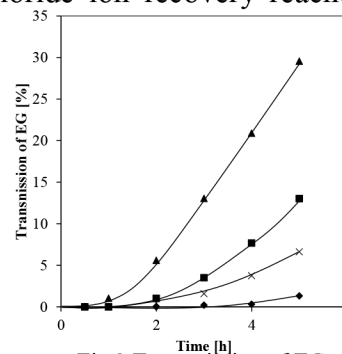


Fig.2 Transmission of EG

[▲:CP2, ×:CP2(AgCl-supported),
■:S, ◆:S(AgCl-supported)]

Keywords: electrodialysis , chlorine circulation , AgCl/Al₂O₃ membrane

1) T. Yoshioka, T. Kameda, S. Imai, A. Okuwaki, *Polym. Degrad, Stab*, **93**, 1138-1141, (2008)

P09

Lead Removal from Cathode Ray Tube Glass in the Presence of PVC and Calcium Hydroxide

Kenshi Takahashi, Guido Grause, Tomohito Kameda,
Toshiaki Yoshioka

Graduate School of Environmental Studies; Tohoku University, Sendai, Japan



Abstract

In recent years, the amount of waste cathode ray tube (CRT) glass has increased because flat-panel displays are rapidly replacing CRT monitors. The funnel glass (FG) fraction of CRT contains between 20 and 30 wt% lead. Therefore, it is necessary to develop a process for lead removal from funnel glass. Earlier¹⁾ we proposed a chloride volatilization process making use of PVC as chlorination agent. However lead removal was negligible because the hydrogen chloride produced by PVC pyrolysis barely reacted with FG. In this study, we examined the enhanced lead chloride volatilization from FG in the presence of PVC and calcium hydroxide.

FG powder (particle size <106 μm) mixed with PVC and calcium hydroxide was treated in an electric heated tube reactor, batch-wise at 1000 °C for 10 - 120 min. The lead content in the residue was determined after digestion with HNO₃, HF, and H₂O₂ by ICP-AES.

At a Ca/Cl molar ratio of 2 and a holding time of 120 min, lead volatilization was far higher than in the sole presence of PVC. Fig.1 shows thermal decomposition behavior of the mixtures of PVC and calcium hydroxide. As seen in Fig.1, the mixture had weight losses at 300, 400 and 450 °C caused by the dehydrochlorination of PVC, the pyrolysis of calcium hydroxide, and the pyrolysis of the residual polyene, respectively. Moreover, calcium chloride was probably volatilized from 850 °C. It can be assumed that calcium hydroxide absorbed hydrogen chloride and calcium chloride was formed. Then the calcium chloride acted as chlorination agent that led to the improvement of lead volatilization (Scheme 1).

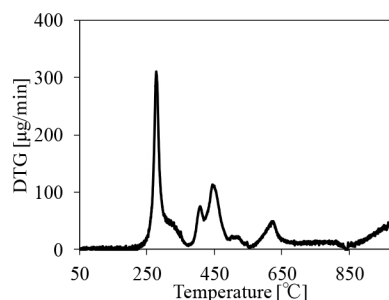
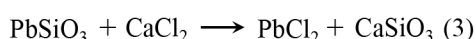
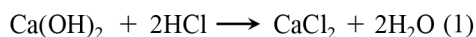


Fig.1 Thermal decomposition behavior of the mixtures of PVC and calcium hydroxide



Scheme 1 Reactions leading to the removal of lead

Keywords: cathode ray tube, lead removal, PVC

1) G. Grause, N. Yamamoto, T. Kameda, T. Yoshioka, *Int. J. Environ. Sci. Tec.*, in press, DOI

10.1007/s13762-013-0286-0

Selective adsorption of substituted phenols by Cu-Al layered double hydroxide intercalated with 1-naphthol-3,8-disulfonate

Tomomi Uchiyama, T. Kameda, T. Yoshioka

Graduate School of Environmental Studies, Tohoku University, Sendai, Japan



Abstract

Layered double hydroxides (LDHs) intercalated with aromatic anion are able to selectively take up aromatics from aqueous solutions. This is attributed to the extent of aromatic interactions between the aromatic rings of the intercalated aromatics and the aromatics in the aqueous solutions with different electronic densities.¹⁾

In this study, Cu–Al LDH intercalated with 1-naphthol-3,8-disulfonate (NDS²⁻) was prepared by coprecipitation. The adsorption of 5 kinds of substituted phenols, shown in Table 1, onto the LDH intercalated with NDS²⁻ was examined. Adsorbed amounts were determined by HPLC. NDS²⁻ has one OH group and two SO₃⁻ groups, which are electron donating and weakly electron withdrawing, respectively, attached to its aromatic core. Therefore, the naphthalene core of NDS is electron rich. The density of electrons in the aromatic rings of the substituted phenols is expected to increase in the following order: N-phe < DCI-phe < Cl-phe < MM-phe < Me-phe.

Fig.1 shows the uptake of each aromatic compound by the Cu-Al-NDS²⁻ LDH. The adsorption amounts from a single solution by the Cu-Al-NDS²⁻ LDH was as follows: N-phe > DCI-phe > Cl-phe > MM-phe > Me-phe. The maximum and minimum adsorption amounts were 78.0% for N-phe and 14.4% for Me-phe. Even from a mixed solution which contained all of them, adsorption decreased in the same order as that from the single solution.

The different adsorption amounts of the various phenols are probably caused by differences in the extent of the π - π stacking interactions.

Keywords: LDH, adsorption, aromatic interaction

1) T. Kameda *et al.*, *Bull. Chem. Soc. Jpn.*, **82**, 1436-1440 (2009).

Table1 Substituted phenols used in this study

<i>m</i> -nitrophenol (N-phe)	3,5-dichlorophenol (DCI-phe)	<i>p</i> -chlorophenol (Cl-phe)	2-methoxy-4-methylphenol (MM-phe)	<i>p</i> -methoxyphenol (Me-phe)

Electron density of aromatic rings

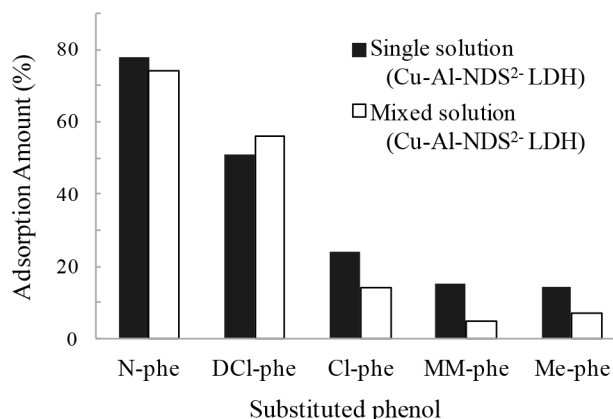


Fig.1 Adsorption of each of the substituted phenols by Cu-Al-NDS²⁻ LDH

Concentration of Cs⁺ using perfluorooctanoic acid and nitrobenzene

Kotaro Hayashi, G.Grause, T.Kameda, T.Yoshioka

Tohoku University, Sendai, Japan



Abstract

The major problem of Fukushima daiichi nuclear power plant is the clean-up of areas that have been heavily contaminated by radioactivity. Cesium is one of the major radioactive elements, with ¹³⁷Cs having a half life of 30 years. Zeolites can be used for the removal of Cs⁺ from sludge and wastewater, but this would produce large amounts of radioactive waste. Some of the metals can be concentrated by porphyrin and ionic associate, and by organic solvents. In the present study, the concentration of Cs⁺ using perfluorooctanoic acid and nitrobenzene was evaluated.

① Concentration of Cs⁺ using perfluorooctanoic acid : Metal chloride(Cs, K, Cd), and $\alpha,\beta,\gamma,\sigma$ -tetrakis(4-sulfophenyl) porphyrin were added and measured by spectrophotometry. The produced solution and ionic associate (perfluorooctanoic acid, hexyltriphenylphosphonium bromide) were separated from the water phase by centrifugation. The water phase was analyzed by ICP-MS. ② Concentration of Cs⁺ using nitrobenzene : The aqueous solution containing cesium chloride was mixed with the organic solution containing dibenzo-24-crown-8-ether (DB24C8) and 2,4-dinitro-1-naphthol(NOL). After the centrifugation, the water phase was analyzed by ICP-MS. The evaluation of concentration of metal ions was expressed as eq 1, 2.

$$E(\%) = (C_{w0} - C_{w1})/C_{w0} \times 100 \quad (1)$$

$$D(-) = C_{org}/C_{w1} = V_{w1}/V_{org} \times E / (100-E) \quad (2)$$

where C_{w0} is the initial concentration of metal ions in aqueous phase and C_{w1} is the concentration of metal ions in aqueous phase after the experiment.

① : The formation complex with Cd²⁺ and porphyrin was recognized by the shift of wavelength from 413 nm to 430 nm as compared to no metal (figure 1). However, the formation complexes of porphyrin with either Cs⁺ or K⁺ were not recognized. From the results shown in table 1, it can be seen that Cd²⁺ was concentrated to ionic associate, but Cs⁺ was not. ② : Table 2 shows that the extraction rate of Cs⁺ decreased by reducing the volume of nitrobenzene. However, the highest distribution was 120, which indicates the possibility of concentration of Cs⁺.

Keywords: ionic associate, porphyrin

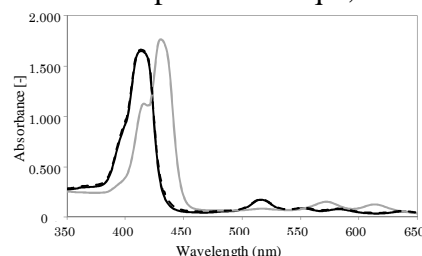


Figure 1. Change of absorbance upon addition of metal ions (—: Cs, - - - : Cd, : No metal)

Table 1. Extraction rate and distribution rate of metal ions using ionic associate ($V_{w1}=19.95$ ml, $V_{org}=0.05$ ml)

Metal	C_{w0} (mol/l)	C_{w1} (mol/l)	E(%)	D(-)
Cs	3.76×10^{-6}	3.87×10^{-6}	—	—
Cd	4.48×10^{-6}	4.19×10^{-7}	90.6	1.93×10^3

Table 2. Extraction rate and distribution rate of Cs⁺ using nitrobenzene (DB24C8= 5.0×10^{-2} mol/l, NOL= 1×10^{-1} mol/l, $C_{w0} = 9.30 \times 10^{-5}$ mol/l, $V_{w1}=10$ ml)

V_{org} (ml)	C_{w1} (mol/l)	E(%)	D(-)
10	1.48×10^{-6}	98.4	11.9
5	1.53×10^{-6}	98.4	120
1	1.15×10^{-5}	87.7	71.1
0.1	7.66×10^{-5}	17.6	21.4

A Microfluidics for Real Time DNA Molecules Replication

Chia-Chin Ho, M.-S Hung*

Department of Biomechatronic Engineering, National Chiayi University,
Chiayi 600, Taiwan

*Corresponding author: Min-Sheng Hung, email: mshung@mail.ncyu.edu.tw



Abstract

The goal of this study was to design and fabricate a microfluidic device to achieve rapid single DNA replication. Numerous studies have demonstrated that rapid polymerase chain reactions (PCR) in microchips can increase the speed of DNA analysis [1], or have developed microfluidic systems to realize real-time PCR in micro droplets [2]. To achieve a real-time DNA replication, a few DNA molecules were injected into a polydimethylsiloxane (PDMS) microfluidic device and isolated in micro-chambers while being fed with oil, as illustrated in Figs. 1(a) and 1(b). The hydrophilic property of PDMS treated with O₂ plasma resulted in the micro-chambers being completely filled with the DNA solution. The injected DNA solution included (1) a 1× buffer (10mM Tris-HCl, 50mM KCl, 0.01% (w/v) gelatin, 1.5mM MgCl₂, 0.1% Triton X-100, pH 9.0), (2) two designed primers, and (3) dNTPs and Taq DNA polymerase with a 1× buffer. After the DNA molecule was observed in the micro-chamber as demonstrated in Fig. 1(c), the microfluidic device was placed on a hot plate for DNA replication by the thermal cycle. Oil was injected to prevent the evaporation of the DNA solution from the thermal cycle. Finally, the replicated DNA in the micro-chamber was confirmed by the number of fluorescent spots evident under a fluorescence microscope. The real-time DNA replication technique developed in this study can be used to decrease the time needed for gene analysis, and can be used to rapidly detect genetic variation.

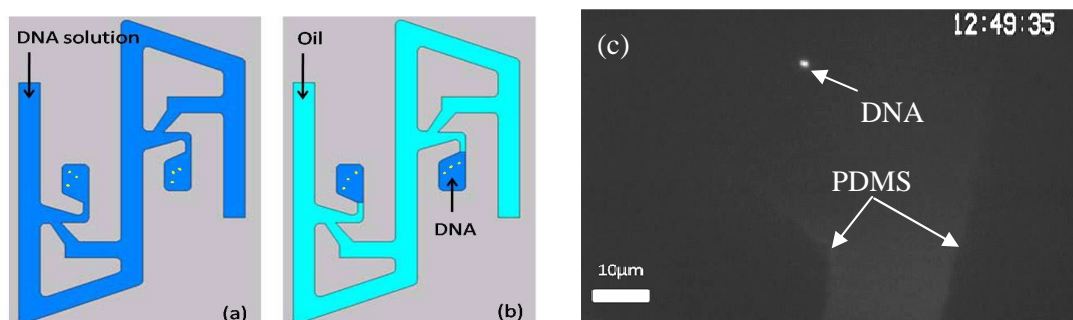


Figure 1 Real time DNA replication in a isolated micro-chamber, (a) DNA solution filled in micro-chambers, (b) DNA solution is isolated using injecting oil, (c) a DNA molecule isolated in a micro-chamber.

References:

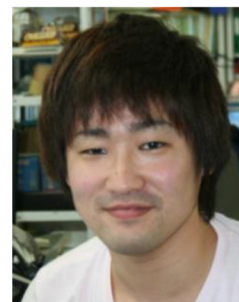
- [1] M. U. Kopp, A. J. de Mello, and A. Manz, *Science*, **280**(1998)1046-1048.
- [2] W. J. Jeong, J. Y. Kim, J. Choo, E. K. Lee, C. S Han, D. J. Beebe, G. H. Seong, S. H. Lee, *Langmuir*, **21**(2005)3738-3741.

Keywords: microfluidics, DNA replication, real time PCR

Uptake of Nd^{3+} and Sr^{2+} from aqueous solution using Zn-Al layered double hydroxide intercalated with aminocarboxylic acid

Tetsu Shinmyo, T. Kameda, T. Yoshioka

Graduate School of Environmental Studies, Tohoku University, Sendai,
Japan



Abstract

Layered double hydroxides (LDHs) referred to as anionic clays are represented by the chemical formula $[\text{M}^{2+}_{1-x}\text{M}^{3+}_x(\text{OH})_2](\text{A}^n)_{x/n} \cdot m\text{H}_2\text{O}$, where M^{2+} could be Mg^{2+} , Zn^{2+} , etc.; M^{3+} could be Al^{3+} , Fe^{3+} , etc.; A^n could be CO_3^{2-} , Cl^- , etc.; and x is the $\text{M}^{3+}/(\text{M}^{2+} + \text{M}^{3+})$ molar ratio ($0.20 \leq x \leq 0.33$). LDHs have anion-exchange capabilities and LDHs intercalated with EDTA, which can form complex with various metal ions, can capture metal ion of a cationic form from aqueous solution¹⁾. In this paper, uptake of rare metal ions such as Nd^{3+} and Sr^{2+} from aqueous solution using Zn-Al LDHs intercalated with TTHA (TTHA·Zn-Al LDHs) prepared by coprecipitation process is reported.

Figures 1 and 2 show variations in the uptake of Nd^{3+} and Sr^{2+} with time. In all cases, the uptake increased along with time. Its increase by TTHA·Zn-Al LDHs is larger than that of $\text{NO}_3\cdot\text{Zn-Al}$ LDHs as for Nd^{3+} uptake. This suggests that $[\text{Nd}(\text{TTHA})]^{2-}$ complexes are formed in the interlayer of TTHA·Zn-Al LDHs. Nd^{3+} uptake increased with the increase of the TTHA/ Nd^{3+} molar ratio and reached 90% at TTHA/ Nd^{3+} =5. Uptake of Sr^{2+} by TTHA·Zn-Al LDHs is almost as much as that of $\text{NO}_3\cdot\text{Zn-Al}$ LDHs, so Sr^{2+} uptake is thought to be mainly due to SrCO_3 precipitation. The uptake of Nd^{3+} is greater than that of Sr^{2+} , and that of Sr^{2+} is low because the difference of the complex formation constant is $[\text{Nd}(\text{TTHA})]^{2-}$ (22.8) and $[\text{Sr}(\text{TTHA})]^{3-}$ (9.26).

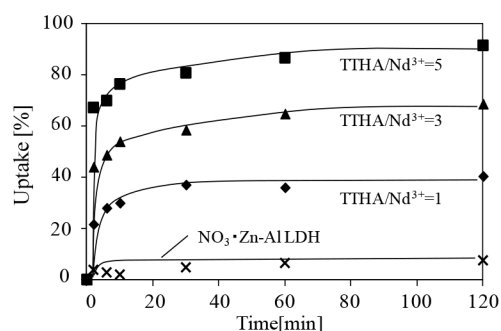


Figure 1 Variations in the uptake of Nd^{3+} with time.

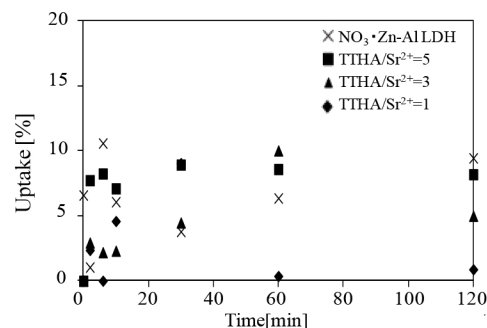


Figure 2 Variations in the uptake of Sr^{2+} with time.

Keywords: Zn-Al LDH, rare metal, TTHA

1) T.Kameda, S.Saito, Y.Umetsu, *Sep. Purif. Technol.*, **47**, 20-26, (2005).

Ultrahigh Surface Area Graphene Oxide Nanoribbons for Electrochemical Detection of Ascorbic Acid, Dopamine and Uric Acid

Chun-Yi Chiu, Chun-Hao Su, Chia-Liang Sun

Department of Chemical and Materials Engineering, Chang Gung University, Kwei-Shan, Tao-Yuan 333, Taiwan



Abstract

In this study, graphene oxide nanoribbons (GONRs) were synthesized from the facile unzipping of multiwalled carbon nanotubes (MWCNTs) with the help of microwave energy. [1] A core-shell MWCNT/GONR-modified glassy carbon (MWCNT/GONR/GC) electrode was used to electrochemically detect ascorbic acid (AA), dopamine (DA), and uric acid (UA). Furthermore, it was found that different GONRs can be synthesized by using various MWCNTs as the raw materials. **Figure 1** shows the comparison of the specific surface area (SSA) values of MWCNT and GONR. The SSA value of our GONR(K) is larger than 2,500 m²/g but still lower than that of 3D graphene reported recently. [2] **Figure 2** illustrates the cyclic voltammograms of GONR(K) and GONR(J) from the detection of DA in 0.1M PBS solution. The GONR(K) with larger SSA value exhibits better oxidation current than GONR(J). It is suggested that the ultrahigh surface area of GONR(K) does partially contribute to the electrochemical oxidation current of analytes.

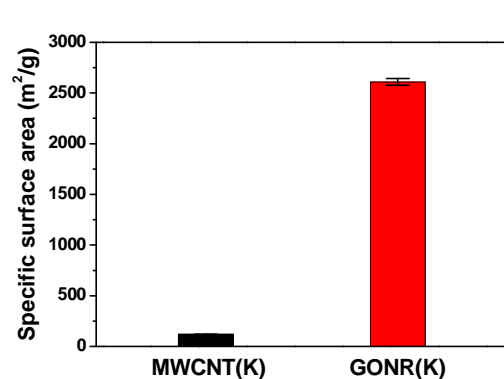


Figure 1

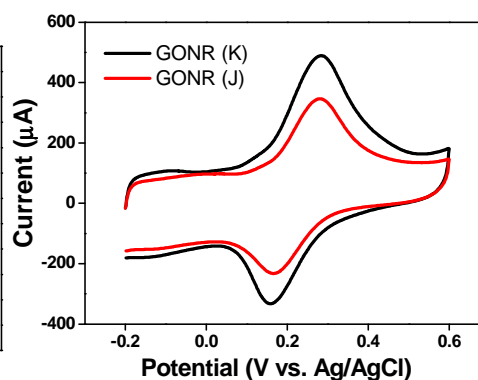


Figure 2

Keywords: Carbon nanotube, graphene nanoribbon, ascorbic acid, dopamine, uric acid

- 1) C.L. Sun, C.T. Chang, H.H. Lee, J. Zhou, J. Wang, T.K. Sham, W.F. Pong, *ACS Nano*, **2011**, 5, 7788.
- 2) L. Zhang, F. Zhang, X. Yang, G. Long, Y. Wu, T. Zhang, K. Leng, Y. Huang, Y. Ma, A. Yu, Y. Chen, *Sci. Rep.*, **2013**, 3, 1408.

Laser-induced Heating for Rapid Targeted DNA Replication

Chih-Pin Chen, M.-S Hung*

Department of Biomechatronic Engineering, National Chiayi University,
Chiayi 600, Taiwan

*Corresponding author: Min-Sheng Hung, email: mshung@mail.ncyu.edu.tw



Abstract

In this study, a microfluidics and an infrared laser are integrated to develop a microfluidic system that performs target DNA replication. Numerous previous studies have investigated laser photothermal effects and its effects on biomolecules by using a laser to heat cells or analyzing the denaturation of DNA [1]. Applying nanotechnology in bioscience assists the development of rapid, low-cost nanobiotechnology approaches that are capable of detecting multiple targets. To demonstrate the replication of the targeted DNA by laser heating, we use double-strand (ds-) DNA (• DNA, 48kb) as the sample. As shown in Figs. 1(a) and 1(b), both ends of the strands are anchored onto 2 electrodes by dielectrophoresis [2], and irradiated with a focused IR laser while monitoring under a fluorescence microscope. The temperature of the laser spot is calibrated from an experiment with the temperature dependent dye tetramethylrhodamine TAMRA (Invitrogen). Figure 1(c) shows the result of DNA stretch and immobilization on the Al electrode of glass surface. After immobilized DNA was observed, then (1) a 1× buffer (10mM Tris-HCl, 50mM KCl, 0.01% (w/v) gelatin, 1.5mM MgCl₂, 0.1% Triton X-100, pH 9.0) was fed to wash surplus DNA, (2) designed primer, dNTPs and Taq DNA polymerase with 1× buffer were fed, (3) the approximately at the center of • DNA was irradiated with a laser for thermal cycle, (4) the replicated DNA was recovered and confirmed using PCR assay and gel electrophoresis.

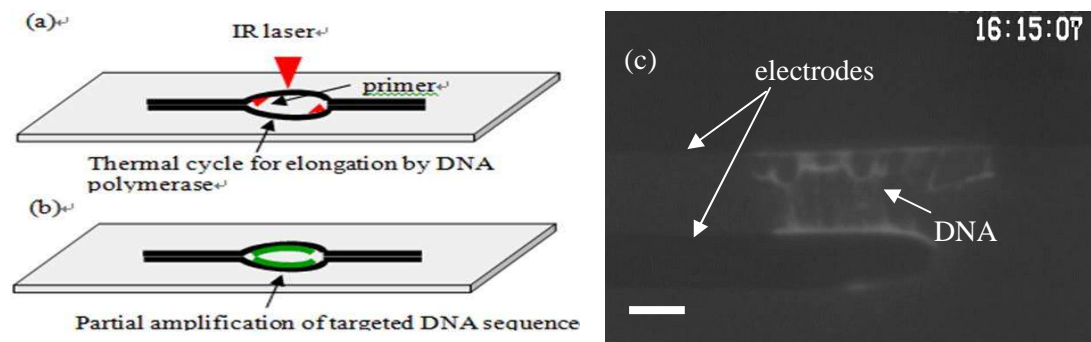


Figure 1 Targeted DNA replication by laser irradiation, (a) laser irradiation, (b) targeted DNA replication, (c) DNA immobilization onto electrodes. (Scale bar 10 μ m)

Keywords: microfluidics, DNA stretch, laser, DNA replication

[1] M.-S. Hung, O. Kurosawa, M. Washizu, *Molecular and Cellular Probes*, 26(2012)107-112.

[2] M. Washizu, O. Kurosawa, I. Arai, N. Shimamoto, *IEEE Transactions on Industry Applications*, 31(1995) 447-456.

Control of selectivity by solvent permittivity in inclusion of methylamines with crystals of thiacalix[4]arene

Ikuko Miyoshi, Y. Kitamoto, O. Shibata, N. Morohashi, T. Hattori

Graduate School of Engineering, Tohoku University, Sendai, Japan



Abstract

The selectivity of molecular recognition is often strongly affected by the permittivity (ϵ) of the solvent employed.¹ Recently, we have found that powdery crystals of *p*-*tert*-butylthiacalix[4]arene (**1**) selectively absorb Me₂NH from a 1:1 aqueous mixture of Me₂NH and Me₃N by forming inclusion crystals. In this study, we wish to report that the inclusion selectivity can be controlled by solvent permittivity.

Powdery crystals of compound **1** were suspended in two-component mixed solvents, in which 0.43 M each of Me₂NH and Me₃N were dissolved; the solvent permittivity was varied by changing the volumetric ratio of the two solvents. After each suspension was stirred at 70 °C for 7 days, the crystals were collected by filtration to determine the inclusion ratio (\bar{n}), which is defined by the average number of guest molecules included into a host molecule. The inclusion selectivity drastically changed within a narrow ϵ range ($65.9 < \epsilon < 88.9$) and almost complete Me₂NH and Me₃N selectivities (~97%) were achieved in the lower and higher ϵ ranges, respectively (Fig. 1). The time course of \bar{n} determined for a high-permittivity solvent revealed that Me₂NH was first included into the crystals and gradually displaced with Me₃N (Fig. 2). In contrast, the initially included Me₂NH remained in the crystals in a low-permittivity solvent. In the inclusion crystals, Me₂NH molecules are associated with each other, whereas each Me₃N molecule is included into the cavity of a host molecule (Fig. 3). In addition, the thermal stability of **1**·Me₃N crystal was higher than that of **1**·Me₂NH. Based on these observations, it is concluded that in a low-permittivity solvent, intermolecular hydrogen bonds between amine molecules prevents Me₃N from being incorporated into the crystals. On the other hand, in a high-permittivity solvent, solvation retards the aggregation of amines, which allows the host crystals to selectively include Me₂NH under kinetic control and Me₃N under thermodynamic control.

a) In the inclusion crystals, Me₂NH molecules are associated with each other, whereas each Me₃N molecule is included into the cavity of a host molecule (Fig. 3). In addition, the thermal stability of **1**·Me₃N crystal was higher than that of **1**·Me₂NH. Based on these observations, it is concluded that in a low-permittivity solvent, intermolecular hydrogen bonds between amine molecules prevents Me₃N from being incorporated into the crystals. On the other hand, in a high-permittivity solvent, solvation retards the aggregation of amines, which allows the host crystals to selectively include Me₂NH under kinetic control and Me₃N under thermodynamic control.

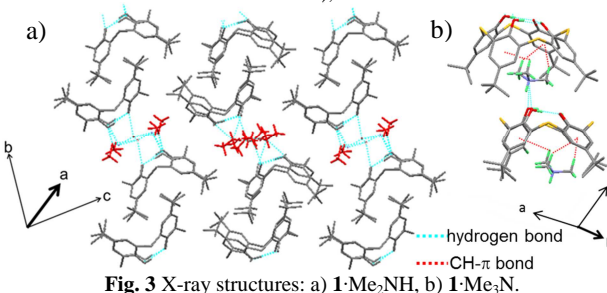


Fig. 3 X-ray structures: a) **1**·Me₂NH, b) **1**·Me₃N.

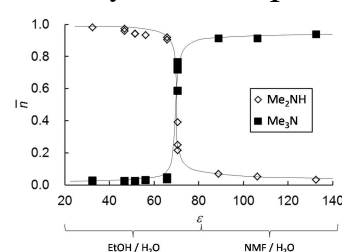


Fig. 1 The ϵ -dependence of inclusion ratio of amines absorbed into the crystals of **1**. Conditions: 70 °C, 7 d.

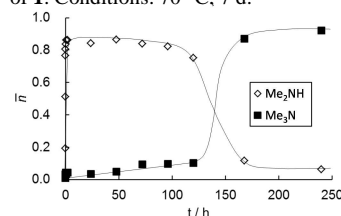


Fig. 2 Inclusion of amines with the crystals of **1** from a high-permittivity solution. Conditions: NMF-H₂O (5.12:4.88) ($\epsilon = 132.6$), 30 °C.

Keywords: Host-guest chemistry, Recognition field, Dielectric constant

1) Kitamoto, Y.; Suzuki, K.; Morohashi, N.; Sakai, K.; Hattori, T. *J. Org. Chem.* **2013**, 78, 597.

P19

Removal of heavy metals in solution by Fe²⁺ doped Mg-Al layered double hydroxides

Eisuke Kondo, Tomohito Kameda, Toshiaki Yoshioka

Graduate School of Environmental Studies, Tohoku University, Sendai, Japan



Abstract

【Introduction】 Heavy metals such as hexavalent chromium, selenium, arsenic, and antimony do not precipitate as metal hydroxides in solution because they exist as oxyanions in both acid and basic mediums. Therefore, the process of removal by coprecipitation method after reduction treatment in two stages is required. Mg-Al layered double hydroxides (Mg-Al LDHs) are anion-exchange materials and their host layer metals have various compositions other than Mg²⁺ and Al³⁺. In this study, doped Fe²⁺ was used as reductant for heavy metals in the host layer of Mg-Al LDH and the removal of the heavy metal oxyanions was examined. This research aims to efficiently remove these heavy metal oxyanions in a single stage process.

【Experiment】 Mg-Al LDH and Fe²⁺-doped LDH (Mg-Al-Fe LDH) was prepared by coprecipitation method, with Mg/Al and Mg: Al: Fe ratios of 3 and 3: 1: 1, respectively. Next, 500 mL of 1 mM of each solution were prepared and each LDH was added with varying stoichiometric proportions of Al/Metals. The removal experiment was done at 308 K for 2 h by stirring at 300 rpm, and concentrations of each metal were determined by ICP-AES.

【Results & Discussion】 Removal of heavy metals after 2 h are presented in Figure 1. Mg-Al-Fe LDH showed a higher removal than Mg-Al LDH for chromium, selenium and arsenic. The adsorption mechanism of LDH is anion exchange in the interlayer promoted by positive electric charge. The factor causing a high removal is the increasing positive electric charge, and the oxyanion reduction by Fe²⁺ oxidizing. However, the adsorption rate was lowered in antimony. This occurred due to the pace of Fe²⁺ oxidation, as it is very slow so that it cannot reach the adsorption equilibrium after two hours.

In fact, compared to the results after four hours of reaction, the adsorption rate of Mg-Al-Fe LDH exceeded that of Mg-Al LDH.

Keywords: Layered Double Hydroxides, Heavy Metal Oxyanions, Reduction

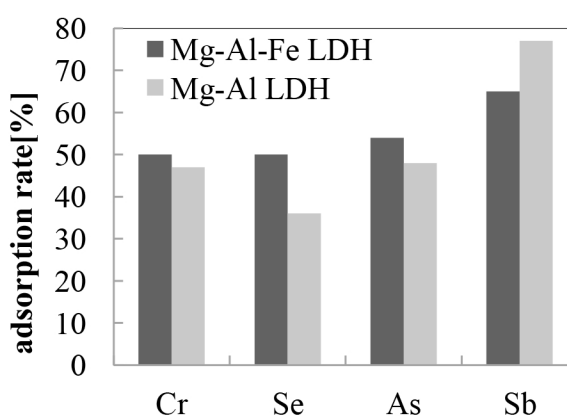


Figure 1 Removal of heavy metals after 2 h
(Al/Metals = 1)

Influence of various factors on spatial structure of nanoparticles in polymer nanocomposite thin films

Yang Liu¹, T. Fujii¹, M. Kubo¹, K. Sugioka¹, T. Tsukada¹,
S. Takami², T. Adschiri³

¹Department of Chemical Engineering, Tohoku University, Sendai, Japan.

²Institute of Multidisciplinary Research for Advanced Materials, Tohoku University, Sendai, Japan.

³WPI Advanced Institute for Materials Research; Tohoku University, Sendai, Japan.



Abstract

Polymer nanocomposite thin films have attracted much attention because of their novel properties which depend on the combination of host polymers and functional nanoparticles as well as the spatial structure of nanoparticles in polymer matrices. In this work, we have investigated the spatial structure of oleic-modified CeO₂ nanoparticles (NPs), which were prepared by the supercritical hydrothermal synthesis method^[1], in polystyrene (PS) nanocomposite thin films by transmission electron microscope (TEM). The surface morphologies of the thin films were also observed by an atomic force microscope (AFM).

Toluene solutions containing PS (Mw=50000, $T_g = 379$ K) and oleic acid-modified CeO₂ NPs were spun-coat onto silicon substrates to prepare nanocomposite thin films. Then, the films were annealed at 433 K for 6 h in air. Besides, the films whose surfaces were entirely covered with the epoxy resin adhesive were annealed for 1 h. The thickness of the films was measured by ellipsometry.

Figure 1 shows the TEM images of the spatial structure of NPs in PS films. Before annealing (Fig.1(a)), a single or two-layers of NPs segregated to the film surface. After annealing for 6 h (Fig.1(b)), the NPs moved a distance of 30 nm away from the film surface. When the film surface was covered with epoxy adhesive (Fig.1(c)), the NPs completely segregated to the substrate surface.

Figure 2 shows the surface morphologies of the PS nanocomposite thin films. The film without annealing (Fig.2(a)) was flat. Annealing the film, however, the surface undulation was observed at 1 h (Fig.2(b)), and then, the surface became flat again at 6h (Fig.2(c)). Such time variation of the surface morphology might be caused by the migration of NPs.

Keywords: nanocomposite film, spatial structure, nanoparticles, annealing

1) Zhang, J, et al., *Adv. Mater.* **2007**, 19, 203-206.

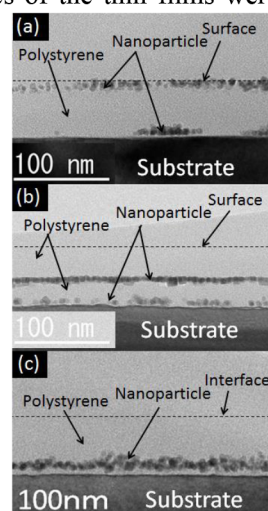


Figure1. TEM images of films.
(a) Before annealing.
(b) After annealing for 6h in air.
(c) After annealing for 1h when surface of film was covered with the epoxy resin.

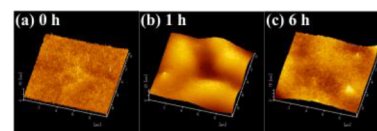


Figure2. AFM images of the morphologies of film surface.

Fundamental study on incubation and condensation of culture medium for extraction from *Nannochloropsis* species

Yuri Hamabe, Masaki Ota, Yoshiyuki Sato, Hiroshi Inomata

Research Center of Supercritical Fluid Technology, Graduate School of Engineering, Tohoku University, Sendai, Japan



Abstract

A green microalgae, *Nannochloropsis*, is considered as one of promising resources to be used in such fields as functional foods, biodiesel and feedstuff since it accumulates valuable fatty acids and lipids. Contained amount of these metabolites depend on the type of algae strains and incubation conditions. Therefore, to utilize this resource efficiently, it is essential to select a strain that will give appropriate metabolites for the objectives. Optimization of incubation conditions as well as establishment of pretreatment process for the effective extraction of target components from algae is also required. In this work, three strains of *Nannochloropsis* were cultured to make a selection of a model strain. Subsequently, ultrasonic atomization technique was applied to culture condensation.

Three strains of *Nannochloropsis* (*Nannochloropsis granulata*, *Nannochloropsis salina*, *Nannochloropsis oceanica*) obtained from National Institute of Technology and Evaluation Biological Resource Center was cultured in artificial seawater with DAIGO IMK medium (Nihon Pharmaceutical Co. Ltd.). Incubation conditions were regulated at a temperature of 22 °C, light intensity of 170 $\mu\text{mol-photon}/(\text{m}^2 \cdot \text{s})$ provided by LED light source, total gas flow rate of 100 cm^3/min and gas composition of $\text{N}_2:\text{CO}_2=99:1$ (v/v). Specific growth rate was determined according to equation (1), where C and X are the concentration and turbidity of culture respectively, and t is the incubation time. Fatty acid content was analyzed by GC-FID.

As shown in Fig. 1, *N. salina* achieved the highest specific growth rate among the three strains. Fatty acid content per dry weight was 43.7 wt % for *N. granulata*, 44.5 wt % for *N. salina* and 17.7 wt% for *N. oceanica*. *N. salina* gave the highest fatty acid productivity, considering both growth and fatty acid accumulation. Currently, ultrasonic atomization apparatus for culture medium collection and culture condensation is being prepared.

$$\mu = \frac{1}{C} \frac{dC}{dt} \approx \frac{1}{X} \frac{dX}{dt} \quad (1)$$

C : cell density [g/dm^3] X : optical density [-],
 t : incubation time [h]

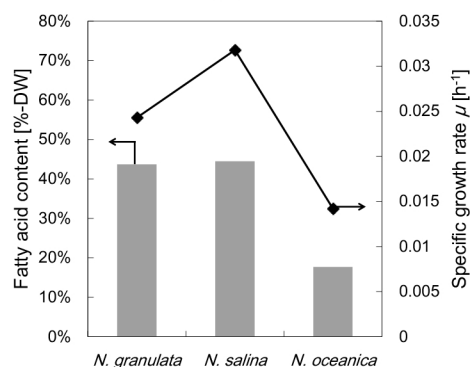


Fig. 1 Specific growth rate and fatty acid content of each strain

Solid Acid Catalysts for Cellulose Hydrolysis in 1-butyl-3-methylimidazolium chloride ([Bmim][Cl])

Shiho Matsuda¹, M. Watanabe², T. M. Aida¹, R. L. Smith Jr.^{1,2}

¹Graduate School of Environmental Studies, ²Research Center of Supercritical Fluid Technology; Tohoku University, Sendai, Japan



Abstract

Saccharides such as glucose are key compounds for sustainable society because their available amount is huge and they are sustainable carbon sources. One of the most likely resources of saccharide is cellulose. Cellulose can selectively be hydrolyzed efficiently into glucose in [Bmim][Cl]-water mixture with water addition in the presence of a solid acid such as Dowex¹⁾, however the suitable catalysts for the cellulose hydrolysis via sequential water addition in ionic liquids is still unclear. In this work, 3 types of solid acid catalysts (ion exchange resin, carbon catalyst, and zeolite) were examined.

A 5% glucose solution in [Bmim][Cl] and 0.5 g catalyst were loaded into a glass reactor and heated in a microwave oven. An amount of water was added sequentially during the reaction. After the reaction, the solid acid was separated by filtration and the liquid product was analyzed by HPLC. Yields were defined on a molar basis.

As shown in Figure 1, the highest yield of saccharides (glucose and cellobiose) was obtained in the presence of Amberlyst-15. The hydrothermal char with fuming sulfuric acid treatment (HC-SA) showed high catalytic activity. Two types of zeolite (MOR: mordenite, and FAU: faujacite) showed relatively high activity among the zeolites. For ion exchange resin and carbon

catalyst, -SO₃H group was active site²⁾ and the lower activity of Dowex is probably due to smaller surface area compared with Amberlyst-15. For zeolite, protons from water adsorption make up the active sites. Since MOR and FAU have 12 member-ring and its pore size is larger than MFI, it is probable that active site in the pore of the zeolite can readily approach those of cellulose (1,4-β-glucosidic bond).

Keywords: cellulose, glucose, ionic liquid, solid acid catalyst, microwave heating

1) X.Qi *et al.*, *Cellulose*, **18**,1327(2011), 2) Guo H. *et al.*, *Biores. Technol.*, **116**, 355(2012)

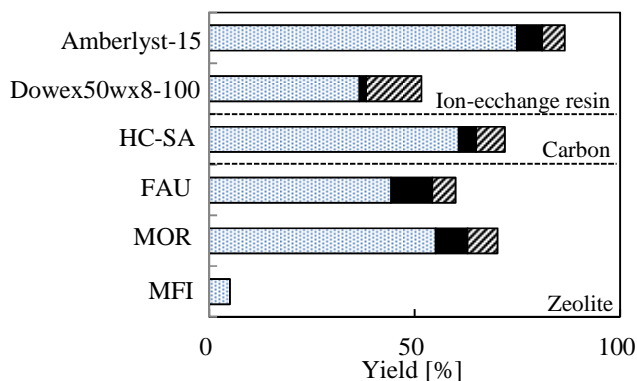


Figure 1 Product yields obtained by catalytic hydrolysis of cellulose (Cellulose 0.05 g, [Bmim][Cl] 0.05 g, catalyst 0.05 g, 120 °C, 20 min, Water content: 5 wt% at 0 min, 25 wt% at 2 min, 35 wt% at 10 min)
 ■:Glucose, ■:Cellobiose, ▨:HMF

Numerical simulations of SiGe single crystal growth by TLZ method in ISS

Keita Abe^{*1}, Sara Sumioka¹, Ken-ichi Sugioka¹, Masaki Kubo¹, Takao Tsukada¹, Kyoichi Kinoshita², Yasutomo Arai², Yuko Inatomi²

1) Department of Chemical Engineering, Tohoku University, 6-6-07 Aramaki, Aoba-ku, Sendai 980-8579, Japan,

2) Institute of Space and Astronautical Science, Japan Aerospace Exploration Agency (JAXA), 2-1-1 Sengen, Tsukuba, Ibaraki 305-8505, Japan



Abstract

Single crystals of SiGe, especially Si_{0.5}Ge_{0.5}, attract the attentions as the post Si semiconductor substrates which enable to produce high-speed and low energy electronic devices. Recently, Kinoshita *et al.*^[1] have developed the traveling liquidus-zone (TLZ) method for the production of homogeneous SiGe bulk single crystals. Currently, in order to clarify the effect of free convection on the TLZ crystal growth of SiGe, the crystal growth experiments under microgravity environment in International Space Station (ISS) have been planned and are being performed this year by JAXA (Hicari project).

In this work, to understand transport phenomena in the TLZ crystal growth process of SiGe under microgravity, a mathematical model for the crystal growth of SiGe by the TLZ method has been developed under the axisymmetric assumption. The self-made code based on this model can predict numerically the velocity field in the melt, the thermal fields in the melt, crystal and crucible, Si concentration fields in the melt and crystal, and the melt/crystal interface shapes. The boundary conditions for temperature at the outer wall of the crucible were determined by a global analysis of heat transfer in the TLZ furnace using a commercial software FLUENT. Figures 1 (a),(b) and (c) show the numerical results of temperature field in the furnace (left side) and Si composition field in the molten zone (right side) during dissolution and crystal growth. The furnace geometry and operational conditions were set to the same as the experimental ones. Firstly, Si feed and seed were dissolved into the molten Ge, and consequently, the molten zone became longer (Figure 1(b)). At 300 min, the SiGe crystal began to grow (Figure 1(b)), and at 7370 min, grew up to 14.9 mm in length (Figure 1(c)).

Keywords: Numerical Simulation, SiGe single crystal growth, TLZ method, ISS

1) K.Kinoshita. *et al.*, *J.Crystal Growth*, **237-239**, 1859(2002)

* k.abe@pcel.che.tohoku.ac.jp

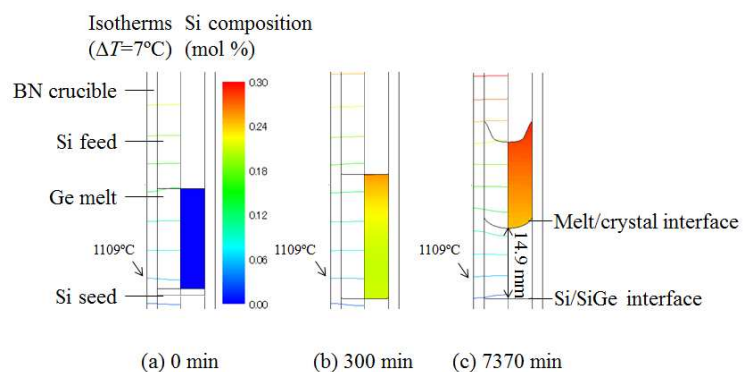


Figure 1 Numerical results of temperature field in the furnace (left side) and Si composition field in the molten zone (right side) during dissolution and crystal growth.

Low-Invasive, Quantitative and Single Cell Level Evaluation of Differentiation State of Embryonic Stem Cells by SECM

Yoshiharu Matsumae¹, T. Arai¹, Y. Takahashi², K. Ino.¹, H. Shiku¹, T. Matsue^{1,2}

¹Graduate School of Environmental Studies, Tohoku University, Sendai, Japan

²Advanced Institute for Materials Research, Tohoku University, Sendai, Japan



Abstract

Embryonic stem (ES) cells which have the capacity to differentiate into a wide range of cell types are a useful resource for regenerative medicine and can be used for studying pathogenesis and drug screening. It is essential to develop a low-invasive and quantitative measurement technique to precisely monitor the differentiation states of ES cells. As an evaluation method for the differentiation states, we have proposed electrochemical methods to detect activities of alkaline phosphatase (ALP), which is an enzymatic differentiation marker. Scanning electrochemical microscopy (SECM) is well suited for single-cell measurements of cellular enzymatic activities. We report here the low-invasive and quantitative electrochemical estimation of the differentiation states of ES cells at the single-cell level by SECM¹.

SECM measurements were conducted using HEPES-based saline solution (pH 9.5) containing 4.7 mM p-aminophenylphosphate (PAPP) monosodium salt for the detection of ALP activities. ALP catalyzed the hydrolysis of PAPP, yielding p-aminophenol (PAP) as an enzymatic product, which was detected electrochemically using a microelectrode probe set at +0.3 V vs. Ag/AgCl/KCl (sat.) (Fig. 1). A disk-type platinum electrode with a diameter of 20 μm was used as an SECM microelectrode probe.

Fig. 2 shows optical microscope images (a, b) and SECM results (c). The current responses for ES cells were considerably larger than those of differentiated cells. This result indicates that SECM can distinguish the differentiation states of a single living ES cell from the electrochemical responses attributable to endogenous ALP activity.

Keywords: embryonic stem cell, scanning electrochemical microscopy, alkaline phosphatase

1) Y. Matsumae. *et. al.*, *Chem. Comm.*, **49**, 6498(2013)

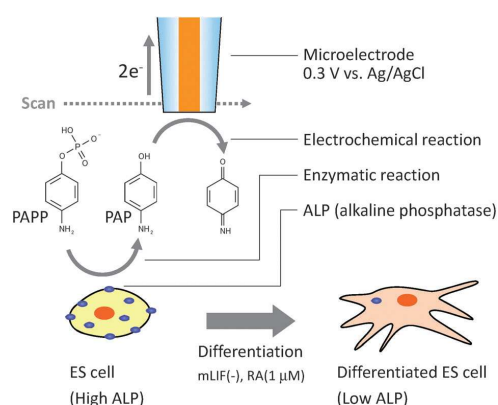


Fig. 1 Schematic diagrams of ALP detection of a single cell using SECM

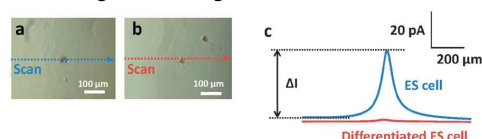


Fig. 2 Optical images of a single ES cell (a) and differentiated ES cell (b). Current response in one-line scan images (c).

P27

Sorting, culture and functional evaluation of mouse mesodermal embryoid bodies

Y. Zhou¹, T. Arai¹, S. Yamada¹, I. Fujisawa¹, K. Ino¹, H. Shiku¹, T. Matsue^{1,2}

¹Graduate School of Environmental Studies, Tohoku University,

²WPI-AIMR



Abstract

Although embryoid bodies (EBs) have been applied for differentiation into various somatic cells and tissues *in vitro*, problems are remained such as heterogeneous and random differentiation and necrosis inside. Our research aimed to produce the purified mesodermal EBs and their functional characterization to improve cardiomyocyte differentiation procedure.

Methods: First we used flow cytometry to sort Flk1(+) mesodermal progenitor cells from EBs formed with hanging drop culture method. After re-cultured EBs in 96well-plate, we measured their respiratory activity by

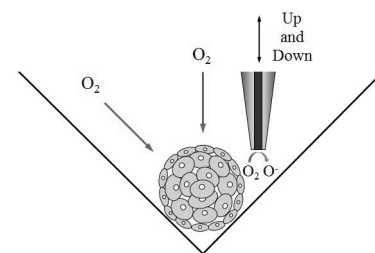


Figure.1 Principle of SECM

scanning electrochemical microscope (SECM) noninvasively. Comprehensive gene expression analyses of mesodermal EBs were performed by using 48.48 dynamic arrays. Results: After sorting and re-culture, EBs specifically expressed mesodermal markers (Nkx2.5, Tnt2, Pecam1) and not expressed endodermal markers or ectodermal markers. We found two types of proliferation patterns of the mesodermal EBs. SECM measurement showed EBs from flk(+) cells had higher respiratory activity than flk(-) cells despite they were the same in morphology. We also found mesodermal EBs with suppressed proliferation during 10 days had higher respiratory activity per cell than those with significant growth. The gene expression profiles suggested that the differentiation to cardiomyocytes was much promoted for the smaller mesodermal EBs. Conclusion: With the mesodermal progenitor marker flk1, we can easily separate and re-culture mesodermal EBs. In contrast to conventional EBs with random differentiation, mesodermal EBs with suppressed proliferation indicated beating behavior effectively and had the potential to differentiate to cardiomyocytes. Furthermore, the respiratory activity of EBs was strongly correlated with the level of cardiac differentiation.

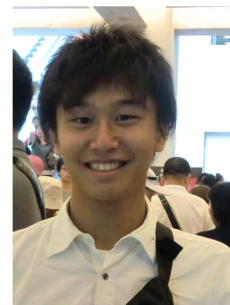
Keywords: mesodermal embryoid bodies, respiratory activity, gene expression

Construction of small bispecific antibody mutants with enhanced anti-tumor activity

Katsuhiko Hosokawa, R. Asano, S. Taki, M. Umetsu, I. Kumagai

Department of Biomolecular Engineering, Graduate School of Engineering,

Tohoku University, Sendai, Japan



Abstract

Antibodies recognize specific antigens using the fragment of variable region (Fv), which comprises the variable domains of the heavy (VH) and of the light chain (VL). Bispecific diabody is one of the smallest recombinant bispecific antibodies,

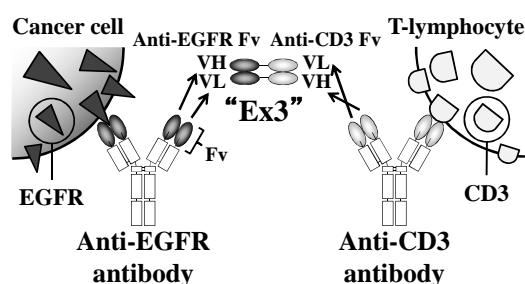


Figure1 Schematic diagram of Ex3 bispecific diabody

consisting of only two different Fvs. We previously reported the construction of Ex3, a humanized bispecific diabody with specificity for epidermal growth factor receptor (EGFR) on cancer cells and CD3 on T-lymphocytes. Ex3 induces marked anti-tumor activity by recruiting T-lymphocytes against cancer cells. We also constructed a humanized Ex3 for clinical application; however, a substantial reduction in binding affinity for EGFR was observed. To recover the affinity of Ex3, affinity selection was performed using anti-EGFR Fv displayed phage and we successfully isolated several promising VH and VL mutants, respectively¹⁾. Then, these mutants were introduced into Ex3 to prepare high affinity Ex3 mutants, and the highest cytotoxicity was observed with one of the mutants, Ex3 mH1. Here, for further functional enhancement, we tried to construct additional 14 Ex3 mutants and to evaluate their functions.

We constructed 14 different expression vectors for Ex3s with VH and/or VL mutations. Ex3 mutants were prepared using bacterial expression system, and purified by immobilized metal affinity chromatography followed by gel filtration chromatography. The results of surface plasmon resonance imaging showed the increase in the affinity of some Ex3 mutants than that of Ex3 mH1. Further, some Ex3 mutants also showed higher cytotoxicity. However, the affinities of Ex3 mutants had a low correlation with those of corresponding anti-EGFR Fv mutants, so the anti-EGFR Fv mutant with the highest affinity could not produce the most functional Ex3 mutant. Therefore, for further functional enhancement of Ex3, we may need to develop a novel affinity selection method using bispecific diabody directly displayed phage.

Keywords: bispecific antibody, cancer immunotherapy, CD3, EGFR

1) T. Nakanishi *et al.*, *Protein Eng. Des. Sel.*, **26**, 113(2013)

In vivo assembly design: multivalent antibody generation

Rui Todokoro, Hikaru Nakazawa, Ryutaro Asano,
Izumi Kumagai, Mitsuo Umetsu

Dept. Biomol. Eng., Grad. Sch. Eng., Tohoku Univ.



[Introduction] Sustained structural biology approach for genome sequences of various species gets to hierarchically describe protein structures; proteins are hierarchically designed from functional module units. The hierarchical understanding of proteins enabled us to generate recombinant chimera proteins with artificial structural format. Here, we propose a unique format for generating multivalent antibodies which can be expressed in *E.coli*, by fusing antigen-recognition domain of antibody on multimeric proteins.

[Results and Discussion] In order to identify the appropriate multimeric protein for backbones of multivalent antibody expressed in *E.coli*, we developed a new ligation method by which we can produced the expression vector in one pot at one time (iPaT method).

Variable domain of heavy chain of a heavy chain camel antibody (VHH) with affinity for epidermal growth factor receptor (EGFR) is fused at the N-terminus of *Pyrococcus horikoshii* copper uptake and transport protein cutA (trimer), human p53 protein, *Streptomyces avidinii* streptavidin (tetramer), horse H-type ferritin, and human L-type ferritin (24mer), by simultaneously ligate the gene fragments coding the multimeric proteins into the vectors containing the VHH gene fragment in a microtube (Fig1.). Consequently, all the expression vectors are prepared.

In this study, we prepared the VHH-fused cutA and p53 and we measured CD spectra to analyze the secondary structures. As a result, the CD spectra seem to show the mixture of characters of VHH and multivalent protein, indicating that each domain of prepared VHH-fused multivalent proteins had native-like secondary structure. We further applied flow cytometry to estimate the binding activity to EGFR on cancer cells. Consequently, our data showed that VHH-fused multivalent proteins had higher avidity than monomeric VHH.

[Conclusions] We generated the variety of expression vector by using new ligation method and prepared two new multivalent antibodies.

[Keywords] protein engineering, multimeric protein, *E.coli*

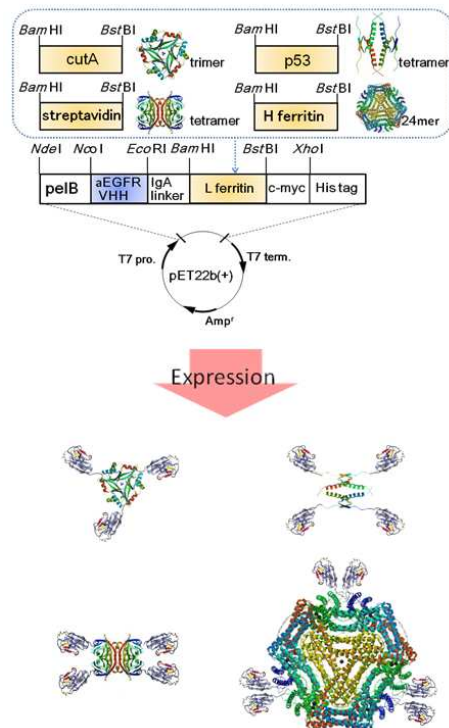


Fig1. Expression vector

Design of bispecific interface molecules for biosensor utilizing camel antibody with affinity for ZnO surface

Takuma Sujino, Hikaru Nakazawa, Ryutaro Asano,
Izumi Kumagai and Mitsuo Umetsu
Dept. Biomol. Eng., Grad. Sch. Eng., Tohoku Univ.



Abstract

Some biosensors have a sensor chip bearing antibody for detecting a specific target molecule and antibody's capturing action is transduced to optical or electrical signals. The density and orientation of immobilized antibody are critical for detection sensitivity of sensors, but several complicated processes should be considered for designing the surface of sensor chip. Recently, we devised a method for creating a camel antibody with high affinity for a specific inorganic material, and the material-binding antibody can spontaneously and high-densely bind to the material surface. In this study, we tried to design the bispecific interface molecules from material-binding antibody and antigen-binding antibody fragments, which can spontaneously immobilize antigen-binding probes on bare sensor chip.

We constructed the bispecific interface molecule by fusing the C terminus of single variable domain of the heavy chain of the heavy chain camel antibody (VHH) with affinity for ZnO surface to the N terminus of humanized single chain fragment of variable domain (scFv) against epidermal growth factor receptor (EGFR), via an immunoglobulin A (IgA) linker. Further, we fused the ZnO-binding VHH to the heavy chain (VH) or light chain (VL) via an IgA linker and co-expressed it with the other chain (VL or VH, respectively). We expressed the recombinant proteins in *E. coli* and confirmed the expression by means of SDS-PAGE and western blotting methods. Purification and measurement of binding affinities are in progress.

Keywords: protein engineering, bispecific antibody, ZnO surface

Estimation Kamlet-Taft Solvatochromic Parameters and Solubility Parameter of Binary Solvent Mixtures for Nucleophilic Substitution and Homogeneous Reaction



Alif Duereh, Masaki Ota, Yoshiyuki Sato, Hiroshi Inomata

Department of Chemical Engineering, Research Center of Supercritical Fluid Technology;
Graduate School of Engineering, Tohoku University, Sendai, Japan

Abstract

A solvent plays an important role on chemical reaction such as rate reaction and selectivity. The characteristics of solvents influenced on chemical reaction can be described by the Kamlet-Taft solvatochromic parameters [1] which consist of 3 components as Π^* for polarity /polarizability, β for the hydrogen-bond accepting, and α for the hydrogen-bond donating. A homogeneous solution can be obtained by predicting the solubility parameter of reactant, product, and solvent. In last decade, many chemists have employed binary solvent mixtures as alternative for pure solvents in order to adjust physical properties and/or avoidable toxic solvent.

In this study, we proposed the advantages of using aqueous-organic solvent mixtures of water and tetrahydrofuran (THF) for replacing pure solvent. The values of Π^* , β , and α of water and THF mixtures as a function of mole fraction of THF at 25 °C are shown in Fig.1 which was reported from Migron et al. [2]. As a result, the decrease of Π^* and α values of mixed solvents were gradual and large, respectively, with increasing mole fraction of THF. In contrast, the β values rose to 0.75 at 0.3 of mole fraction THF, higher than the β values of pure solvents due to solvent-solvent interaction, and remained stable at 0.75 till 0.8 of mole fraction THF. From the Fig. 1, interestingly, using mixed THF and water in THF rich composition, in the range 0.7-0.9 of mole fraction of THF, might be used in a nucleophilic substitution reaction which requires lone-pair electron from the solvent because the β values are higher than the α values, and also the α values are relative low in these range, namely the mixed solvents behave likely an aprotic polar solvent which can donate lone-pair electron.

The most important advantage of using the mixed solvents is adjustable its solubility parameter which generally was estimated by averaging solubility parameter of pure solvents from volume fraction. Thus, the solubility parameter of mixed THF and water are varied between pure THF and pure water, 19-48 MPa^{0.5} [3] that we can use it in wide range of solubility parameter.

Conclusively, the nucleophilic substitution reaction, which a reactant and a product have solubility parameter in range 20-22 MPa^{0.5}, might be used the mixed solvents, THF/water, in range 0.7-0.9 of mole fraction of THF for obtaining homogeneous solution.

Keywords: Kamlet-Taft solvatochromic parameters, solubility parameter

- 1) M. J. Kamlet et al., J. Am. Chem. Soc., 1977, 99(18), 6027-6038.
- 2) Y. Migron et al., J. Chem. Soc. Faraday Trans., 1991, 87(9), 1339-1343.
- 3) C. M. Hasen, Hansen solubility parameters: a user's handbook, CRC Press, Boca Raton, London, New York, 2nd edn., 2007.

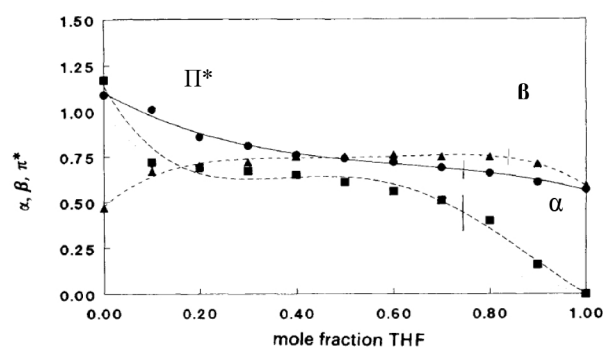


Fig. 1 Values of Π^* (●), β (▲), and α (■) of water and THF mixtures as a function of mole fraction THF [2]

P32

A field emission lighting device employing highly crystalline single-walled carbon nanotubes

Sharon Marie Garrido, Norihiro Shimoi, Adriana Ledezma Estrada, Toshimasa Hojo, Yasumitsu Tanaka and Kazuyuki Tohji

Graduate School of Environmental Studies, Tohoku University

6-6-20 Aoba, Aramaki, Aoba-ku, Sendai 980-8579, Japan



Abstract

To obtain a homogeneously dispersed carbon nanotubes (CNTs) plane with a stable field emission and low FE current fluctuation, it is important to disperse and align the highly crystalline CNTs uniformly. In particular, highly crystalline single-walled nanotubes (SWNTs) can be expected to emit electrons stably with a low turn-on and driving voltage, but their homogeneous dispersion has not yet been reported. In this research, we developed a new cathode for a visible ray flat plane-emission device formed from a mixture of highly crystalline single-wall carbon nanotubes (SWNTs) dispersed into an organic $\text{In}_2\text{O}_3\text{-SnO}_2$ solution. A thin film cathode was fabricated by a simple coating process for the mixture onto a conductive substrate.

The turn-on field of a diode using the optimized cathode was $1.2 \text{ V} / \mu\text{m}$, and the brightness homogeneity in that plane was within 5%.

Favorable brightness homogeneity from the lighting device to control the content of SWNTs in the coated mixture could be obtained by employing highly crystalline SWNTs. Furthermore, brightness efficiency, which is an important factor in comparing luminance devices, totaled more than 50 lm/W . This flat plane-emission device has the potential to provide a new approach to lighting in everyday life as it contributes to energy saving through its low power consumption.

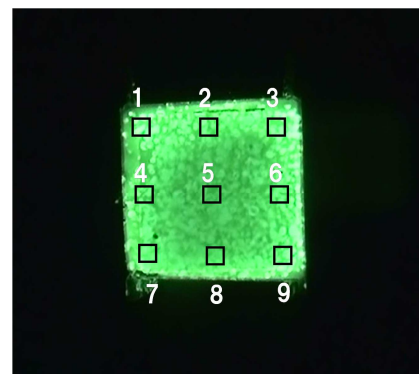


Figure Light emission homogeneity among nine areas captured by CCD.

Keywords: field emission, carbon nanotubes, cathode, homogeneous, brightness efficiency

Evaluation of specific strength of ultimet thin MWCNT fiber based on uncertainty

Hikaru Nishizaka^{1,2}, Yoshinori Sato¹, Kenichi Motomiya¹,
Kazuyuki Tohji¹

¹Graduate School of Environmental Studies, ²Research Fellow of the Japan
Society for the Promotion of Science



Abstract

Carbon nanotubes (CNTs) possess extraordinary mechanical properties. CNT fibers have a flexible structure and consist of highly aligned CNTs [1], which is an advantage in fabricating macroscale CNT materials capable of fully utilizing the excellent mechanical properties of individual CNTs. However, the mechanical properties of CNT fibers are much lower than those of individual CNTs. The load transfer between CNTs in a fiber has currently been transferred by increasing fiber density [2] and introducing polymer chains adjacent CNTs [3]. The specific strength of a fiber (S) is calculated using the following formula [4]:

$$S = \frac{F}{L}$$

where F is a breaking force on the tensile test curve and L is the linear density of the CNT fiber in tex (1 tex = 1 mg/m). Reliability is relatively low at lower linear density, because the error of the linear density mainly depends on the accuracy of a microbalance. Hence, the error of S is relatively large at lower L . In order to precisely evaluate the specific strength of an ultra-light CNT fiber, assessing the reliability of S and its error is of great significance.

Here, we quantitatively expressed the reliability of specific strength based on uncertainty. Uncertainty of specific strength was calculated using the law of propagation of uncertainty. Multi-walled carbon nanotube (MWCNT) fibers were spun from vertically aligned MWCNT arrays synthesized by chemical vapor deposition. The mass per unit length and breaking tensile load of fibers then were measured by an electric microbalance (UMX2, METTLER TOLEDO) and tensile tester (model5848, INSTRON), respectively. Additivity of variance was employed and the combined standard uncertainty (CSU) of each reading was equal to the root-mean-square of standard uncertainties, which were attributed to certain factors such as repeatability and linearity. The CSU of specific strength was then calculated using the CSU of each reading and the law of propagation of uncertainty. The reliability of specific strength is inversely proportional to the CSU.

Keywords: carbon nanotubes, carbon nanotube fibers, specific strength, uncertainty

- 1) K. L. Jiang *et al.* Nature, **419**, 801 (2002), 2) K. Liu *et al.* Nanotechnology, **21**, 045708 (2010),
3) K. Liu *et al.* ACS Nano, **4**, 5827 (2010), 4) M. Miao *et al.* Carbon, **48**, 2802 (2010)

P34

Microbial community dynamic and process performance on chicken manure fermentation at a wide range of ammonia concentration

Qigui Niu¹, Wei Qiao¹, Toshimasa Hojo¹, Yu-You Li^{1,2}

1. Graduate School of Environmental Studies, Tohoku University

2. Department of Civil and Environmental Engineering, Graduate School of Engineering,

Tohoku University



Abstract

With the increase in intensive and mechanized poultry breeding industries, large amounts of waste are being produced. Annually, about 13 million tons of chicken manure (CM) is generated in Japan (MAFF, 2008). Since the organic matter in CM is highly biodegradable, methane fermentation is considered the best method to minimize waste and recover bioenergy. A 12L mesophilic CSTR of chicken manure fermentation was operated for 400 days to evaluate process stability, inhibition occurrence and the recovery behavior suffering TAN concentrations from 2000mg/L to 16000mg/L (Fig.1). A biogas production of 0.35-0.4L/gVS_{in} and a COD conversion of 68% were achieved when TAN concentration was lower than 5000mg/L. Ammonia inhibition occurred due to the addition of NH₄HCO₃ to the substrate. The biogas and COD conversion decreased to 0.3L/gVS_{in} and 20% at TAN 10000mg/L and was totally suppressed at TAN 16000mg/L. Carbohydrate and protein conversion decreased by 33% and 77% after inhibition. After extreme inhibition, the reactor was diluted and washed; reducing TAN and FA to 4000mg/L and 300mg/L respectively, and the recovered biogas production was 0.5L/gVS_{in}. The extended Monod model manifested the different sensitivities of hydrolysis, acidogenesis and methanogenesis to inhibition. VFA accumulation accompanied an increase in ammonia and exerted a toxic on microorganism. Successfully recovery was proved from a seriously inhibited system with a TAN of 16000 mg/L. 16SrDNA cloning and TRFLP were used to detect Bacterial and Archaeal community's dynamics (Fig.2). The Bacterial and Archaeal proportion shifted significantly with VFA accumulation and biogas production following TAN variation. While Aceticlastic Methanosaeta was 2% in the steady stage, it was 5% in the inhibition stage at a high TAN and VFA concentration. Aceticlastic Methanosarcina acetivorans increased from 17% to 72% in the recovered stage. Hydrogenotrophic Methanoculleus bourgensis MS2 increased from 2% in the steady stage to 30% in the inhibition stage and decreased to 13% in the recovered stage according to the resilience of performance. The dominant phylum of Firmicutes was 74% and 92% with and without inhibition and 58% in the recovery stage. The results reveals that TAN has an obvious effect on the microbial community dynamics.

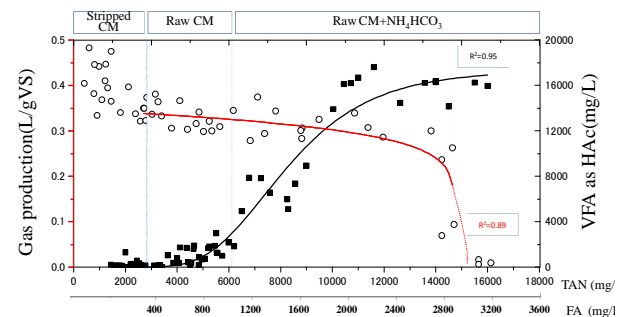


Fig.1. Ammonia inhibition on biogas production and VFA

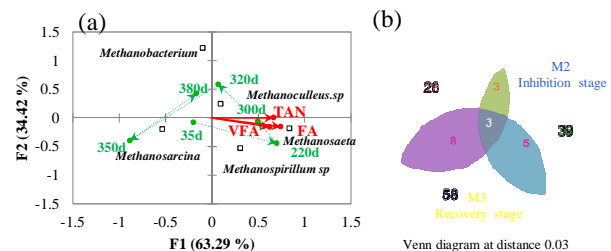


Fig.2. Microbial community dynamic ((a) Methanogens, (b) bacteria Venn diagram at distance of 0.03)

Keywords: chicken manure; mesophilic methane fermentation; functional resilience; ammonia inhibition; microbial community shift

Evaluation of the steam assisted thermal dehydrochlorination of poly(vinyl chloride)

Juan D. Fonseca, G. Grause, T. Kameda, T. Yoshioka

Graduate School of Environmental Studies, Tohoku University, Sendai, Japan



Abstract

PVC is a versatile and low cost material used in a wide array of applications. However, the disposal of PVC-based waste is problematic because of its high content of chlorine. When incinerated, corrosive hydrochloric acid is produced, endangering equipment. Moreover, PVC is also a precursor for carcinogenic dioxin formation, resulting in the release of dangerous pollutants into the atmosphere. Because of this, PVC waste often ends up in sanitary landfill where plasticizers, most of which are suspected endocrine disruptors, can leach into ground water. Proper dechlorination pretreatment allows PVC waste to be processed along with other waste plastic streams and for this reason there has been many research done on both dry thermal processing and wet processing using solvents. The present research investigates an intermediate alternative process that is based on the application of steam and the effect that steam addition has upon the thermal dehydrochlorination of PVC materials.

0.5 g of either PVC resin or flexible PVC was placed on a ceramic boat inside a horizontal glass-tube reactor. A total gas flow of 200 ml min⁻¹ with varying compositions of steam (0, 25, 50 and 75 vol%) was maintained. For each steam concentration, the reactor temperature was set to a temperature between 150 and 250 °C for reaction time intervals ranging from 15 to 180 minutes. Steam and HCl were collected in iced water traps at the outlet of the reactor and analyzed using ion chromatography. The dechlorination rate was calculated in relation to the initial amount of chlorine present in the sample mass: 57 wt% for PVC resin and 28 wt% for flexible PVC. Reaction kinetics for steam dechlorination of PVC resin was obtained using thermo gravimetric analysis performed in helium and steam atmosphere. The structure of residue was examined by SEM photography and FT-IR.

For both samples used the most effective steam concentration was 50 vol% with most of the dechlorination occurring between 15 and 60 minutes after initiation. At 250 °C, the addition of steam increased the maximum dechlorination by about 15% for both PVC resin and flexible PVC (figure 1). The steam assisted dehydrochlorination reaction proceeded under an apparent first order reaction with an activation energy of 120 kJ mol⁻¹ and depended strongly on the temperature. Reaction rates were 40-50% faster when a steam concentration of 50 vol% was applied. According to these results, the use of steam dechlorination as a pretreatment step for the utilization of waste PVC has various advantages over the dry thermal decomposition of PVC in an inert atmosphere.

Keywords: flexible PVC, dechlorination, atmospheric pressure

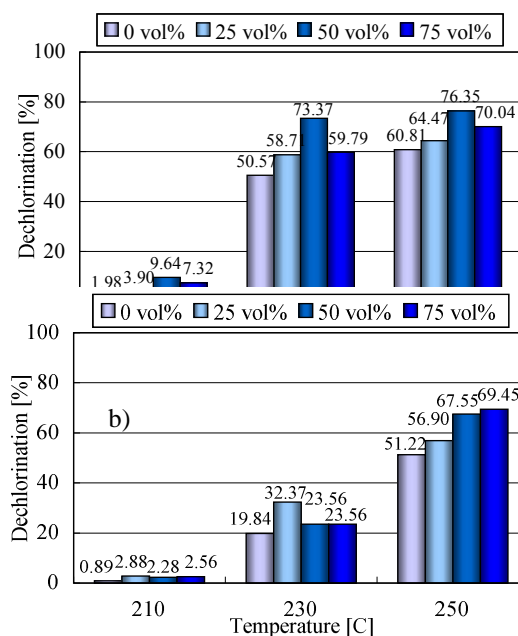


Figure 1. Dehydrochlorination of a) PVC resin and b) flexible PVC after 60 min, under various temperatures and steam contents.